PERFORMANCE ANALYSIS OF DPSK SYSTEMS WITH MIMO EMPLOYING EGC OVER WIRELESS FADING CHANNELS

by

IYAD ABDELRAZZAQE AL FALUJAH

A Dissertation Presented to the Faculty of the Graduate School of The University of Texas at Arlington in Partial Fulfillment

of the Requirements

for the Degree of

DOCTOR OF PHILOSOPHY

THE UNIVERSITY OF TEXAS AT ARLINGTON

May 2007

In memory of my parents, Abdelrazzaqe and Haleemah Al Falujah, and to my brothers and sisters with love.

ACKNOWLEDGEMENTS

First and foremost, I would like to express my deepest gratitude to my advisor Professor Vasant K. Prabhu for his support and guidance throughout my years at UTA. Starting from the day when I first learned that I would be his advisee, I have always been excited to have the opportunity to work with him. I realize that sometimes a single discussion with him has led to ideas for a full research paper, and I feel fortunate to have seen a glimpse of his wisdom. With his encouragement of independent research and high-quality scholarly work, inspiration, constant guidance and dedication, I feel I have improved myself to become a better researcher and writer, and I consider myself privileged to have experienced a rewarding graduate study.

I am also thankful to the members of my dissertation committee: Dr. Jonathan Bredow, Dr. Chien-Pai Han, Dr. Michael T. Manry, and Dr Mingyu Lu for their interest in my research and for taking time to serve in my dissertation committee.

I am grateful to all the teachers who taught me during the years I spent in school, in Jordan, Iraq, and the Unites States.

Thanks must go to my old colleagues in the Telecommunication Research Group, Dr. Dongdong Li, Dr. Feng Liu, Dr. Chen Liao, and Dr. Mahmoud Smadi for their valuable help, enthusiasm, and humor. I am also grateful to my friends Dr. Hussam Al-Shammari, Dr. Murad Abu Khalaf, Mohammad Mayyas, and Jareer H. Abdel-Qader for making my time here more enjoyable.

Finally, I owe a huge debt of gratitude to my brothers and sisters, Tawfeeq, Jihad, Suhair, Rawhyyah, Nihad, Najah, Shahir, Sameer, Mohammad-Ameen, Ayman, and Wajeeh for their endless support and love throughout not only the course of my Ph.D. studies, but my entire life.

April 16, 2007

ABSTRACT

PERFORMANCE ANALYSIS OF DPSK SYSTEMS WITH MIMO EMPLOYING EGC OVER WIRELESS FADING CHANNELS

Publication No. _____

IYAD ABDELRAZZAQE AL FALUJAH, Ph.D.

The University of Texas at Arlington, 2007

Supervising Professor: Vasant K. Prabhu

The proliferation of digital wireless communication services has increased the congestion of the available radio spectrum. In addition to that, wireless communications are encountered by multipath channel fading. To alleviate the scarcity of the radio spectrum and multipath channel fading, attention in this dissertation is placed on differentially coherent phase shift keying (DPSK) systems with equal gain combining (EGC) diversity reception. DPSK systems are capable of achieving high spectral efficiency with adequate performance over wireless fading channels. Several wireless communication systems have adopted DPSK such as the time division multiple access (TDMA) version of the North American Digital Cellular (NADC) system. DPSK systems together with multiple-input multiple-output (MIMO) antenna systems have the potential to further improve the diversity gain and increase the spectral efficiency in wireless communication systems.

This dissertation analyzes the error rates of a variety of wireless digital techniques over fading channels with particular emphasis on the DPSK systems. This work leads to a useful framework to analyze the error rates of digital techniques over fading channels, and the proposal of a reduced-complexity and low-cost MIMO system for wireless communications. This dissertation also simplifies and generalizes the previous results of the error rates of wireless communication techniques over independent and correlated fading without resorting to approximations. In addition to that, this study investigates the impact of fading correlation and imperfect phase recovery on the performance of noncoherent and coherent digital wireless communication systems respectively. From practical point of view, this research study is expected to be helpful in the design of the practical radio communication receivers.

First, this research starts with a study of the DPSK systems over independent and correlated fading channels. We present two approaches to analyze the average bit error probability (BEP) of differential quaternary phase shift keying (DQPSK) systems with equal gain combining (EGC) diversity reception over fading channels. The first approach relies on the integral definition of the associated Legendre functions, which can lead to finite-series closed-form expressions for the average BEP of DQPSK over L independent Rayleigh and Nakagami-m, when the product Lm is integer, fading channels. In the second approach, we propose a finite sum of a finite-range integral for the average BEP of DQPSK with EGC over arbitrarily Nakagami-m and Rician fading channels. Besides, a finite-series closed-form expression is given for the average BEP of differential binary phase shift keying (DBPSK) with EGC over independent Rician fading channels. It is observed that the performance degradation due to the correlation among the diversity branches in Rician fading channels is severer than that in Nakagami-m fading channels as a result of the presence of the specular component.

Second, we propose and analyze a reduced-complexity and low-cost DPSK system with MIMO employing EGC (MIMO EGC) diversity reception. The proposed structure provides a reduced-complexity and low-cost receiver for MIMO systems compared to the coherent phase shift keying system (PSK) with MIMO employing maximal ratio combining (MIMO MRC). The average BEP for DBPSK and DQPSK with MIMO EGC over independent Rayleigh fading channels has been derived. The associated Legendre functions approach has been used to analyze the average BEP of DQPSK with MIMO EGC. Finite closed-form expressions for the average BEP of DBPSK and DQPSK are presented.

Third, we present another useful utilization of the associated Legendre functions approach. The associated Legendre functions approach is devoted to analyze the performance of coherent PSK systems over fading channels in the presence of imperfect phase recovery. We address an evaluation (without any kind of approximation) for the average BEP of the PSK systems with imperfect phase recovery over fading channels. Moreover, using the Fourier series expansion and the associated Legendre functions, the exact average BEP of the binary and quaternary phase shift keying (BPSK and QPSK respectively) on a single channel (no diversity) in the presence of different kinds of slow fading channels (Rayleigh, Nakagami-m, and Rician), phase recovery error, and additive white Gaussian noise (AWGN) has been evaluated. The detection loss and phase precision for both of BPSK and QPSK have been calculated. The series expressions of the average BEP proposed in our study are found to be converged with reasonable number of terms.

Fourth, we turn our attention onto the performance of the square M-ary quadrature amplitude modulation (MQAM) with maximal ratio combining (MRC) receive diversity. We present closed-form expressions for the average SEP of MQAM with arbitrarily fading index m. Two models of MQAM receivers are analyzed. Closed-form expressions are provided for the average SEP in terms of the Appell and Gauss hypergeometric functions.

Simplified error expressions are proposed when the product Lm is either integer or half integer.

Finally this dissertation is concluded with summarized remarks and future extensions.

PREFACE

This dissertation is based on a research in the area of performance analysis of wireless transmission techniques conducted under the supervision of Prof. Vasant K. Prabhu. Many of the results presented here appear in conference proceedings and in manuscripts published in refereed journals.

Performance analysis of DPSK systems over fading channels is based on results in

- I. Al Falujah, and V. K. Prabhu, "Error Performance of DQPSK with EGC Diversity Reception over Fading Channels," *IEEE Trans. Wire. Comm.*, (to appear 2007).

- I. Al Falujah, and V. K. Prabhu, "Performance Analysis of DPSK with Diversity Reception over Equal-Correlated Nakagami-m and Independent Rician Fading," *Proc. IEEE Veh. Technol. Conf.* (VTC 2005-Fall), vol. 3, 1479-1483, Sept. 2005.

- I. Al Falujah, and V. K. Prabhu, "Error Performance of DQPSK with EGC Diversity Reception over Arbitrarily Correlated Fading Channels," *Proc. of the 2006 IEEE Veh. Technol. Conf.* (VTC 2006-Fall), Montreal, Canada, September 2006.

The error rates of DPSK system with MIMO EGC diversity reception over Rayleigh fading channels are based on results in

- I. Al Falujah, and V. K. Prabhu, "Error Rates of DPSK System with MIMO EGC Diversity Reception over Rayleigh Fading Channels," *IEEE Trans. Comm.*, (to

appear 2007).

- I. Al Falujah, and V. K. Prabhu, "Error Rates of DPSK System with MIMO EGC Diversity Reception over Rayleigh Fading Channels," *Proc. of the 2006 IEEE Veh. Technol. Conf.* (VTC 2006-Fall), Montreal, Canada, September 2006.

The performance analysis of PSK systems in the presence of slow fading, imperfect carrier phase recovery, and AWGN is based on results in

- I. Al Falujah, and V. K. Prabhu, "Performance Analysis of PSK Systems in the Presence of Slow Fading, Imperfect Carrier Phase Recovery, and AWGN," *Proc. IEE—Commun.*, vol. 152, pp. 903-911, Dec. 2005.

- I. Al Falujah, and V. K. Prabhu, "Performance Analysis of PSK Systems in the Presence of Slow Fading, Imperfect Carrier Phase Recovery, and AWGN," *Proc. IEEE Can. Conf. Electrical Computer Engineering (CCECE 05)*, Saskatchewan , Canada, pp. 1859-1862, May 2005.

In the course of this research, we also obtain results on MQAM with MRC over Nakagami-m fading channels which appeared in

- I. Al Falujah, and V. K. Prabhu, "Performance Analysis of MQAM with MRC over Nakagami-m Fading Channels," *Electronics Letters*, vol. 42, pp. 231 - 232, Feb. 2006.

- I. Al Falujah, and V. K. Prabhu, "Performance Analysis of MQAM with MRC over Nakagami-m Fading Channels," *Proc. of the IEEE Wireless Communications and*

Networking Conference (WCNC 2006), Las Vegas, NV, April 2006.

TABLE OF CONTENTS

LIST OF FIGURES

LIST OF TABLES

CHAPTER 1

INTRODUCTION

1.1 Introduction

Wireless communication systems represent one of the most attractive features of today's modern communication systems. The main goal of wireless radio communications is to provide reliable and cost effective voice, video, or data communications to anyone, any where, and at any time [1]. Carrying out this objective is encountered by many challenges. The principal phenomena that makes our objective difficult to achieve is the time-varying multipath fading [2]. In the time-varying multipath channel fading, the multiple propagation paths between the transmitter and receiver produce a received signal suffering from random envelope and phase fluctuations. The multipath fading effects (the random envelope and phase fluctuations) can lead to a severe system performance degradation of wireless communication systems.

1.2 Multipath Fading Channels

The signals transmitted through multipath fading channels undergo several effects [3]. The main effects are the time varying nature of the multipath fading channel and the time delay spread of the multiple received replicas of the transmitted signal.

1.2.1 Slow and Fast fading

The time variation of the multipath fading channel (changes in the amplitudes, delays, and the number of multipath received components) can be observed over a large

time scale. The coherence time T_c determines the time duration over which the channel impulse response is invariant, and it is related to the channel Doppler spread f_d as [3]

$$T_c \simeq \frac{1}{f_d} \tag{1.1}$$

Multipath fading can be classified into fast and slow regarding the symbol duration T_s and channel's coherence time T_c. Slow fading refers to the situation for which $T_s < T_c$ i.e. the channel is static over some symbol intervals. Thus, in slow fading many successive symbols can be influenced by the same fading level, which may lead to burst errors. On the other hand, fast fading occurs when $T_s < T_c$ and in this case the channel impulse response changes rapidly within the symbol duration.

1.2.2 Frequency-Flat and Frequency-Selective fading

The transmitted signal reaches the receiver along different paths, the arrival of the signal via different paths causes a time dispersion and frequency selective fading. The time delay spread $\tau_{\max}$ equals the difference between the time arrival of the first received component (line of sight (LOS) or multipath) and the last received component associated with a single transmitted pulse. The coherence bandwidth f_c specifies the range of frequencies over which the fading process is correlated. The relationship between the coherence bandwidth and the time delay spread is

$$\tau_{\max} \simeq \frac{1}{f_c} \tag{1.2}$$

Frequency flat fading (nonselective) is observed in wireless channels when the spectral components of the transmitted signal are affected in similar manner (narrowband fading models). However, frequency selective fading is captured when the spectral components are affected by different amplitude gains and phase shifts (wideband fading models).

In this dissertation, we will concentrate on the performance evaluation of flat and slow multipath fading channels (narrowband fading models).

1.3 Envelope Distribution in Narroband Fading Models

The various received replicas of the transmitted signal add constructively and destructively at the receiver due to the phase mismatch among them. The random envelope and phase fluctuations can be characterized statistically. In narrowband fading models, the fading envelope and phase can be considered constant during the symbol signalling interval. In coherent digital communication systems the random phase can be compensated using phase recovery techniques [2], whereas in noncoherent modulations the phase information is not required. Thus, the phase variation does not affect the performance evaluation for both of the coherent systems with perfect phase recovery and noncoherent systems. The random fading amplitude can be considered as a random variable whose distribution depends on the particular propagation environment [3]. In the following, the most common fading envelope probability density functions (pdf) are explained:

1.3.1 Rayleigh Fading

In Rayleigh fading, there is no LOS component in the multipath fading, and the pdf of the fading envelope is given by

$$f_\alpha(\alpha) = \frac{2\alpha}{\Omega} \exp(-\frac{\alpha^2}{\Omega}), \quad \alpha \geq 0 \tag{1.3}$$

where $\Omega = \mathrm{E}\{\alpha^2\}$ and $\mathrm{E}\{.\}$ denotes the expectation. Rayleigh distribution often agrees with experimental data of mobile systems, in which LOS component does not exist [3].

1.3.2 Nakagami-m Fading

In Nakagami-m fading, the pdf of the fading amplitude can be written as [4]

$$f_\alpha(\alpha) = \frac{2m^m \alpha^{2m-1}}{\Omega^m \Gamma(m)} \exp\left(-\frac{m\alpha^2}{\Omega}\right), \quad \alpha \geq 0 \tag{1.4}$$

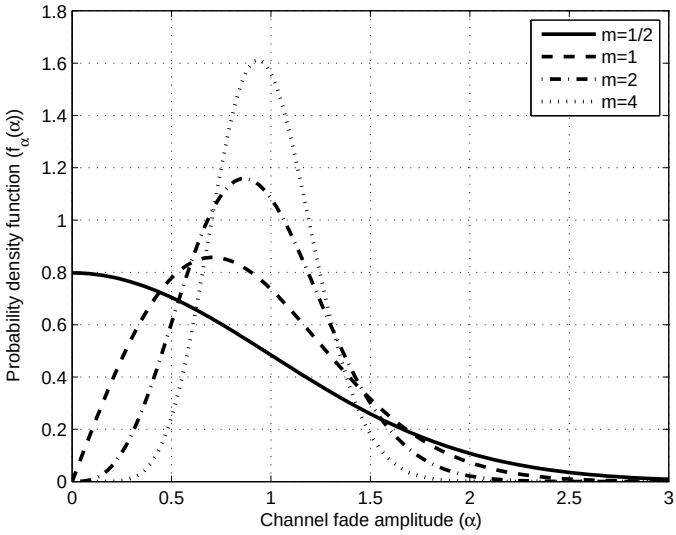

Figure 1.1. The Nakagami-m pdf for $\Omega = 1$ and various values of the fading index m.

where $\Gamma(.)$ is the Gamma function and m is the Nakagami-m fading parameter, which ranges from 0.5 to ∞ , and Ω is the mean squared of α. Nakagami-m fading model can model several fading environments including Rayleigh fading ($m = 1$), one-sided Gaussian distribution ($m = \frac{1}{2}$), and unfaded channel ($m = \infty$). Nakagami-m fading is observed to provide the best fit to land mobile and indoor-mobile multipath propagations [3]. Figure 1.1 shows the Nakagami-m pdf for $\Omega = 1$ and various values of the fading index m.

The kth moment of a Nakagami-m distributed random variable is [2]

$$\mu_k = \mathrm{E}\{\alpha^k\} = \frac{\Gamma(m + k/2)}{\Gamma(m)} \left(\frac{\Omega}{m}\right)^{k/2} \tag{1.5}$$

1.3.3 Rician Fading

In Rician fading environment, there is a fundamental LOS signal from the transmitter to the receiver with additional weaker paths resulting from reflections. The pdf of the fading amplitude α is given by [5]

$$f_\alpha(\alpha) = \frac{2(1+K)\alpha}{\Omega} \exp\left(-\frac{(1+K)\alpha^2 + \Omega K}{\Omega}\right) I_0\left(2\alpha\sqrt{\frac{K(1+K)}{\Omega}}\right), \qquad \alpha \geq 0 \quad (1.6)$$

where K is the Rician fading parameter, which ranges from 0 to ∞, and Ω is the mean squared of α. For the special case ($K = 0$), the distribution deteriorate into Rayleigh fading statistics.

The kth moment of a Rician distributed random variable is [2]

$$\mu_k = \mathrm{E}\{\alpha^k\} = \left(\frac{\Omega}{K+1}\right)^{(k/2)} e^{-K}\Gamma(1+k/2)\ {}_1F_1\left(1; 1+k/2; K\right) \quad (1.7)$$

where ${}_1F_1(.;.;.)$ is the confluent hypergeometric function [6].

The Rician distribution relates to Nakagami-m through a simple formulas

$$\begin{aligned} m &= \frac{(1+K)^2}{2K+1}, \qquad K \geq 0 \\ K &= \frac{\sqrt{m^2-m}}{m-\sqrt{m^2-m}}, \qquad m \geq 1 \end{aligned} \quad (1.8)$$

The above two relations gives the one to one mapping between Rician and Nakagami-m distributions. Apart from the Rayleigh case ($m = 1$ and $K = 0$), the resulting two distributions (Rician and Nakagami-m) from the corresponding interrelations equations are shown to approximate each other [3]. However, the Nakagami-m case with $1/2 \leq m < 1$ is not covered by the Rician statistics. Figure 1.2 shows the Rician pdf for $\Omega = 1$ and various values of the fading index K.

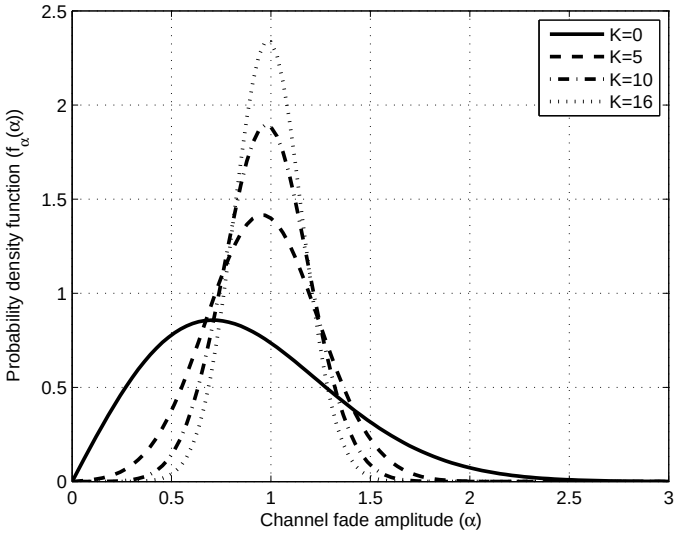

Figure 1.2. The Rician pdf for $\Omega = 1$ and various values of the fading index K.

1.4 Diversity Techniques to Mitigate Multipath Fading Channel

Diversity techniques, or alternatively multichannel reception techniques, represent one of the most powerful techniques that can be used to mitigate the effects of multipath channel fading [2],[7],[8]. The main reason behind the usefulness of diversity techniques is to supply the receiver with multiple versions of the same transmitted signals over independent channels, so that the probability of all the signals suffer severe fading is less than the probability of single signal suffer deep fading [2]. Many replicas of the information bearing signal can be obtained by extracting the signals via different techniques, one way is to employ frequency diversity in which the information bearing signal is transmitted on L carriers provided that the separation between successive carriers equals or exceeds the coherence bandwidth of the channel. The main disadvantage of frequency diversity is that this scheme does not posses bandwidth efficiency. The second possible way to achieve diversity is to send the information bearing signal on L different time slots (time

diversity). A third commonly used scheme of diversity is based on using multiple antenna separated wide enough with respect to carrier wavelength at the transmitter and/or the receiver (space diversity). Space diversity does not require any additional bandwidth and it has the benefit of achieving a signal to noise ratio (SNR) to support the communication link without increasing the total transmitted power [1]. Diversity techniques can be classified into two main types: microdiversity and macrodiversity techniques [9]. Microdiversity is used to combat the effects of multipath channel fading. On the other hand macrodiversity is used to mitigate the effects of shadowing from building and objects.

1.5 Receiver Diversity Combining Techniques

Diversity techniques are used to improve the performance of wireless communication systems over fading channels. Significant improvement in performance of communication systems can be achieved using appropriate combining techniques with a certain degree of complexity. Diversity combining involves weighted linear sum of the multiple received signals. Combining the received signals in diversity systems can be classified into four types, which depend essentially on the complexity restrictions put on the communication system and the amount of channel state information (CSI), random amplitude and phase introduced by the channel, available at the receiver [3],[10].

1.5.1 Maximal Ratio Combining (MRC)

In MRC the received signals form the L diversity branches are co-phased and individually weighted by their respective complex fading gain and combined. In the absence of interference, MRC is the optimal combining scheme (regardless of fading statistics), but comes at the expense of complexity since MRC needs the knowledge of all channel fading parameters [3]. Since MRC involves estimating the amplitude of the

received signals, this scheme can be used in conjunction with unequal energy signals like M-ary quadrature amplitude modulation (MQAM), M-ary pulse amplitude modulation (MPAM), or any other amplitude modulation. It should be pointed out that MRC scheme is not practical with differential form of modulation techniques, because MRC requires the knowledge of phase, so it is better in terms of performance to employ coherent schemes rather than noncoherent reception [3].

1.5.2 Equal Gain Combining (EGC)

In the EGC technique, the outputs of the different diversity branches are co-phased and weighted equally before being summed to give the resultant output. Since EGC scheme does not require the knowledge of the amplitude, it is is widely used in equal energy modulation techniques as the M-ary phase shift keying (M-PSK). Moreover, it benefits in a reduced complexity of the receiver structure relative to MRC receiver [3].

1.5.3 Selection Combining (SC)

The two preceding techniques (MRC and EGC) require all or some of the CSI, also they require a demodulator for each diversity branch [3]. On the other hand, SC chooses the branch which yields the maximum SNR. Selection diversity does not require co-phasing, which results in a simple receiver structure compared to MRC and EGC [10]. The main disadvantage of this scheme of combining is the requirement of continuous monitoring of the SNR on all branches.

1.5.4 Switch and Stay Combining (SSC)

A SSC diversity searches all the diversity branches until it finds one that has a SNR exceeding a predetermined threshold and it stays there until the SNR drops below a

predetermined threshold, when this happens the receiver switches to another branch [10]. There are several criteria behind choosing which branch to switch to [10]. The simplest one is to switch in a random manner to another branch (switch and stay strategy) [9]. SSC diversity requires neither continuous monitoring of all the diversity branches nor co-phasing the received signals on the L branches. Hence SSC is the least complexity of all diversity combining schemes.

1.6 Practical Limitations of Diversity Systems

The performance of wireless communication systems with diversity reception over fading channels are subject to some limitations related to the implementation of diversity systems [11]. Combining the received signals before or after the detection and the effect of correlation between the received signals are examples of these limitations that degrade the performance of diversity systems.

1.7 Predetection and Postdetection combining

Diversity combining can be classified into predetection and postdetection combining. In predetection combining, the received signals are combined coherently before they are detected, whereas the postdetection combining implies that the received signals are detected before combining takes place in the baseband region. In coherent systems, the performance of predetection and postdetection combining diversity is equal when the weighting factors are identical for both of combining techniques. However, predetection combining offers a better performance than postdetection in case of noncoherent and differential coherent systems. The improvement in performance of predetection over postdetection comes at the expense of complexity and cost, because RF co-phasing is required before detection [11].

1.8 Impact of Fading Correlation

In space diversity, the multiple antennas at the transmitter and/or the receiver, should be separated wide enough with respect to the carrier wavelength, so that independent channel fading can be assumed. If the separation distance between the multiple antennas decreases, the correlation between the received signals at different branches should be taken into account. In many cases, it is difficult to achieve independent signals and branches on the diversity receiver. The limited frequency separation between frequency diversity and closely mounted antennas are major reasons for the correlated signals [8].

1.9 Organization of This Dissertation

This dissertation analyzes the error rates of a variety of wireless digital techniques over fading channels with particular emphasis on the differential phase shift keying (DPSK) systems. The primary goals of this present work are: first, we develop a useful framework to analyze the error rates of digital techniques over fading channels. This framework is based on the integral definition of the associated Legendre functions. Second, it is intended to propose and analyze a reduced-complexity and low-cost multiple-input multiple-output (MIMO) system for wireless communications. The proposed structure is based on differential phase shift keying (DPSK) system with MIMO employing EGC receive diversity. Third, we also aim to simplify and generalize the previous results of the error rates of wireless communication techniques over independent and correlated fading without resorting to approximations. Fourth, we plan to study the impacts of fading correlation on the performance of DPSK systems, and imperfect phase recovery on the performance of PSK systems. From practical point of view, this research study is

expected to be helpful in the design of the practical radio communication receivers. The main results of the present work are explained below.

This research starts with a study of the DPSK systems over independent and correlated fading channels in Chapter two. Focus was placed on the performance of differentially coherent reception techniques as they have gained an increased importance in digital communication systems [12]. The reasons behind this increased importance can be summarized as follows: first, the noncoherent receptions of PSK systems avoid the need for carrier recovery, and therefore achieve fast synchronization. Second, unlike the coherent receivers, differential coherent systems are capable to resolve the phase ambiguity of $2\pi/M$, where M is the constellation size. Third, the receiver implementation in case of differential systems is simpler than coherent receivers. For these reasons, the American and Japanese digital cellular standards suggest differential quaternary phase shift keying (DQPSK) as the modulation of choice for the current digital mobile communication systems [13]. In Chapter two, we analyze the performance of differential binary and quaternary phase shift keying (DBPSK and DQPSK respectively) with diversity reception over independent and correlated Nakagami-m and Rician fading channels. The average bit error probability (BEP) of DBPSK and DQPSK are derived with two major schemes of diversity reception: predetection with MRC and postdetection with EGC. The average BEP of DPSK with diversity reception over independent fading channels has been studied extensively in the literature [2],[14], [15]. For example, Simon and Alouini have presented a moment generating function (MGF)-based approach to analyze the average BEP for coherent, differential coherent, and noncoherent modulation formats over several fading channels [3],[15]. In [15], the authors used an alternative form of the Marcum Q-function to reach BEP expressions, which involve a single finite-range integral. In general, the average BEP of DQPSK over independent fading channels can be expressed as either infinite-series expression or as a single finite-range integral. The independent

assumption of diversity reception can simplify the performance analysis of the DPSK systems. As a result of that, these studies may fail to reflect the real penalty due to the fading environment. The effect of correlated channel fading on the performance of DPSK systems has been considered by many authors, for example [16],[17], and [18] to name a few. Ma and Lim in [16], analyzed the average BEP of DBPSK and DQPSK over arbitrarily correlated Rician fading channels. Their approach is based on evaluating the probability of being the demodulator's decision statistic smaller than zero (half-plane decision technique), however, the average BEP of DBPSK and DQPSK is given in terms of triple sums (the middle summation is infinite whereas the outer and inner summations are finite). Ma and Zhang presented a double finite-range integral expression for the error probability of M-ary DPSK in [17]. In [18], the authors have presented an infinite-series of a finite-range integral for the average BEP of DQPSK with EGC over arbitrarily correlated Nakagami-m fading channels. In this Chapter, we present two approaches to analyze the average BEP of DQPSK systems over fading channels. The first approach relies on the integral definition of the associated Legendre functions, which can lead to finite-series closed-form expressions for the average BEP of DQPSK over L independent Rayleigh and Nakagami-m, when the product Lm is integer, fading channels. In the second approach, we propose a finite sum of a finite-range integral for the average BEP of DQPSK with EGC over arbitrarily Nakagami-m and Rician fading channels. In addition to presenting the associated Legendre functions approach, the novelty of the results in Chapter two lies in presenting relatively simple-to-numerically evaluates BEP expressions for the average BEP of DQPSK over independent and correlated fading channels. Besides, a finite-series closed-form expression is given for the average BEP of differential binary phase shift keying (DBPSK) with EGC over independent Rician fading channels. It is observed that the performance degradation due to the correlation among the di-

versity branches in Rician fading channels is severer than that in Nakagami-m fading channels as a result of the presence of the specular component.

In Chapter three, we propose and analyze a reduced-complexity and low-cost DPSK system with MIMO employing EGC diversity reception. Multiple-transmit multiple-receive antenna systems can introduce additional system performance improvement relative to the system with receiver diversity and single transmit antenna. Having a perfect channel state information (CSI) at both the transmitter and the receiver, MIMO with MRC (MIMO MRC) can be realized by transmitting in the direction of the eigenvector corresponding to the largest eigenvalue of the channel, which leads to attain the maximum signal to noise ratio (SNR) at the receiver [19]. Performance analysis of MIMO MRC has been conducted by several authors [20],[21],[22],[23]. All previous studies tackled the performance of MIMO MRC systems, which require a perfect knowledge of the CSI at both the transmitter and the receiver sides, leading to increased system complexity and cost. Because of the limitations on the size, cost, and complexity of the receiver unit, (for example the mobile unit in the downlink case), the design of reduced-complexity and low-cost receivers for MIMO systems, which still keeps much of the advantages and benefits of the full-complexity MIMO system, is of great concern to the researchers and engineers. A promised approach to achieve this goal without considerable prejudice to performance quality, is to employ DPSK techniques. In DPSK system with MIMO employing EGC (MIMO EGC), the signal processing is performed at the transmitter (or base station) with the receiver (mobile unit) having a simplified structure that requires only limited signal processing. Moreover, MIMO EGC has much simpler amplifier requirements than MIMO MRC, since it does not require the antenna amplifiers to modify the amplitudes nor the phases of the received signals. In this Chapter, we consider DPSK systems with MIMO EGC diversity reception that require only knowing the CSI at the transmitter side. The objective of this Chapter is to present the proposed structure of DPSK with

MIMO employing EGC receive diversity system and analyze its performance in terms of the average bit error probability (BEP). To the best of our knowledge, this is the first study that analyzes the error rates of DPSK systems with MIMO EGC diversity.

In Chapter four, we present another useful utilization of the associated Legendre functions approach. In this Chapter, the associated Legendre functions approach is devoted to analyze the performance of coherent PSK systems over fading channels in the presence of imperfect phase recovery. Coherent reception techniques require a perfect knowledge of the carrier's phase [2]. The receiver can estimate the carrier's phase using either a suppressed carrier-tracking loop or a pilot tone [24]. Due to thermal noise, which is present in the recovery circuit, and due to the multipath channel fading, the estimation process results in a residual carrier phase error, this situation is denoted by partially coherent reception [25]. Imperfect phase recovery can introduce a severe system performance degradation. Thus, many research studies have been conducted to analyze the performance coherent PSK systems with imperfect phase recovery [26],[27],[28]. However, there are very limited analytical results about the impact of fading channels on the performance of PSK systems with imperfect phase recovery [29],[30],[31], [32]. These studies are either limited to Rayleigh fading channels [29] or based on some kind of approximations [30],[31], [32]. By contrast, Chapter four presents an evaluation (without any kind of approximation) for the average BEP of the PSK systems with imperfect phase recovery. Moreover, using Fourier series expansion and associated Legendre functions, the exact average BEP of the binary and quaternary phase shift keying (BPSK and QPSK respectively) on a single channel (no diversity) in the presence of different kinds of slow fading channels (Rayleigh, Nakagami-m, and Rician), phase recovery error, and additive white Gaussian noise (AWGN) has been evaluated. The detection loss and phase precision for both of BPSK and QPSK have been calculated. The series expressions

of the average BEP proposed in our study are found to be convergent with reasonable number of terms.

In Chapter five, we turn our attention onto the performance of the square M-ary quadrature amplitude modulation (MQAM) with maximal ratio combining (MRC) receive diversity. The average SEP of MQAM over Nakagami-m has been studied by many authors [33], [34]. In [33], the average SEP of MQAM is given in terms of a single finite-range integral. The authors in [34] proposed closed-form expressions for the average SEP of MQAM over independent Nakagami-m fading channels with integer fading index m. In contrast, this Chapter presents closed-form expressions for the average SEP of MQAM with arbitrarily fading index m. Two models of MQAM receivers are analyzed. Closed-form expressions are provided for the average SEP in terms of the Appell and Gauss hypergeometric functions. Simplified error expressions are proposed when the product Lm is either integer or half integer. The distinction between the performance of the two MQAM schemes is discussed. In addition to that, our analysis is extended to include the performance of MQAM over equal-correlated Nakagami-m fading.

Finally, Chapter five summarizes the dissertation and discusses future areas of research.

CHAPTER 2

DPSK WITH RECEIVE DIVERSITY RECEPTION

In this Chapter, the average bit error probability (BEP) of differential phase shift keying (DPSK) is analyzed over independent and correlated Nakagami-m and Rician fading channels. Particular emphasis is placed on the performance of differential quaternary phase shift keying (DQPSK). The average BEP of DPSK is demonstrated with two major schemes of diversity reception: predetection with maximal ratio combining (MRC) and postdetection with equal gain combining (EGC). Finite closed-form expressions for the average BEP of differential binary phase shift keying (DBPSK) over independent Rician fading channels and for the average BEP of DQPSK over L independent Nakagami-m fading channels, when the product Lm is integer, are presented. The error expressions of DQPSK over arbitrarily correlated fading channels are given in terms of a finite-sum of a finite-range integral. The penalty in signal to noise ratio (SNR) due to arbitrarily correlated channel fading is investigated. It is observed that the performance degradation due to the correlation among the diversity branches in Rician fading channels is severer than that in Nakagami-m fading channels as a result of the presence of the specular component. The distinction between the performance of predetection and postdetection diversity combining of DPSK systems is expalined. Finally, the accuracy of the results is verified by computer simulation.

2.1 Introduction

The average BEP of differential phase shift keying (DPSK) systems over additive white Gaussian noise (AWGN) has been studied extensively in the literature. Starting with the pioneering work of Proakis in multichannel reception [2]. Proakis has addressed the average BEP of differentially coherent reception of diversity signal transmission. Moreover, closed-form expression for the average BEP of differential binary phase shift keying (DBPSK) with equal gain combining (EGC) over L independent Rayleigh fading channels has been provided. Weng and Leung in [14] provide a new closed-form expression for the BEP of DBPSK with postdetection EGC diversity over Nakagami-m fading channels. Recently, Simon and Alouini have presented a moment generating function (MGF)-based approach to analyze the average BEP for coherent, differential coherent, and noncoherent modulation formats over several fading channels [3],[15]. In [15], the authors used alternative form of the Marcum Q-function to reach BEP expressions, which involve a single finite-range integral. The previous studies tackled the performance of DPSK systems with diversity combining schemes operating in mutually independent branch fading environments. The effect of correlated fading channels on the performance of DPSK systems has been considered by many authors [35],[36],[37],[38], [16], [17], and [18]. Ma and Lim in [16], analyzed the average BEP of DBPSK and DQPSK over arbitrarily correlated Rician fading channels. Their approach is based on evaluating the probability of being the demodulator's decision statistic smaller than zero (half-plane decision technique), however, the average BEP of DBPSK and DQPSK is given in terms of triple sums (the middle summation is infinite whereas the outer and inner summations are finite). Ma and Zhang presented a double finite-range integral expression for the error probability of M-ary DPSK in [17]. In [18], the authors have presented an infinite-series of a finite-range integral for the average BEP of DQPSK

with EGC over arbitrarily correlated Nakagami-m fading channels. In this Chapter, we present two approaches to analyze the average BEP of DQPSK over fading channels. The first approach relies on the integral definition of the associated Legendre functions, which can lead to finite-series closed-form expressions for the average BEP of DQPSK over L independent Rayleigh and Nakagami-m, when the product Lm is integer, fading channels. In the second approach, we propose a finite sum of a finite-range integral for the average BEP of DQPSK with EGC over arbitrarily Nakagami-m and Rician fading channels. To the best of our knowledge, the exact average BEP of DQPSK over correlated fading channels is expressed (in the literature) as a double infinite series, twofold integral, or as an infinite sum of a finite range integral. In this chapter, we first derive the average BEP of DBPSK and DQPSK with diversity reception over equal-correlated Nakagami-m and independent Rician fading channels. Derivation the average BEP of DQPSK is achieved using the associated Legendre approach, which relies on the integral definition of the associated Legendre functions. This approach can lead to finite-series closed-form expressions for the average BEP of DQPSK over L independent Rayleigh and Nakagami-m, when the product Lm is integer, fading channels. Second, we propose a finite sum of a finite-range integral for the average BEP of DQPSK with EGC over arbitrarily Nakagami-m and Rician fading channels. The problem is formulated in section 2.2. Section 2.3 clarifies the conditional average BEP of DBPSK and DQPSK. In section 2.4, the average BEP of DBPSK and DQPSK over equal-correlated Nakagami-m is obtained once for predetection MRC and second for postdetection EGC by averaging the conditional probability over the probability density function (pdf) of the total signal to noise ratio (SNR) per bit at the combiner output. In section 2.5, we derive the BEP of DBPSK and DQPSK over independent Rician fading for both of the predetection and postdetection combining. Section 2.6 introduces an alternative approach for evaluating

the average BEP of DQPSK over arbitrarily correlated fading channles. Results are discussed in section 2.7. Finally, concluding remarks are presented in section 2.8.

2.2 System Model

DPSK modulation schemes are characterized by the fact that the information sequence is contained in the phase difference of the received carrier between two successive signaling intervals. The low-pass representation of the transmitted signal during the ith signalling interval can be expressed as:

$$s_i(t) = \begin{cases} u_M(t)\exp(\jmath\ \theta_i), & 0 \le t \le T \\ 0, & \text{elsewhere} \end{cases} \tag{2.1}$$

where $u_M(t)$ is the pulse shaping signal and it is assumed to be constant during the pulse interval T (rectangular shaping pulse) and it has the following form

$$u_M(t) = \begin{cases} \sqrt{\frac{2E_s}{T}}, & 0 \le t \le T \\ 0, & \text{elsewhere} \end{cases} \tag{2.2}$$

in which $E_s = E_b \log_2 M$ is the symbol energy and E_b is the bit energy. The modulation phase θ_i is chosen such that the relative phase difference $\triangle\theta_i = \theta_i - \theta_{i-1}$ belongs to $\{0, \pi\}$ in case of DBPSK and $\{-3\pi/4, -\pi/4, \pi/4, 3\pi/4\}$ in case of DQPSK.

The low-pass equivalent of the ith received signal on the ℓth channel is given by

$$r_{i,\ell}(t) = \alpha_\ell u_M(t)\exp[\jmath\ (\theta_i + \ \varphi_\ell)\ ] + n_\ell(t) \tag{2.3}$$

where φ_ℓ is a random phase shift introduced by the ℓth channel, which is uniformly distributed between $[-\pi, \pi]$. The additive noise term $n_\ell(t)$ represents the zero mean complex-valued Gaussian noise, and it has a single-sided power spectral density of $2N_0$ W/Hz. All noise terms are assumed to be mutually statistically independent. The fading amplitude α_ℓ is due to the time-variant multipath characteristics on the ℓth channel.

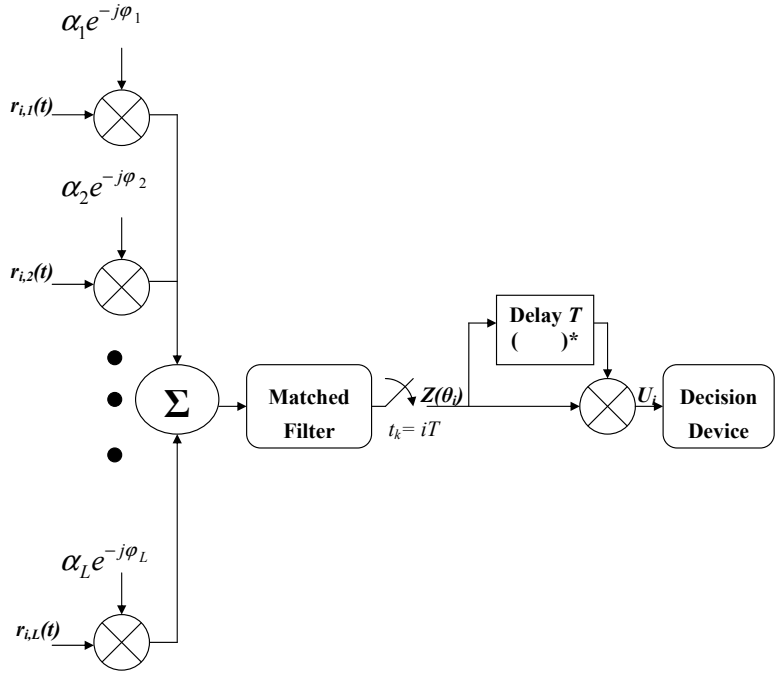

Figure 2.1. DPSK receiver with predetection MRC diversity, where $(\ )^*$ denotes the complex conjugate.

The channel parameters α_ℓ and φ_ℓ are assumed to be slowly varying, so that they can be considered constant over two consecutive signaling intervals.

2.2.1 Predetection combining

Figure 2.2 shows the block diagram of a DPSK receiver with predetection MRC diversity. In predetection combining, the received signals are combined coherently before they are detected. The output of the matched filter $Z(\theta_i)$ is

$$Z(\theta_i) = 2E_s \exp(\jmath\ \theta_i) \sum_{\ell=1}^{L} \alpha_\ell^2 + v \tag{2.4}$$

where the noise term v is given by

$$\begin{aligned} v &= \sum_{\ell=1}^{L} \alpha_\ell \exp(-\jmath\ \varphi_\ell) \int_0^T n_\ell(t) u_M(t) dt \\ &= v_I + \jmath\ v_Q \end{aligned} \tag{2.5}$$

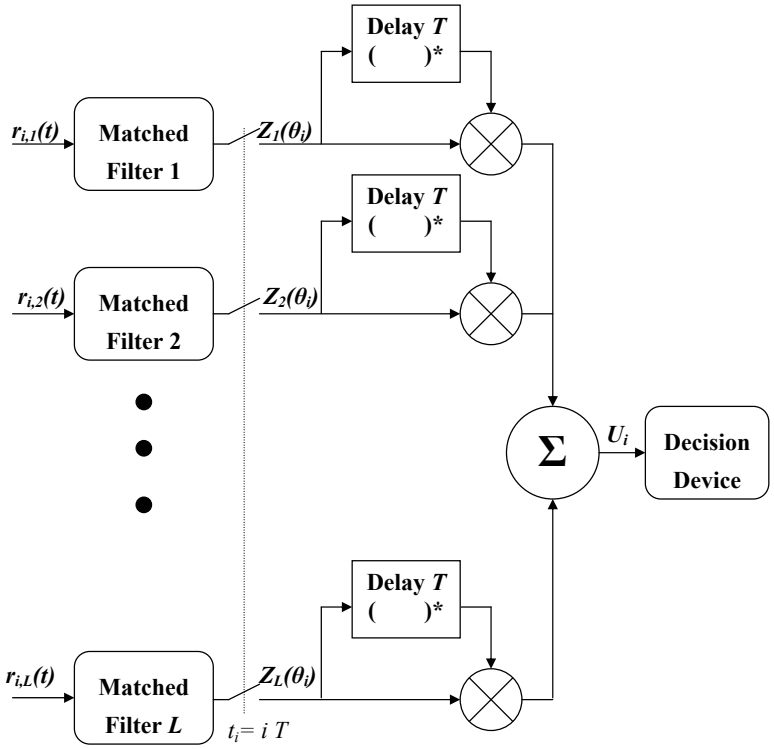

Figure 2.2. DPSK receiver with postdetection EGC diversity.

where v_I and v_Q are zero mean Gaussian-distributed random processes with equal variances

$$\sigma_{v_I}^2 = \sigma_{v_Q}^2 = 2E_s N_0 \sum_{\ell=1}^{L} \alpha_\ell^2 \tag{2.6}$$

After sampling, the combined signal is multiplied with the complex conjugate of the previous sample. The input to the decision device U_i is

$$U_i = Z(\theta_i) Z^*(\theta_{i-1}) \tag{2.7}$$

where $(\ )^*$ denotes the complex conjugate.

2.2.2 Postdetection combining

In predetection combining diversity receiver, the signals have to be combined coherently before detection, but this requirement requires a phase estimation which in turn

will increase the complexity and the cost of the receiver. In addition to that, since the channel phase is required to be estimated, then the designer might choose coherent detection schemes to achieve better performance. Postdetection combiner offers a trade off between the receiver complexity and performance. In postdetection combiner, the received signals are detected before combining takes place in the baseband region. Figure 2.2 shows the block diagram of a DPSK receiver with postdetection EGC diversity. The output of the matched filter for the ℓth channel is given by

$$Z_\ell(\theta_i) = 2E_s\alpha_\ell \exp[\jmath\ (\theta_i + \ \varphi_\ell)\ ] + v_\ell,\ i = 1, 2, \ldots, M \tag{2.8}$$

where the noise term v_ℓ is given by

$$\begin{aligned} v_\ell &= \int_0^T n_\ell(t) u_M(t) dt \\ &= v_{\ell,I} + \jmath\ v_{\ell,Q} \end{aligned} \tag{2.9}$$

and it can be shown that $v_{\ell,I}$ and $v_{\ell,Q}$ are zero mean Gaussian-distributed random processes with equal variances

$$\sigma^2_{v_{\ell,I}} = \sigma^2_{v_{\ell,Q}} = 2E_sN_0 \tag{2.10}$$

The decision variable U_i at the output of the postdetection combiner (shown in Fig.2) can be written as

$$U_i = \sum_{\ell=1}^{L} Z_\ell(\theta_i) Z^*_\ell(\theta_{i-1}) \tag{2.11}$$

2.3 Conditional Probability

In [2], [39], and [40], Proakis analyzed the performance of matched filter reception of M-phase signals, and he gave formulas for the bit error expressions of binary and quaternary phase shift keying (BPSK and QPSK respectively) in which the demodulator's decision statistic is in the form $\Sigma_{k=1}^{L} X_k Y_k^*$, where X_k is the sampled output of the matched filter on the kth branch and Y_k is the estimate of the kth channel's gain and phase shift.

Both of X_k and Y_k were assumed to be uncorrelated Gaussian random variables with nonzero means. Since the decision variable U_i at the output of the combiner is equivalent to $\Sigma_{k=1}^{L} X_k Y_k^*$, Proakis analysis can be extended to the differential detection techniques. The conditional BEP (on the fading power) of DBPSK and DQPSK with Gray coding for both of the diversity schemes, can be written in terms of the generalized Marcum Q-function ($Q_\ell(.,.)$) [3],[15]

$$\begin{aligned} P(e|\gamma_t) =& Q_1(a\sqrt{\gamma_t}, b\sqrt{\gamma_t}) - \exp\left[-\frac{(a^2+b^2)\gamma_t}{2}\right] I_0(ab\gamma_t) \left[1 - \frac{\sum_{\ell=0}^{L-1} \binom{2L-1}{\ell} \eta^\ell}{(1+\eta)^{2L-1}}\right] \\ &+ \frac{1}{(1+\eta)^{2L-1}} \sum_{\ell=2}^{L} \binom{2L-1}{L-\ell} \eta^{L-\ell} \left\{Q_\ell(a\sqrt{\gamma_t}, b\sqrt{\gamma_t}) - Q_1(a\sqrt{\gamma_t}, b\sqrt{\gamma_t})\right\} \\ &- \frac{1}{(1+\eta)^{2L-1}} \sum_{\ell=2}^{L} \binom{2L-1}{L-\ell} \eta^{L-1+\ell} \left\{Q_\ell(b\sqrt{\gamma_t}, a\sqrt{\gamma_t}) - Q_1(b\sqrt{\gamma_t}, a\sqrt{\gamma_t})\right\} \end{aligned} \tag{2.12}$$

where the last two summations contribute only for the BEP expression of postdetection combining, γ_t is the total conditional SNR per bit and it is defined as

$$\gamma_t = \frac{E_b}{N_0} \sum_{\ell=1}^{L} \alpha_\ell^2 = \sum_{\ell=1}^{L} \gamma_\ell \tag{2.13}$$

$Q_\ell(.,.)$ is defined as [41]

$$\begin{aligned} Q_\ell(x,y) &= \exp\left(-\frac{x^2+y^2}{2}\right) \sum_{k=1-\ell}^{\infty} \left(\frac{x}{y}\right)^k I_k(xy), \ \text{x<y} \\ &= 1 - \exp\left(-\frac{x^2+y^2}{2}\right) \sum_{k=\ell}^{\infty} \left(\frac{y}{x}\right)^k I_k(xy), \ \text{x}\geq\text{y} \end{aligned} \tag{2.14}$$

and $I_n(.)$ denotes the nth-order modified Bessel function of the first kind, and the other parameters are defined as

$$\binom{2L-1}{L-\ell} = \frac{(2L-1)!}{(L-\ell)!(L+\ell-1)!}$$

$a = 0,\ b = \sqrt{2},\quad \eta = 1$ for DBPSK, and $a = \sqrt{2-\sqrt{2}},\ b = \sqrt{2+\sqrt{2}},\quad \eta = 1$ for DQPSK.

For predetction combining, the conditional average BEP of DBPSK can be reduced to [35]-[36]

$$P_2(e|\gamma_t) = \frac{1}{2}\exp(-\gamma_t) \tag{2.15}$$

and the average conditional BEP for DQPSK with Gray coding can be expressed as

$$P_4(e|\gamma_t) = \exp(-2\gamma_t)\sum_{k=0}^{\infty} c_k \left(\sqrt{2}-1\right)^k I_k\left(\sqrt{2}\gamma_t\right) \tag{2.16}$$

where

$$c_k = \begin{cases} 0.5, & k = 0 \\ 1, & k \neq 0 \end{cases}$$

In postdetection combining diversity, the conditional BEP of DBPSK takes the form

$$P_2(e|\gamma_t) = \frac{\exp(-\gamma_t)}{2^{2L-1}}\sum_{\ell=0}^{L-1}\gamma_t^{\ell} h_\ell, \quad h_\ell = \frac{1}{\ell!}\sum_{k=0}^{L-1-\ell}\binom{2L-1}{k} \tag{2.17}$$

and the average conditional BEP for DQPSK with Gray coding is

$$P_4(e|\gamma_t) = e^{-2\gamma_t}\left\{\sum_{k=0}^{\infty} c_k(\sqrt{2}-1)^k I_k(\sqrt{2}\gamma_t) + \frac{1}{2^{2L-1}}\sum_{\ell=2}^{L}\binom{2L-1}{L-\ell}\sum_{k=1}^{\ell-1} D_k I_k(\sqrt{2}\gamma_t)\right\} \tag{2.18}$$

where $D_k = (\sqrt{2}+1)^k - (\sqrt{2}-1)^k$.

2.4 Equal-Correlated Nakagami-m Channel Fading

If the channel fades α_ℓ's on all the channels are assumed to be frequency-nonselective, slowly varying, and Nakagami-m distributed. The pdf of α_ℓ can be written as [4]

$$f_{\alpha_\ell}(\alpha_\ell) = \frac{2m_\ell^{m_\ell}\alpha_\ell^{2m_\ell-1}}{\Omega_\ell^{m_\ell}\Gamma(m_\ell)}\exp\left(-\frac{m_\ell\alpha_\ell^2}{\Omega_\ell}\right), \quad \alpha_\ell \geq 0 \tag{2.19}$$

where $\Gamma(.)$ is the Gamma function and m_ℓ is the Nakagami-m fading parameter for the ℓth branch, which ranges from 0.5 to ∞ , and Ω_ℓ is the mean of α_ℓ^2.

In many real-life applications, it is difficult to achieve independent signals and branches on the diversity receiver as a result of the physical constraint on the antenna spacing [36]. In equal-correlated Nakagami-m fading, the power correlation between any two fading envelopes is assumed to be constant and it is given by

$$\lambda = \frac{\mathrm{cov}(\alpha_i^2, \alpha_j^2)}{\sqrt{\mathrm{var}(\alpha_i^2)\mathrm{var}(\alpha_j^2)}}, \quad i \neq j, \quad i, j = 1, 2, \cdots, L \tag{2.20}$$

Assuming the fades α_ℓ's on all the channels are identically distributed ($m_\ell = m$ and $\Omega_\ell = \Omega, \forall \ell \in \{1, 2, ..., L\}$), then the pdf of the total conditional SNR γ_t can be expressed as [36] and [42]

$$f_{\gamma_t}(\gamma_t) = \frac{m^{Lm}\gamma_t^{Lm-1}\exp\left(-\frac{m\gamma_t}{\bar{\gamma}(1-\rho)}\right)}{\bar{\gamma}^{Lm}(1-\rho)^{m(L-1)}(1-\rho+L\rho)^m\Gamma(Lm)}\ {}_1F_1\left(m; Lm; \frac{Lm\rho\gamma_t}{\bar{\gamma}(1-\rho)(1-\rho+L\rho)}\right) \tag{2.21}$$

where $\rho = \sqrt{\lambda}$, $\gamma_t \geq 0$, and $\bar{\gamma} = \frac{\Omega E_b}{N_0}$ is the average SNR per bit per branch, and ${}_1F_1(x; y; z)$ is the confluent hypergeometric function [6]. It should be pointed out that ρ is the correlation coefficient between the accompanying Gaussian process that are used to generate the Nakagami-m random variables at the input of the L-branch receiver [43].

Aalo in [36] has given an expression for the average BEP of DBPSK with predetection combining as

$$P_2(e) = \frac{1}{2}\left(\frac{m^L}{(m+\bar{\gamma}(1-\rho+L\rho))(m+\bar{\gamma}(1-\rho))^{L-1}}\right)^m \tag{2.22}$$

The average BEP of DQPSK with predetection combining is

$$\begin{aligned} P_4(e) =& \frac{m^{Lm}\exp(-\jmath\pi[Lm+1])}{(\sqrt{2}\bar{\gamma})^{Lm}(1-\rho)^{m(L-1)}(1-\rho+L\rho)^m}\sum_{k=0}^{\infty}\frac{(-1)^k(m)_k(Lm\rho)^k}{k!(Lm)_k[\sqrt{2}\bar{\gamma}(1-\rho)(1-\rho+L\rho)]^k} \\ &\times \frac{1}{\Gamma(Lm)}\sum_{i=0}^{\infty}\frac{c_i(\sqrt{2}-1)^i Q_{i-\frac{1}{2}}^{k+Lm-\frac{1}{2}}(z_1)}{\sqrt{\frac{-\pi}{2}}\,(z_1^2-1)^{\frac{1}{2}(k+Lm-\frac{1}{2})}} \end{aligned} \tag{2.23}$$

where $z_1 = \sqrt{2} + \frac{m}{\sqrt{2}(1-\rho)\bar{\gamma}}$, $(x)_k = \frac{\Gamma(x+k)}{\Gamma(k)}$, and we have used the fact that [44]

$$Q_\nu^\mu(z) = \sqrt{\frac{\pi}{2}}(z^2-1)^{\frac{\mu}{2}} \int_0^\infty \exp(-tz + \jmath\mu\pi) I_{\nu+\frac{1}{2}}(t) t^{\mu-\frac{1}{2}} dt \tag{2.24}$$

provided that $\mathrm{Re}(\nu+\mu) > -1, \mathrm{Re}(z) > 1$. $Q_\nu^\mu(.)$ is the associated Legendre function of the second kind with order μ and degree ν. In the literature, there are many algorithms to compute the associated Legendre functions when the absolute value of the argument is less than one, but there are few techniques (for certain values of the order and degree) to compute the associated Legendre functions when the argument is greater than one [45]-[46],[47]-[48]. In Appendix A, we address an efficient recursive algorithm to evaluate the associated Legendre function of the first and second kinds.

The average BEP of DQPSK with predetection combining under uncorrelated Nakagami-m channel fading ($\rho = 0$) is

$$P_4(e) = \frac{m^{Lm}\exp(-\jmath\,\pi[Lm-\frac{1}{2}])}{\sqrt{\frac{\pi}{2}}(\sqrt{2}\bar{\gamma})^{Lm}\Gamma(Lm)(z_{11}^2-1)^{\frac{1}{2}(Lm-\frac{1}{2})}} \sum_{k=0}^{\infty} c_k(\sqrt{2}-1)^k Q_{k-\frac{1}{2}}^{Lm-\frac{1}{2}}(z_{11}) \tag{2.25}$$

where $z_{11} = \sqrt{2} + \frac{m}{\sqrt{2}\bar{\gamma}}$.

For the postdetection combining, the average BEP of DBPSK can be shown to be

$$\begin{aligned} P_2(e) =& \frac{(1-\rho)^m}{(m+\bar{\gamma}(1-\rho))^{Lm}(1-\rho+L\rho)^m\Gamma(Lm)} \frac{m^{Lm}}{2^{2L-1}} \sum_{\ell=0}^{L-1} \frac{h_\ell \Gamma(Lm+\ell)(\bar{\gamma}(1-\rho))^\ell}{(m+\bar{\gamma}(1-\rho))^\ell} \\ & \times\ {}_2F_1(m, Lm+\ell; Lm; z_2) \end{aligned} \tag{2.26}$$

where ${}_2F_1(w,x;y;z)$ is the Gaussian hypergeometric function [6], and z_2 is

$$z_2 = \frac{Lm\rho}{(1-\rho+L\rho)(m+\bar{\gamma}(1-\rho))}$$

The average BEP of DQPSK is given by

$$P_4(e) = \frac{m^{Lm}\exp(-\jmath\pi[Lm+1])}{(\sqrt{2}\bar{\gamma})^{Lm}(1-\rho)^{m(L-1)}(1-\rho+L\rho)^m}\sum_{k=0}^{\infty}\frac{(-1)^k(m)_k(Lm\rho)^k}{k!(Lm)_k[\sqrt{2}\bar{\gamma}(1-\rho)(1-\rho+L\rho)]^k} \times \frac{1}{\Gamma(Lm)}\left\{\sum_{i=0}^{\infty}\frac{c_i(\sqrt{2}-1)^i Q_{i-\frac{1}{2}}^{k+Lm-\frac{1}{2}}(z_1)}{\sqrt{\frac{-\pi}{2}}\,(z_1^2-1)^{\frac{1}{2}(k+Lm-\frac{1}{2})}} + \sum_{\ell=2}^{L}\frac{\binom{2L-1}{L-\ell}}{2^{(2L-1)}}\sum_{i=1}^{\ell-1}\frac{D_i Q_{i-\frac{1}{2}}^{k+Lm-\frac{1}{2}}(z_1)}{(z_1^2-1)^{\frac{1}{2}(k+Lm-\frac{1}{2})}}\right\} \tag{2.27}$$

and the average BEP of DQPSK in the case of zero power correlation between the L branches is

$$P_4(e) = \frac{m^{Lm}\exp(-\jmath\,\pi[Lm-\frac{1}{2}])}{\sqrt{\frac{\pi}{2}}(\sqrt{2}\bar{\gamma})^{Lm}\Gamma(Lm)\,(z_{11}^2-1)^{\frac{2Lm-1}{4}}}\left\{\sum_{k=0}^{\infty}c_k(\sqrt{2}-1)^k Q_{k-\frac{1}{2}}^{Lm-\frac{1}{2}}(z_{11}) + \frac{1}{2^{2L-1}}\sum_{\ell=2}^{L}\binom{2L-1}{L-\ell}\sum_{k=1}^{\ell-1}D_k Q_{k-\frac{1}{2}}^{Lm-\frac{1}{2}}(z_{11})\right\} \tag{2.28}$$

The infinite series expressions for the average BEP of DQPSK over L independent Nakagami-m fading channels can be reduced to finite expressions when the product Lm is integer. This implies that $P_4(e)$ can be provided in a finite-series closed-form expression whenever the product Lm is integer. This case includes integer fading index and many more cases such as $(m = 0.5, L = 2), (m = 0.75, L = 4)$. For the particular case of Rayleigh fading, it can be shown (using equation (A4) in Appendix A) that the average BEP of DQPSK with postdetection EGC over a single channel is

$$P_4(e) = \frac{1+\bar{\gamma}(4-\sqrt{2})+\sqrt{1+4\bar{\gamma}+2\bar{\gamma}^2}}{2\sqrt{1+4\bar{\gamma}+2\bar{\gamma}^2}(1+\bar{\gamma}\,\sqrt{2}+\sqrt{1+4\bar{\gamma}+2\bar{\gamma}^2})} \tag{2.29}$$

which is equivalent to the result reported by Tellambura and Bhargava in [49], namely,

$$P_4(e) = \frac{1}{2}\left(1-\frac{\sqrt{2}\bar{\gamma}}{\sqrt{1+4\bar{\gamma}+2\bar{\gamma}^2}}\right) \tag{2.30}$$

the average BEP of dual-branch DQPSK with postdetection EGC is

$$P_4(e) = \frac{1}{2\bar{\gamma}^2(z_{11}^2-1)^{\frac{3}{2}}}\left\{\frac{1}{4}-\frac{z_{11}}{2}+\frac{\sqrt{z_{11}^2-1}(\sqrt{2}-1)(z_{11}+\sqrt{z_{11}^2-1})}{(z_{11}+\sqrt{z_{11}^2-1}+1-\sqrt{2})^2} + \frac{z_{11}(z_{11}+\sqrt{z_{11}^2-1})}{(z_{11}+\sqrt{z_{11}^2-1}+1-\sqrt{2})}\right\} \tag{2.31}$$

where z_{11} is defined in (3.25). The average BEP of triple-branch DQPSK is

$$\begin{aligned}P_4(e) =&\frac{1}{2\sqrt{2}\bar{\gamma}^3}\left\{\frac{3z_{11}}{(z_{11}^2-1)}\left(\frac{z_{11}(z_{11}+\sqrt{z_{11}^2-1})}{(z_{11}^2-1)^{\frac{3}{2}}(z_{11}+\sqrt{z_{11}^2-1}+1-\sqrt{2})}\right.\right.\\&\left.+\frac{(\sqrt{2}-1)(z_{11}+\sqrt{z_{11}^2-1})}{(z_{11}^2-1)(z_{11}+\sqrt{z_{11}^2-1}+1-\sqrt{2})^2}\right)-\frac{z_{11}+\sqrt{z_{11}^2-1}}{(z_{11}^2-1)^{\frac{3}{2}}(z_{11}+\sqrt{z_{11}^2-1}+1-\sqrt{2})}\\&+\frac{(\sqrt{2}-1)(z_{11}+\sqrt{z_{11}^2-1}+\sqrt{2}-1)(z_{11}+\sqrt{z_{11}^2-1})}{(z_{11}+\sqrt{z_{11}^2-1}+1-\sqrt{2})^3(z_{11}^2-1)^{\frac{3}{2}}}-\frac{1+2z_{11}^2}{2(z_{11}^2-1)^{\frac{5}{2}}}\\&\left.+\frac{1}{32(z_{11}^2-1)^{\frac{5}{2}}}\left(\frac{12\sqrt{2}(z_{11}^2-1)}{(z_{11}+\sqrt{z_{11}^2-1})^2}+36z_{11}+\frac{12\sqrt{2}z_{11}(z_{11}+2\sqrt{z_{11}^2-1})}{(z_{11}+\sqrt{z_{11}^2-1})^2}\right)\right\}\end{aligned} \tag{2.32}$$

2.5 Statistically Independent Rician (Channel Fading

In Rician fading environment, the pdf of α_ℓ is given by [5]

$$f_{\alpha_\ell}(\alpha_\ell)=\frac{2(1+K_\ell)\alpha_\ell}{\Omega_\ell}\exp\left(-\frac{(1+K_\ell)\alpha_\ell^2+\Omega_\ell K_\ell}{\Omega_\ell}\right)I_0\left(2\alpha_\ell\sqrt{\frac{K_\ell(1+K_\ell)}{\Omega_\ell}}\right),\qquad \alpha_\ell\geq 0 \tag{2.33}$$

where K_ℓ is the Rician fading parameter, which ranges from 0 to ∞, and Ω_ℓ is the mean squared of α_ℓ. The fading power α_ℓ^2 has a non-central Chi-square distribution with two degrees of freedom and γ_t is also a non-central Chi-square with $2L$ degrees of freedom. It can be shown that the pdf of γ_t is given by [2]

$$\begin{aligned}f_{\gamma_t}(\gamma_t)=&\frac{(L+K_t)^{\frac{L+1}{2}}}{\bar{\gamma_t}^{\frac{L+1}{2}}}\frac{\gamma_t^{\frac{L-1}{2}}}{K_t^{\frac{L-1}{2}}}\exp\left(-\frac{(L+K_t)\gamma_t}{\bar{\gamma_t}}\right)\exp(-K_t)I_{L-1}\left(2\sqrt{\frac{K_t(L+K_t)\gamma_t}{\bar{\gamma_t}}}\right)\\&\gamma_t\geq 0,\qquad K_t=\sum_{\ell=1}^{L}K_\ell,\qquad \bar{\gamma_t}=\frac{E_b}{N_0}\sum_{\ell=1}^{L}\Omega_\ell\end{aligned} \tag{2.34}$$

The average BEP of DBPSK with predetection combining is

$$P_2(e)=\frac{1}{2}\left(\frac{L+K_t}{L+K_t+\bar{\gamma_t}}\right)^L\exp\left(-\frac{K_t\bar{\gamma_t}}{K_t+L+\bar{\gamma_t}}\right) \tag{2.35}$$

and the average BEP of DQPSK with predetction combining is

$$P_4(e) = \frac{(L+K_t)^L}{\bar{\gamma_t}^L\ 2^{\frac{1}{2}(L-1)}} \sum_{k=0}^{\infty} \frac{(-1)^{L+k+1}(K_t(L+K_t))^k}{(\sqrt{2}\bar{\gamma_t})^k k!\Gamma(L+k)} \exp(-K_t) \sum_{i=0}^{\infty} \frac{c_i(\sqrt{2}-1)^i Q_{i-\frac{1}{2}}^{L+k-\frac{1}{2}}(z_3)}{\sqrt{-\pi}(z_2^3-1)^{\frac{1}{2}(L+k-\frac{1}{2})}} \tag{2.36}$$

where $z_3 = \frac{L+K_t+2\bar{\gamma_t}}{\sqrt{2}\bar{\gamma_t}}$, and we have used the fact [6]

$$I_m(x) = \left(\frac{x}{2}\right)^m \sum_{k=0}^{\infty} \frac{x^{2k}}{4^k k!\Gamma(m+k+1)} \tag{2.37}$$

In case of postdetection combining, the average BEP of DBPSK is

$$P_2(e) = \frac{(L+K_t)^L \exp(-K_t)}{(L+K_t+\bar{\gamma_t})^L \Gamma(L)} \sum_{\ell=0}^{L-1} \frac{\Gamma(L+\ell)\bar{\gamma_t}^\ell h_\ell}{(L+K_t+\bar{\gamma_t})^\ell} \frac{1}{2^{2L-1}}\ {}_1F_1\left(L+\ell; L; \frac{K_t(K_t+L)}{K_t+L+\bar{\gamma_t}}\right) \tag{2.38}$$

The average BEP of DBPSK in (2.38) can be reduced to finite-series closed-form expression. Equation (2.38) can be rewritten as

$$P_2(e) = \frac{(L+K_t)^L e^{(z_3-K_t)}}{(L+K_t+\bar{\gamma_t})^L 2^{2L-1}} \sum_{\ell=0}^{L-1} \frac{(L)_\ell\ h_\ell\ \bar{\gamma_t}^\ell}{(L+K_t+\bar{\gamma_t})^\ell} \sum_{j=0}^{\ell} \frac{(-\ell)_j(-z_3)^j}{(L)_j} \tag{2.39}$$

where $z_3 = K_t(K_t+L)/(K_t+L+\bar{\gamma_t})$, $(\delta)_j$ is the shifted factorial (Pochhammer symbol) [6], and we have used the fact that [6]

$${}_1F_1\left(a; b; z\right) = e^z\ {}_1F_1\left(b-a; b; -z\right) \tag{2.40}$$

Note that the result given in (2.39) is simpler than the error expression proposed in [50, eq. 7], since the later needs to precalculate the lookup table of the required enumerations, which becomes more complicated to find as L increases. The average BEP of DQPSK is

$$P_4(e) = \frac{(L+K_t)^L}{\bar{\gamma_t}^L 2^{\frac{1}{2}(L-1)}} \sum_{k=0}^{\infty} \frac{(-1)^{k+L+1}(K_t(L+K_t))^k}{k!\Gamma(L+k)(\sqrt{2}\bar{\gamma_t})^k} \exp(-K_t) \left\{ \sum_{i=0}^{\infty} \frac{c_i(\sqrt{2}-1)^i Q_{i-\frac{1}{2}}^{L+k-\frac{1}{2}}(z_3)}{\sqrt{-\pi}(z_2^3-1)^{\frac{1}{2}(L+k-\frac{1}{2})}} \right.$$
$$\left. + \sum_{\ell=2}^{L} \frac{\binom{2L-1}{L-\ell}}{2^{2L-1}} \sum_{i=1}^{\ell-1} \frac{D_i Q_{i-\frac{1}{2}}^{L+k-\frac{1}{2}}(z_3)}{\sqrt{-\pi}(z_2^3-1)^{\frac{1}{2}(L+k-\frac{1}{2})}} \right\} \tag{2.41}$$

2.6 BEP of DQPSK over Arbitrarily Correlated Fading Channels

The average conditional BEP of DQPSK with Gray coding can be rewritten as

$$P_4(e|\gamma_t) = Q\left(a\sqrt{\gamma_t}, b\sqrt{\gamma_t}\right) - \frac{1}{2}e^{-2\gamma_t}I_0(\sqrt{2}\gamma_t) + \frac{e^{-2\gamma_t}}{2^{2L-1}}\sum_{\ell=2}^{L}\binom{2L-1}{L-\ell}\sum_{k=1}^{\ell-1}D_k I_k(\sqrt{2}\gamma_t) \tag{2.42}$$

The first two terms in (2.42) can be expressed as a single finite-range integral by using the formula introduced by Pawula in [51]

$$Q_1\left(\sqrt{U-W}, \sqrt{U+W}\right) - \frac{1}{2}\,e^{-U}I_0(V) = \frac{1}{2\pi}\int_0^{\pi}\exp\left[-\frac{W^2}{U - V\cos(\phi)}\right]d\phi \tag{2.43}$$

provided that $W = \sqrt{U^2 - V^2}$. Using this transformation, $P_4(e|\gamma_t)$ can be written as

$$P_4(e|\gamma_t) = \frac{1}{2\pi}\int_0^{\pi} e^{-\frac{\sqrt{2}\gamma_t}{\sqrt{2}-\cos(\phi)}}d\phi + \sum_{\ell=2}^{L}\binom{2L-1}{L-\ell}\sum_{k=1}^{\ell-1}\frac{D_k}{\pi 2^{2L-1}}\int_0^{\pi}\cos(k\phi)e^{-\gamma_t(2-\sqrt{2}\cos(\phi))}d\phi \tag{2.44}$$

where we have used the fact that [18],[6]

$$I_n(z) = \frac{1}{\pi}\int_0^{\pi} e^{-z\cos(\theta)}\cos(n\theta)d\theta \tag{2.45}$$

The total average BEP of DQPSK is,

$$\begin{aligned} P_4(e) =& \frac{1}{2\pi}\int_0^{\pi}\Phi_{\gamma_t}\left(\frac{\sqrt{2}}{\sqrt{2}-\cos(\phi)}\right)d\phi + \sum_{\ell=2}^{L}\binom{2L-1}{L-\ell}\sum_{k=1}^{\ell-1}\frac{D_k}{\pi 2^{2L-1}} \\ &\times\int_0^{\pi}\cos(k\phi)\Phi_{\gamma_t}\left(2-\sqrt{2}\cos(\phi)\right)d\phi \end{aligned} \tag{2.46}$$

and $\Phi_{\gamma_t}(\omega)$ is defined as

$$\Phi_{\gamma_t}(\omega) = \mathrm{E}\{e^{-\gamma_t\omega}\} \tag{2.47}$$

where $\mathrm{E}\{.\}$ denotes the statistical expectation.

For Nakagami-m fading channels, $\Phi_{\gamma_t}(\omega)$ can be shown to be [43]

$$\Phi_{\gamma_t}(\omega) = \left[\det\left(\mathbf{I} + \frac{1}{m}\omega\mathbf{D}_{\bar{\gamma}}\mathbf{M}_X\right)\right]^{-m} \tag{2.48}$$

provided that det(.) denotes the determinant, $\mathbf{I}$ is an $L \times L$ identity matrix, $\mathbf{D}_{\bar{\gamma}}$ is a diagonal matrix defined as

$$\mathbf{D}_{\bar{\gamma}} = \mathrm{diag}\left(\mathrm{E}\{\gamma_1\}, \mathrm{E}\{\gamma_2\}, \ldots, \mathrm{E}\{\gamma_L\}\right) \tag{2.49}$$

and $\mathbf{M}_X$ is the the correlation matrix

$$\mathbf{M}_X = \begin{bmatrix} 1 & \rho_{12} & \rho_{13} & \ldots & \rho_{1L} \\ \rho_{21} & 1 & \rho_{23} & \ldots & \rho_{2L} \\ \rho_{31} & \rho_{32} & 1 & \ldots & \rho_{3L} \\ \vdots & \vdots & \vdots & \ldots & \vdots \\ \rho_{L1} & \rho_{L2} & \rho_{L3} & \ldots & 1 \end{bmatrix} \tag{2.50}$$

where $\rho_{i,j} = \sqrt{\lambda_{i,j}}$ and $\lambda_{i,j}$ is the power correlation defined by

$$\lambda_{ij} = \frac{\mathrm{cov}(\gamma_i, \gamma_j)}{\mathrm{var}(\gamma_i)\mathrm{var}(\gamma_j)},\ i, j = 1, 2, \cdots, L \tag{2.51}$$

In Rician fading environment, the conditional SNR on the ℓth branch γ_ℓ is non-central Chi-square distributed with two degrees of freedom, which is equivalent to the sum of the squares of two independent non-zero mean Gaussian random variables ($\gamma_\ell = x_{1,\ell}^2 + x_{2,\ell}^2$). The Rician fading index K_ℓ can be written as $K_\ell = \mu_\ell^2/P_\ell$, where μ_ℓ^2 and P_ℓ are the average power of the specular and diffuse components on the ℓth channel respectively and they are defined as

$$\begin{aligned} &\mu_\ell^2 = \bar{x}_{1,\ell}^2 + \bar{x}_{2,\ell}^2, \quad \bar{x}_{1,\ell} = \mathrm{E}\left\{x_{1,\ell}\right\} = \mu_\ell \cos(\theta), \quad \bar{x}_{2,\ell} = \mathrm{E}\left\{x_{2,\ell}\right\} = \mu_\ell \sin(\theta) \\ &P_\ell = \sum_{i=1}^{2} \mathrm{E}\left\{\left(x_{i,\ell} - \bar{x}_{i,\ell}\right)^2\right\}, \quad \mathrm{E}\{\gamma_\ell\} = \mu_\ell^2 + P_\ell \end{aligned} \tag{2.52}$$

where θ is the LOS phase angle, which is uniformly distributed $[0, 2\pi]$. Note that the phase of the specular component is assumed to be equal for all the diversity branches in our analysis. In [52], Ma studied the impact of Rician correlated diversity branches with different LOS phase angles on the performance of coherent MRC and noncoherent EGC receivers. His results showed that the LOS phase angles can lead to a significant performance improvement for medium-to-high SNRs.

Consider the L-dimensional vectors $\mathbf{X}_i = [x_{i,1}, x_{i,2}, ..., x_{i,L}]^T, i = 1, 2$, where $(.)^T$ denotes the transpose operator. The elements of the vector $\mathbf{X}_i$ are jointly Gaussian with mean vector $\mathrm{E}\{\mathbf{X}_i\}$ and covariance matrix $\mathbf{R}, \{\mathbf{R}\}_{i,j} = \sqrt{P_i P_j}\ \rho_{ij}/2$. The vectors $\mathbf{X}_1$ and $\mathbf{X}_2$ are statistically independent, and then it can be shown that

$$\Phi_{\gamma_t}(\omega) = \mathrm{E}\left\{\exp\left(-\omega\left[\mathbf{X}_1^T\mathbf{X}_1 + \mathbf{X}_2^T\mathbf{X}_2\right]\right)\right\} = \frac{\exp\left(-\omega\boldsymbol{\mu}^T[I + \omega\mathbf{R}]^{-1}\boldsymbol{\mu}\right)}{\det\left(I + \omega\mathbf{R}\right)} \tag{2.53}$$

where $\boldsymbol{\mu}$ is the $L \times 1$ mean vector whose elements are defined as $\{\boldsymbol{\mu}\}_\ell = \mu_\ell$.

2.7 Discussion of Results

The average BEP versus average SNR per branch (with identical average SNR in all branches) for DQPSK with arbitrarily correlated diversity reception is plotted in Figures 2.3,2.4. The correlation matrix M_X for all the performance curves given in this study is [53]

$$\mathbf{M}_X = \begin{bmatrix} 1 & 0.795 & 0.605 & 0.375 \\ 0.795 & 1 & 0.795 & 0.605 \\ 0.605 & 0.795 & 1 & 0.795 \\ 0.375 & 0.605 & 0.795 & 1 \end{bmatrix} \tag{2.54}$$

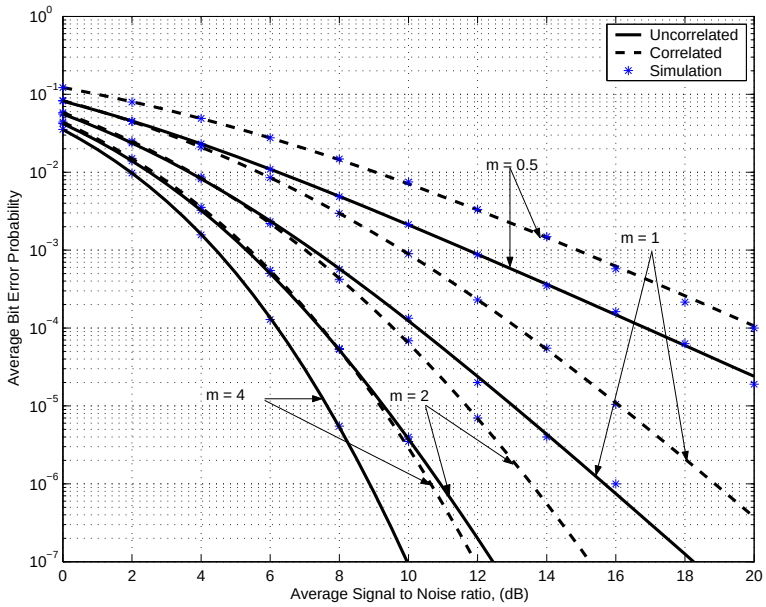

Figure 2.3. Average BEP of DQPSK with diversity reception ($L = 4$) over arbitrarily correlated Nakagami-m fading channels.

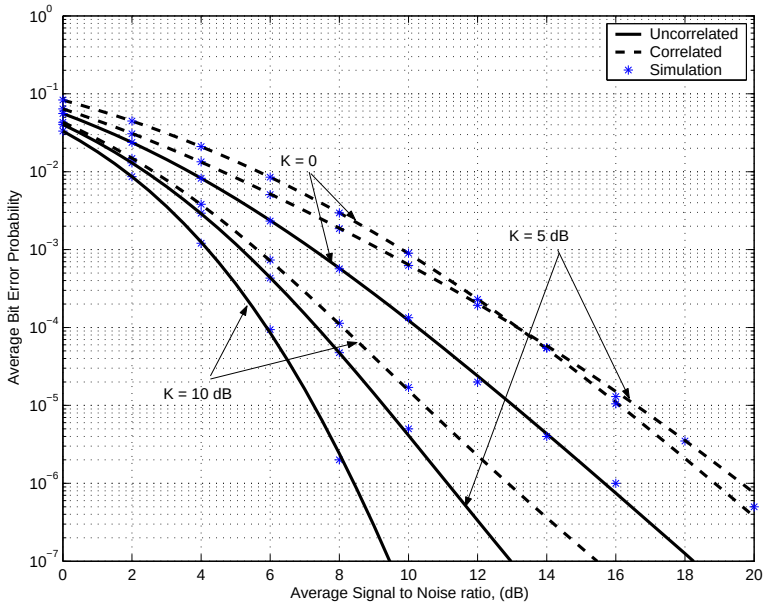

Figure 2.4. Average BEP of DQPSK with diversity reception ($L = 4$) over arbitrarily correlated Rician fading channels.

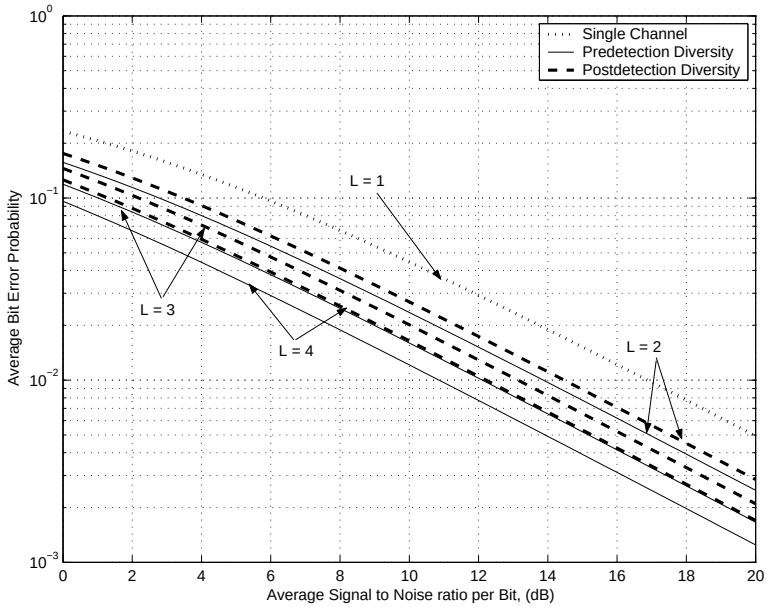

Figure 2.5. Average BEP of DQPSK over equal-correlated Rayleigh fading channels when $\rho = 1$.

The accuracy of the results is verified by computer simulation. Figures 2.3 and 2.4 show an excellent agreement between the numerical and simulation results. Comparison between the average BEP curves in Figures 2.3, 2.4 reveals that the correlation between the L branches causes extra system performance degradation relative to the original penalty due to the present noise impairments (channel fading and AWGN). It is obvious in Figure 2.4 that the degradation due to correlation, moves the BEP (with $K = 5$ dB) curve over the BEP with Rayleigh fading channels ($K = 0$) at about SNR=13.2 dB. Similar observation was reported by Chang and McLane in [54, Fig. 3]. This can be attributed to the correlation among the scattering components in the different diversity branches. In diversity reception, the system performance can be improved relative to the scatter component. In Figure 2.4, the phases of the LOS components are fixed on all diversity branches and the average power of the scatter components in the Rician case is smaller than the Rayleigh case, when they have the same total average signal power. Then,

for small-to-medium K factor, high enough correlation coefficient, and enough diversity branches, the performance degradation due to the correlation is going to be severer in Rician case. Thus, unlike the uncorrelated situation, the performance of DQPSK (with K=5 dB) is inferior than the performance of Rayleigh faded channels after 13.2 dB. In the literature, it is common to translate the increase in a certain average BEP into an equivalent increase of SNR that maintain the same BEP as that without correlation. In our context, we will refer to this increase in SNR as the correlation loss. Computation of correlation loss is important in the design of the practical DQPSK receivers. The correlation loss can be interpreted as an additional margin in the power link budget to compensate the power loss due to correlation. The correlation loss of DQPSK system over arbitrarily correlated Nakagami-m and Rician fading channels at average BEP of 10^{-5} is given in Table 2.1, 2.2 respectively. Notice that, in Tables 2.1, 2.2 the correlation among the diversity branches is assumed to be constant $\rho_{ij} = 0.795, i \neq j, i, j, \in \{1, 2, ..., L\}$. The results in Tables 2.1, 2.2 indicate that the correlation loss is dependent on the severity of the fading environment (m, K, and $\mathbf{M}_X$), diversity order, and error probability level. In Table 2.1, it is observed that the correlation loss is getting smaller for higher fading index m (less severe fading condition) and it is getting larger for higher diversity order L (higher correlation among more diversity branches). In contrast, the results in Table 2.2 (excluding the Rayleigh fading case) do not obey the same behavior of Nakagami-m case, the reason behind this situation can be ascribed to the presence of the specular component. The correlation loss is increased with greater fading index K, however, with sufficiently large fading index K (less severe fading environment), the correlation loss starts to decrease (10 dB in Table 2.2).

An interesting aspect of the correlation among the diversity reception can be observed when $\rho \rightarrow 1.0$. The L-diversity branches of the combiner act as a single channel (no diversity) when $\rho \rightarrow 1.0$. In Figure 2.5, the average BEP of DQPSK over correlated

Table 2.1. Correlation loss on decibels for DQPSK with diversity reception over equal correlated Nakagami-m (ρ=0.795) fading channels at average BEP 10^{-5}

m	$L=2$	$L=4$
0.5	2.171	3.827
1	2.156	3.662
2	1.958	3.075
4	1.402	2.115
6	1.033	1.556
8	0.806	1.217

Table 2.2. Correlation loss on decibels for DQPSK with diversity reception over equal correlated Rician (ρ=0.795) fading channels at average BEP 10^{-5}

K	$L=2$	$L=4$
0	2.156	3.662
3 dB	5.772	8.046
5 dB	7.278	8.846
7 dB	7.581	8.366
10 dB	3.433	4.286
13 dB	1.180	1.677

Rayleigh fading channels is plotted with postdetection EGC and predetection with MRC. The conditional BEP of DQPSK with MRC diversity (It is known also as differential encoded quaternary phase shift keying) can be written as

$$\begin{aligned} P_4(e|\gamma_t) =& Q_1\left(a\sqrt{\gamma_t}, b\sqrt{\gamma_t}\right) - \frac{1}{2}e^{-2\gamma_t} I_0(\sqrt{2}\gamma_t) \\ =& \frac{1}{2\pi}\int_0^{\pi} e^{-\frac{\sqrt{2}\gamma_t}{\sqrt{2}-\cos(\phi)}}\, d\phi \end{aligned} \tag{2.55}$$

and the total average BEP is

$$P_4(e) = \frac{1}{2\pi}\int_0^{\pi} \Phi_{\gamma_t}\left(\frac{\sqrt{2}}{\sqrt{2}-\cos(\phi)}\right) d\phi \tag{2.56}$$

From Figure 2.5, it is apparent that the performance curves of the DQPSK with various diversity orders degrade towards the nondiversity case and the only improvement is the

Table 2.3. Postdetection with EGC penalty over predetection with MRC in decibles for DBPSK and DQPSK over uncorrelated Nakagami-m fading at average BEP 10^{-4}

m	DBPSK		DQPSK	
	$L=2$	$L=4$	$L=2$	$L=4$
0.5	0.969	1.855	0.594	0.971
1	0.884	1.658	0.402	0.645
2	0.782	1.497	0.247	0.466
4	0.700	1.394	0.171	0.384
6	0.666	1.356	0.150	0.360
8	0.649	1.336	0.139	0.347

gain that comes from adding the power from the diversity branches. It can be recognized from Figure 2.5 that improvement in predetection type is more than postdetection type when $\rho = 1$, which can be attributed to the nature of the predetection combiner, where the received signals are combined coherently before detection. For example, in predetection there is a 3 dB gain (comes from doubling the power) for the dual branch combiner. However, in postdetection it decreases to 2.41 dB.

The postdetection combining diversity offers a tradeoff between the receiver complexity and system performance. The postdetection's penalty over predetection combining for independent Nakagami-m and Rician fading channels is shown in Table 2.3 and Table 2.4 respectively. Table 2.3 and 2.4 indicate that the penalty of postdetection over predetection is affected mainly by the diversity order, severity of the fading environment, and the modulation scheme. One conclusion that can be drawn from these results is that the DBPSK's penalty is greater than DQPSK's penalty.

2.8 Conclusion

The average BEP for DQPSK with postdetection EGC diversity over independent and arbitrarily correlated Rayleigh, Nakagami-m, and Rician fading channels has been

Table 2.4. Postdetection EGC penalty over predetection MRC in decibles for DBPSK and DQPSK over Rician fading at average BEP 10^{-4}

K	DBPSK		DQPSK	
	$L=2$	$L=4$	$L=2$	$L=4$
0	0.884	1.658	0.402	0.645
4 dB	0.853	1.544	0.347	0.510
7 dB	0.772	1.445	0.236	0.422
10 dB	0.689	1.369	0.164	0.367

derived using two independent approaches. The associated Legendre function approach can lead to finite closed-form expressions for the average BEP of DQPSK over L independent Rayleigh and Nakagami-m channels, when the product Lm is integer, we believe that these finite-series closed-form expressions provide new results for the average BEP of DQPSK. Besides, a finite-series closed-form expression is proposed for the average BEP of DBPSK with EGC over independent Rician fading channels. In the second approach, the performance of DQPSK is tackled over arbitrarily correlated Nakagami-m and Rician fading channels. To the best of our knowledge, the exact average BEP of DQPSK over arbitrarily correlated channels is expressed (in the literature) as a double infinite series, twofold integral, or as an infinite sum of a finite-range integral. In contrast, our study provides a finite sum of a finite-range integral for the average BEP of DQPSK with EGC over arbitrarily correlated Nakagami-m and Rician fading channels. The novelty of the second approach lies in presenting relatively simple-to-numerically evaluates BEP expression in terms of a finite sum of a finite-range integral. The penalty in signal to noise ratio (SNR) due to arbitrarily correlated channel fading is investigated. It is observed that the system performance degradation due to the correlation among the diversity branches in Rician fading channels is severer than that in Nakagami-m fading channels as a result of the presence of the specular component. The distinction between the performance of

predetection and posdetection diversity combining is presented. The results provided in this study can be helpful in the design of the practical DQPSK receivers. Finally, the accuracy of the results is verified by computer simulation.

CHAPTER 3

DPSK WITH MIMO EMPLOYING EGC DIVERSITY RECEPTION

This Chapter analyzes the average BEP of DBPSK and DQPSK with multiple-input multiple-output (MIMO) systems employing postdetection EGC diversity reception (MIMO EGC) over Rayleigh fading channels. Finite closed-form expressions for the average BEP of DBPSK and DQPSK are presented. The proposed structure for the DPSK with MIMO EGC provides a reduced-complexity and low-cost receiver for MIMO systems compared to the coherent phase-shift keying system (PSK) employing MRC diversity reception (MIMO MRC). Finally, a useful procedure for computing the associated Legendre functions of the second kind with half-odd-integer order and arbitrarily degree is presented.

3.1 Introduction

The principal phenomenon that deteriorates the performance of wireless transmission systems is the time-varying multipath channel fading. One of the most effective techniques that can be used to mitigate the effects of channel fading is to employ multiple antennas at the transmitter and/or the receiver. The performance analysis of receiver diversity with single transmit antenna has been extensively discussed in the literature [30]. Multiple-input multiple-output (MIMO) systems, multiple transmit-receive antennas, can introduce additional system performance improvement relative to the system

with receiver diversity and single transmit antenna. Having a perfect channel state information (CSI) at both the transmitter and the receiver, MIMO with maximal ratio combining (MRC) can be realized by transmitting in the direction of the eigenvector corresponding to the largest eigenvalue of the channel, which leads to attain the maximum signal-to-noise ratio (SNR) at the receiver [19]. Performance analysis of MIMO MRC has been conducted by several authors [20],[21],[22],[23]. Starting with the work of Dighe *et al.* in [20], they analyzed the performance of coherent MIMO MRC systems over Rayleigh fading channels. Moreover, the authors in [20] addressed the exact cumulative distribution function (cdf) of the maximum SNR, and provided finite-series expressions for the probability density function (pdf) of the SNR for different combinations of transmit and receive antenna numbers. The authors in [21], studied the pdf of the maximum SNR with an arbitrary number of transmit antennas and two receive antennas, and evaluated the average probability of error for coherent binary phase-shift keying (BPSK). In [22], Kang and Alouini have addressed the error rates of MIMO MRC systems with and without cochannel interference over Rayleigh fading channels. Grant in [23], presented hypergeometric series of matrix argument-based approach to analyze the average BEP for MIMO MRC over Rayleigh fading channels. All previous studies tackled the performance of MIMO MRC systems, which require a perfect knowledge of the CSI at both the transmitter and the receiver sides, leading to increased system complexity and cost. Because of the limitations on the size, cost, and complexity of the receiver unit, (for example the mobile unit in the downlink case), the design of reduced-complexity and low-cost receivers for MIMO systems, which still keeps much of the advantages and benefits of the full-complexity MIMO system, is of great concern to the researchers and engineers. A promised approach to achieve this goal without considerable penalty to performance quality, is to employ DPSK techniques. In DPSK system with MIMO employing EGC, the signal processing is performed at the transmitter (or base station) with the receiver

(mobile unit) having a simplified structure that requires only limited signal processing. Moreover, MIMO EGC has much simpler amplifier requirements than MIMO MRC, since it does not require the antenna amplifiers to modify the amplitudes nor the phases of the received signals. In this Chapter, we consider DPSK systems with MIMO EGC diversity reception that require only knowing the CSI at the transmitter side. It is worthwhile to note here that the CSI can be obtained at the transmitter without the aid of the receiver [55],[56]. Note that the differential coherent transmission can be received coherently, this scheme is referred as differentially encoded differentially decoded phase-shift keying system or as DPSK with MRC (predetection combining), to resolve the phase ambiguity encountered in coherent transmission over fading channels [56],[17]. The objective of this Chapter is to present the proposed structure of DPSK with MIMO EGC system and analyze its performance in terms of the average bit error probability (BEP). To the best of our knowledge, this is the first study that analyzes the error rates of DPSK systems with MIMO EGC diversity. This Chapter is organized as follows: the problem is formulated in Section 3.2. Section 3.3 clarifies the conditional BEP of DBPSK and DQPSK. In Section 3.4, the average BEP of DBPSK and DQPSK over independent Rayleigh fading channels is obtained for MIMO EGC by averaging the conditional probability over the pdf of the largest eigenvalue of the channel. It should be pointed out that our study is focused on a combination of $2 \times L$ (2 antenna elements at the transmitter and L antenna elements at the receiver with $L \geq 2$) transmit-receive antennas or $L \times 2$ transmit-receive antennas. However, we will show that it can be extended to arbitrary transmit-receive antenna combinations. Directing our analysis toward $L, 2$ combinations is justified from practical point of view [22] since mobile units cannot afford more than two antennas because of space, complexity, and cost limitations. In contrast, base stations are more flexible and can be implemented with more than two antenna elements. An alternative

approach is presented in Section 3.5 to analyze the average BEP of DQPSK. Results are discussed in Section 3.6. Finally, concluding remarks are presented in Section 3.7.

3.2 System Model

We consider a MIMO system, employing N antennas at the transmitter and L antennas at the receiver. The low-pass equivalent of the $(L \times 1)$ received signal vector $\mathbf{r}$ during the mth signalling interval can be expressed as

$$\mathbf{r} = \mathbf{H}_D \mathbf{w}_t s_m(t) + \mathbf{n} \tag{3.1}$$

provided that $\mathbf{n}$ is the complex-valued additive Gaussian noise vector with zero mean, $\mathrm{E}\{\mathbf{n}\mathbf{n}^T\} = \mathbf{0}_L$, and $\mathrm{E}\{\mathbf{n}\mathbf{n}^H\} = N_0\mathbf{I}_L$, where $\mathrm{E}\{.\}$ denotes the statistical average operator, $(.)^T$ denotes the transpose operator, $(.)^H$ denotes the Hermitian operator, $\mathbf{0}_L$ denotes the $L \times L$ zero matrix, and $\mathbf{I}_L$ denotes the $L \times L$ identity matrix. $\mathbf{w}_t$ is the weight vector at the transmitter with $\|\mathbf{w}_t\| = 1$. $\mathbf{H}_D$ denotes the channel gain matrix, which is given by

$$\mathbf{H}_D = \begin{bmatrix} \alpha_{11}e^{\jmath\varphi_{11}} & \alpha_{12}e^{\jmath\varphi_{12}} & \dots & \alpha_{1N}e^{\jmath\varphi_{1N}} \\ \alpha_{21}e^{\jmath\varphi_{21}} & \alpha_{22}e^{\jmath\varphi_{22}} & \dots & \alpha_{2N}e^{\jmath\varphi_{2N}} \\ \alpha_{31}e^{\jmath\varphi_{31}} & \alpha_{32}e^{\jmath\varphi_{32}} & \dots & \alpha_{3N}e^{\jmath\varphi_{3N}} \\ \vdots & \vdots & \dots & \vdots \\ \alpha_{L1}e^{\jmath\varphi_{L1}} & \alpha_{L2}e^{\jmath\varphi_{L2}} & \dots & \alpha_{LN}e^{\jmath\varphi_{LN}} \end{bmatrix} \tag{3.2}$$

$h_{ij} = \alpha_{ij}e^{\jmath\varphi_{ij}}$ is the channel gain from the jth transmitter-antenna element to the ith receiver-antenna element. The random phase shift φ_{ij} is assumed to be uniformly distributed between $[-\pi, \pi]$. The channel parameters α_{ij} and φ_{ij} are assumed to be slowly varying, so that they can be considered constant over two consecutive signaling intervals. $s_m(t)$ is the transmitted DPSK signal during the mth signaling interval, which has the same form as eq. (2.1).

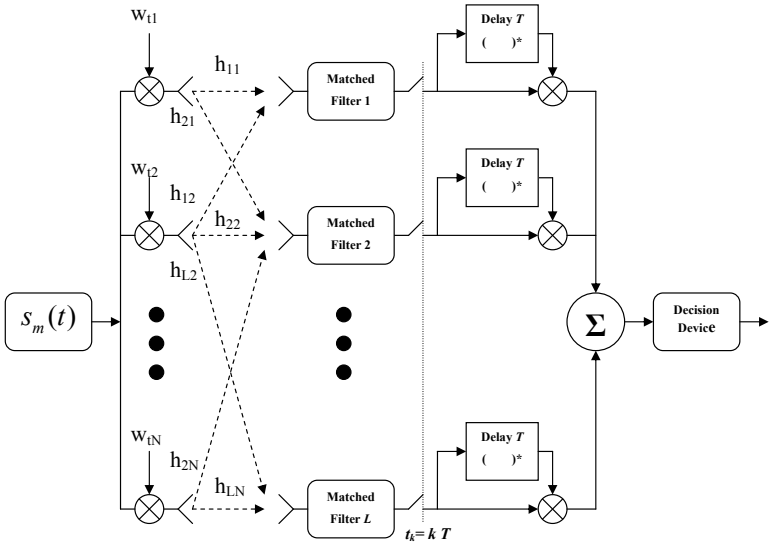

Figure 3.1. DPSK MIMO employing postdetection EGC.

Figure 3.1 shows the block diagram of a DPSK system with MIMO system employing postdetection EGC diversity reception (MIMO EGC). In postdetection combiner, the received signals are detected before combining takes place in the baseband region. The output of the matched filter in a matrix form is given by

$$\mathbf{Z}(\theta_m) = \begin{bmatrix} Z_1(\theta_m) \\ Z_2(\theta_m) \\ \vdots \\ Z_L(\theta_m) \end{bmatrix} = 2E_s e^{\jmath\theta_m}\mathbf{H}_D\mathbf{w}_t + \mathbf{v}_m \tag{3.3}$$

where the noise vector $\mathbf{v}_m$ is given by

$$\mathbf{v}_m = \begin{bmatrix} v_1 \\ v_2 \\ \vdots \\ v_L \end{bmatrix}, \; v_\ell = \int_0^T n_\ell(t)u_M(t)dt = v_{\ell,I} + \jmath\, v_{\ell,Q} \tag{3.4}$$

and it can be shown that $v_{\ell,I}$ and $v_{\ell,Q}$ are zero mean Gaussian-distributed random processes with equal variances

$$\sigma^2_{v_{\ell,I}} = \sigma^2_{v_{\ell,Q}} = 2E_sN_0 \tag{3.5}$$

The decision variable U_m at the output of the postdetection combiner can be written as

$$U_m = \sum_{\ell=1}^{L} Z_\ell(\theta_m) Z^*_\ell(\theta_{m-1}) \tag{3.6}$$

where $(.)^*$ denotes the complex conjugate.

The output conditional SNR (on the channel gain matrix) per bit is given by

$$\gamma = \rho \mathbf{w}_t^H \mathbf{H}_D^H \mathbf{H}_D \mathbf{w}_t \tag{3.7}$$

where $\rho = \frac{E_b}{N_0}$. The maximum SNR can be attained when the weighting vector $\mathbf{w}_t$ is chosen to be the eigenvector corresponding to the largest eigenvalue of $\mathbf{H}_D^H\mathbf{H}_D$ (or equivalently $\mathbf{H}_D\mathbf{H}_D^H$) [19], [22]. Assuming that the channel coefficients are available to the transmitter with $\mathbf{w}_t$ equals the eigenvector corresponding to the largest eigenvalue of $\mathbf{H}_D^H\mathbf{H}_D$ and $\|\mathbf{w}_t\| = 1$, the maximum SNR is

$$\gamma_{max} = \rho\lambda \tag{3.8}$$

where λ is the largest eigenvalue of $\mathbf{H}_D^H\mathbf{H}_D$.

3.3 Conditional Probability

The conditional BEP (on the largest eigenvalue λ) of DBPSK and DQPSK with Gray coding can be written respectively as [2], [39]

$$P_2(e|\lambda) = \frac{e^{-\rho\lambda}}{2^{2L-1}} \sum_{\ell=0}^{L-1} b_\ell \left(\rho\lambda\right)^\ell, b_\ell = \frac{1}{\ell!} \sum_{k=0}^{L-1-\ell} \binom{2L-1}{k} \tag{3.9}$$

$$P_4(e|\lambda) = e^{-2\rho\lambda} \left\{ \sum_{k=0}^{\infty} c_k (\sqrt{2}-1)^k I_k\left(\sqrt{2}\rho\lambda\right) + \frac{1}{2^{2L-1}} \sum_{\ell=2}^{L} \binom{2L-1}{L-\ell} \sum_{k=1}^{\ell-1} D_k I_k\left(\sqrt{2}\rho\lambda\right) \right\} \tag{3.10}$$

where $c_0 = 0.5, c_k = 1\ \forall k \neq 0$, $I_n(.)$ denotes the nth-order modified Bessel function of the first kind, and $D_k = (\sqrt{2}+1)^k - (\sqrt{2}-1)^k$.

3.4 PDF of λ and BEP of DBPSK and DQPSK

The channel fades α_{ij}'s are assumed to be uncorrelated, frequency-nonselective, identically distributed with Rayleigh pdf:

$$f_{\alpha_{ij}}(\alpha) = 2\alpha e^{-\alpha^2}, \quad \alpha \geq 0 \tag{3.11}$$

where, without loss of generality, the mean square of α_{ij} is normalized to one. The columns of $\mathbf{H}_D$ are equivalent to $(L \times 1)$ variate independent and identically distributed (iid) complex Gaussian random vectors. Let $s = \min(N, L)$ and $t = \max(N, L)$, then the s eigenvalues of $\mathbf{H}_D^H \mathbf{H}_D$, denoted as $\Lambda_1, \ldots, \Lambda_s$ are real and positive with probability one and have a joint pdf [57],[20]

$$f_{\Lambda_1,\ldots,\Lambda_s}(\Lambda_1, \ldots, \Lambda_s) = \frac{\left[\prod_{i=1}^{s} \Lambda_i\right]^{t-s} e^{-\left(\sum_{i=1}^{s} \Lambda_i\right)}}{s! \left[\prod_{i=1}^{s} (s-i)!(t-i)!\right]} \left[\prod_{1 \leq i < j \leq s} (\Lambda_i - \Lambda_j)^2\right] \tag{3.12}$$

Suppose that $\Lambda_1 > \Lambda_2 > \ldots > \Lambda_s$, then, the marginal density function of the maximum eigenvalue $\Lambda_1 = \lambda$ can be obtained by integrating (3.12) over the rest of the eigenvalues $\Lambda_2, \ldots, \Lambda_s$. In [20], the authors provided a finite-sum expression for the pdf of the largest eigenvalue λ for several combinations of s, t. For the case of $s = 2$, the pdf of λ can be reduced to a compact expression [22],[21]:

$$f_\lambda(\lambda) = a\lambda^{t-2} e^{-\lambda} \left[\gamma(t+1, \lambda) - 2\lambda\gamma(t, \lambda) + \lambda^2 \gamma(t-1, \lambda)\right] \tag{3.13}$$

where

$$a = \frac{1}{\Gamma(t)\Gamma(t-1)} \tag{3.14}$$

and $\gamma(.,.)$ is the incomplete gamma function defined by [6],[58]:

$$\begin{aligned}\gamma(n,x) =& \int_0^x t^{n-1}e^{-t}dt \\ =& \Gamma(n)\left[1-\sum_{k=0}^{n-1}\frac{x^k}{k!}e^{-x}\right]\end{aligned} \tag{3.15}$$

The pdf of λ can be rewritten in the following expression:

$$f_\lambda(\lambda) = a\left[\lambda^{2t-2}e^{-2\lambda} - t\lambda^{2t-3}e^{-2\lambda} + \left((t-1)t\lambda^{t-2} - 2(t-1)\lambda^{t-1} + \lambda^t\right)e^{-\lambda}\gamma(t-1,\lambda)\right] \tag{3.16}$$

provided that [6]

$$\gamma(d+1,x) = d\gamma(d,x) - x^d e^{-x} \tag{3.17}$$

In order to get the total error probability of DBPSK and DQPSK, the conditional error expressions in (3.9) and (3.10) are needed to be averaged over the pdf of maximum eigenvalue (λ).

3.4.1 DBPSK

The total BEP of DBPSK is

$$\begin{aligned}P_2(e) =& \frac{a}{2^{2L-1}}\sum_{\ell=0}^{L-1} b_\ell \rho^\ell \left[\frac{\Gamma(2t+\ell-1)}{(2+\rho)^{2t+\ell-1}} - \frac{t\Gamma(2t+\ell-2)}{(2+\rho)^{2t+\ell-2}} + \left\{\frac{t(t-1)\Gamma(t+\ell-1)}{(1+\rho)^{t+\ell-1}}\right.\right. \\ & - \frac{2(t-1)\Gamma(t+\ell)}{(1+\rho)^{t+\ell}} + \frac{\Gamma(t+\ell+1)}{(1+\rho)^{t+\ell+1}} - \sum_{j=0}^{t-2}\frac{1}{j!}\left(\frac{t(t-1)\Gamma(j+t+\ell-1)}{(2+\rho)^{j+t+\ell-1}}\right. \\ & \left.\left.\left. - \frac{2(t-1)\Gamma(j+t+\ell)}{(2+\rho)^{j+t+\ell}} + \frac{\Gamma(j+t+\ell+1)}{(2+\rho)^{j+t+\ell+1}}\right)\right\}\Gamma(t-1)\right]\end{aligned} \tag{3.18}$$

where we have used the fact [6]

$$\Gamma(z) = k^z\int_0^\infty t^{z-1}e^{-kt}dt,\ \mathrm{Re}(z)>0, \mathrm{Re}(k)>0 \tag{3.19}$$

Where Re(.) denotes the real part.

3.4.2 DQPSK

The total BEP of DQPSK is

$$P_4(e) = a\left[\frac{g(z_1, 2t-1.5, L)}{(\sqrt{2}\rho)^{2t-1}} - \frac{tg(z_1, 2t-2.5, L)}{(\sqrt{2}\rho)^{2t-2}} + \left\{\frac{t(t-1)g(z_2, t-1.5, L)}{(\sqrt{2}\rho)^{t-1}}\right.\right.$$
$$- \frac{2(t-1)g(z_2, t-0.5, L)}{(\sqrt{2}\rho)^{t}} + \frac{g(z_2, t+0.5, L)}{(\sqrt{2}\rho)^{t+1}} - \sum_{j=0}^{t-2}\frac{1}{j!}\left(\frac{t(t-1)g(z_1, j+t-1.5, L)}{(\sqrt{2}\rho)^{j+t-1}}\right.$$
$$\left.\left.\left. - \frac{2(t-1)g(z_1, j+t-0.5, L)}{(\sqrt{2}\rho)^{j+t}} + \frac{g(z_1, j+t+0.5, L)}{(\sqrt{2}\rho)^{j+t+1}}\right)\right\}\Gamma(t-1)\right] \tag{3.20}$$

In $P_4(e)$, $z_1 = \frac{2+2\rho}{\sqrt{2}\rho}$, $z_2 = \frac{1+2\rho}{\sqrt{2}\rho}$, and $g(z, \mu, L)$ is given by

$$g(z, \mu, L) = \frac{e^{-\jmath\mu}}{\sqrt{\pi/2}}\left\{\sum_{i=0}^{\infty}\frac{c_i(\sqrt{2}-1)^i Q^{\mu}_{i-\frac{1}{2}}(z)}{(z^2-1)^{\frac{\mu}{2}}} + \frac{1}{2^{2L-1}}\sum_{\ell=2}^{L}\binom{2L-1}{L-\ell}\sum_{i=1}^{\ell-1}\frac{D_i Q^{\mu}_{i-\frac{1}{2}}(z)}{(z^2-1)^{\frac{\mu}{2}}}\right\} \tag{3.21}$$

The infinite series expressions for the average BEP of DQPSK can be reduced to finite expressions. For the particular cases of (s, t) equals (2,2) and (2,3), it can be shown, using equation (A.3) combined with (A.4), that the infinite series part in $P_4(e)$, which is equivalent to $g(z, \mu, 1)$, can be reduced into the following

$$g(z, 0.5, 1) = \frac{z + \sqrt{z^2-1} - 1 + \sqrt{2}}{2\sqrt{z^2-1}(z + \sqrt{z^2-1} + 1 - \sqrt{2})} \tag{3.22}$$

$$g(z, 1.5, 1) = \frac{1}{(z^2-1)^{\frac{3}{2}}}\left\{\frac{z(z+\sqrt{z^2-1})}{(z+\sqrt{z^2-1}+1-\sqrt{2})} - \frac{z}{2}\right.$$
$$\left. + \frac{\sqrt{z^2-1}(\sqrt{2}-1)(z+\sqrt{z^2-1})}{(z+\sqrt{z^2-1}+1-\sqrt{2})^2}\right\} \tag{3.23}$$

$$g(z, 2.5, 1) = \frac{(2z^2+1)(z+\sqrt{z^2-1})}{(z^2-1)^{\frac{5}{2}}(z+\sqrt{z^2-1}+1-\sqrt{2})} + \frac{3z(\sqrt{2}-1)(z+\sqrt{z^2-1})}{(z^2-1)^2(z+\sqrt{z^2-1}+1-\sqrt{2})^2}$$
$$+ \frac{(\sqrt{2}-1)(z+\sqrt{z^2-1}+\sqrt{2}-1)(z+\sqrt{z^2-1})}{(z^2-1)^{\frac{3}{2}}(z+\sqrt{z^2-1}+1-\sqrt{2})^3} - \frac{1+2z^2}{2(z^2-1)^{\frac{5}{2}}} \tag{3.24}$$

$$g(z,3.5,1) = \frac{5zg(z,2.5,1)}{z^2-1} - \frac{4g(z,1.5,1)}{z^2-1} + \frac{(\sqrt{2}-1)(z+\sqrt{z^2-1})}{(z^2-1)^2} \times \left\{ \frac{(z+\sqrt{z^2-1})^2 + (\sqrt{2}-1)^2 + 4(\sqrt{2}-1)(z+\sqrt{z^2-1})}{(z+\sqrt{z^2-1}+1-\sqrt{2})^4} \right\} + \frac{z(\sqrt{2}-1)(z+\sqrt{z^2-1})(z+\sqrt{z^2-1}+\sqrt{2}-1)}{(z^2-1)^{\frac{5}{2}}(z+\sqrt{z^2-1}+1-\sqrt{2})^3} \tag{3.25}$$

$$\begin{aligned} g(z,4.5,1) = {} & \frac{7zg(z,3.5,1)}{z^2-1} + \frac{3z^2(\sqrt{2}-1)(z+\sqrt{z^2-1})(z+\sqrt{z^2-1}+\sqrt{2}-1)}{(z^2-1)^{\frac{7}{2}}(z+\sqrt{z^2-1}+1-\sqrt{2})^3} \\ & - \frac{9g(z,2.5,1)}{z^2-1} + \frac{3z(\sqrt{2}-1)(z+\sqrt{z^2-1})}{(z^2-1)^3} \left\{ \frac{(z+\sqrt{z^2-1})^2 + (\sqrt{2}-1)^2}{(z+\sqrt{z^2-1}+1-\sqrt{2})^4} \right. \\ & \left. + \frac{4(\sqrt{2}-1)(z+\sqrt{z^2-1})}{(z+\sqrt{z^2-1}+1-\sqrt{2})^3} \right\} + \frac{(\sqrt{2}-1)(z+\sqrt{z^2-1})}{(z^2-1)^{\frac{5}{2}}(z+\sqrt{z^2-1}+1-\sqrt{2})^5} \\ & + \frac{(\sqrt{2}-1)(z+\sqrt{z^2-1})(z+\sqrt{z^2-1}+\sqrt{2}-1)}{(z^2-1)^{\frac{5}{2}}(z+\sqrt{z^2-1}+1-\sqrt{2})^3} \left\{ (z+\sqrt{z^2-1})^2 \right. \\ & \left. \times \left[(z+\sqrt{z^2-1}) + 11(\sqrt{2}-1) \right] + (\sqrt{2}-1)^3 + 11(z+\sqrt{z^2-1})(\sqrt{2}-1)^2 \right\} \end{aligned} \tag{3.26}$$

The previous analysis was focused on $L, 2$ antenna combinations. However, since the pdf of the largest eigenvalue λ for several combinations of s, t can be expressed as finite-sum expression involving a product of exponential and power functions [20], then, our analysis can be extended to evaluate the error rates for arbitrary s, t combinations.

3.5 Alternative approach for the average BEP of DQPSK

Another way in which the average BEP of DQPSK can be expressed as a finite-sum of a finite-range integral is explained in this Section. The average conditional BEP for DQPSK can also be expressed in terms of the Marcum's Q-function as [2],[39]

$$P_4(e|\lambda) = Q\left(a\sqrt{\rho\lambda}, b\sqrt{\rho\lambda}\right) - \frac{1}{2}e^{-2\rho\lambda}I_0(\sqrt{2}\rho\lambda) + \frac{e^{-2\rho\lambda}}{2^{2L-1}} \sum_{\ell=2}^{L} \binom{2L-1}{L-\ell} \sum_{k=1}^{\ell-1} D_k I_k(\sqrt{2}\rho\lambda) \tag{3.27}$$

where $a = \sqrt{2-\sqrt{2}}, b = \sqrt{2+\sqrt{2}}$, and $Q(x,y)$ is the Marcum's Q-function. The first two terms in (3.27) can be expressed as a single finite-range integral using (2.43).$P_4(e|\lambda)$ can be written as

$$P_4(e|\lambda) = \frac{1}{2\pi}\int_0^{\pi} e^{-\frac{\sqrt{2}\rho\lambda}{\sqrt{2}-\cos(\phi)}}d\phi + \sum_{\ell=2}^{L}\binom{2L-1}{L-\ell}\sum_{k=1}^{\ell-1}\frac{D_k}{\pi 2^{2L-1}}\int_0^{\pi}\cos(k\phi)e^{-\rho\lambda(2-\sqrt{2}\cos(\phi))}d\phi \tag{3.28}$$

The total average BEP of DQPSK is

$$\begin{aligned} P_4(e) =& \frac{1}{2\pi}\int_0^{\pi}\Phi_\lambda\left(\frac{\sqrt{2}\rho}{\sqrt{2}-\cos(\phi)}\right)d\phi \\ &+ \sum_{\ell=2}^{L}\binom{2L-1}{L-\ell}\sum_{k=1}^{\ell-1}\frac{D_k}{\pi 2^{2L-1}}\int_0^{\pi}\cos(k\phi)\Phi_\lambda\left(\rho(2-\sqrt{2}\cos(\phi))\right)d\phi \end{aligned} \tag{3.29}$$

given that $\Phi_\lambda(\omega)$ is given as [22]

$$\begin{aligned} \Phi_\lambda(\omega) =& \mathrm{E}\{e^{-\lambda\omega}\} \\ =& \sum_{i=0}^{2}\frac{\Gamma(t+1-i)\Gamma(t-1+i)}{\Gamma(t)\Gamma(t-1)}\binom{2}{i}\frac{(-1)^i}{(1+\omega)^{t-1+i}} \\ &- \frac{2\Gamma(2t)}{\Gamma(t+2)\Gamma(t)}\sum_{k=0}^{t-2}\left(\sum_{j=k}^{t-2}\frac{(3)_j(2-t)_j}{(t+2)_j(j-k)!}\right)\frac{(-1)^k}{k!(2+\omega)^{2t-3-k}} \end{aligned} \tag{3.30}$$

where $(\delta)_j$ is the shifted factorial (Pochhammer number), defined as $(\delta)_j = \delta(\delta+1)\cdots(\delta+j-1)$ with $(\delta)_0 = 1$ [6]. Note that this approach can also be applied to evaluate the average BEP of DQPSK for arbitrary (s,t) combinations, where $\Phi_\lambda(\omega)$ can be extracted from [20, eq. 26] for arbitrary (s,t) combinations.

3.6 Discussion of Results

The average BEP versus the average SNR per branch (i.e $\frac{E_b}{N_0}$) for DBPSK and DQPSK with MIMO EGC systems over independent Rayleigh fading channels is plotted for various combination of transmit-receive antennas in Figures 3.2,3.3. It should be

pointed that the $\mathrm{E}\{\lambda\} = 1$. Comparison between the average BEP curves (with the same number of $N + L$) in Figures 3.2,3.3 reveals that the increased complexity and cost in the MIMO system are translated into lower error probability compared to the receive diversity system ($N = 1$). In the performance curves of MIMO EGC in Figures 3.2,3.3, the BEP with $t = N, s = L$ outperforms the BEP with $t = L, s = N$. The the reason behind the discrepancy can be explained by recognizing that the MIMO EGC perform coherent transmission in the transmitter side and noncoherent detection in the receiver side. In MIMO MRC system (coherent predetection combining in the receiver side), the average BEP of both $t = N, s = L$ and $t = L, s = N$ combinations can be shown to be the same. With MIMO MRC, the conditional BEP of DBPSK and DQPSK can be written respectively as

$$P_2(e|\lambda) = \frac{1}{2}e^{-\rho\lambda} \tag{3.31}$$

$$P_4(e|\lambda) = e^{-2\rho\lambda}\sum_{k=0}^{\infty} c_k(\sqrt{2}-1)^k I_k\left(\sqrt{2}\rho\lambda\right) \tag{3.32}$$

Figure 3.4 depicts the average BEP of coherent binary phase-shift keying (BPSK) with MIMO MRC and DBPSK with MIMO EGC over Rayleigh fading channels. In the same way, the average BEP of coherent quaternary phase-shift keying (QPSK) with MIMO MRC and DQPSK with MIMO EGC is plotted in Figure 3.5. From the figures (3.4 and 3.5), it is apparent that the performance of DBPSK and DQPSK with MIMO EGC undergoes a system performance degradation relative to the performance of BPSK and QPSK with MIMO MRC respectively. Table 3.1 shows the penalty in SNR of DBPSK and DQPSK with MIMO EGC over BPSK and QPSK with MIMO MRC respectively at average BEP of 10^{-4}. It is worthwhile to note here that the gain penalty in SNR for the DBPSK and DQPSK with EGC receive diversity ($L = 3, 4, 5$) and single transmit antenna ($N = 1$) to achieve the same level of performance (BEP=10^{-4}) with BPSK and

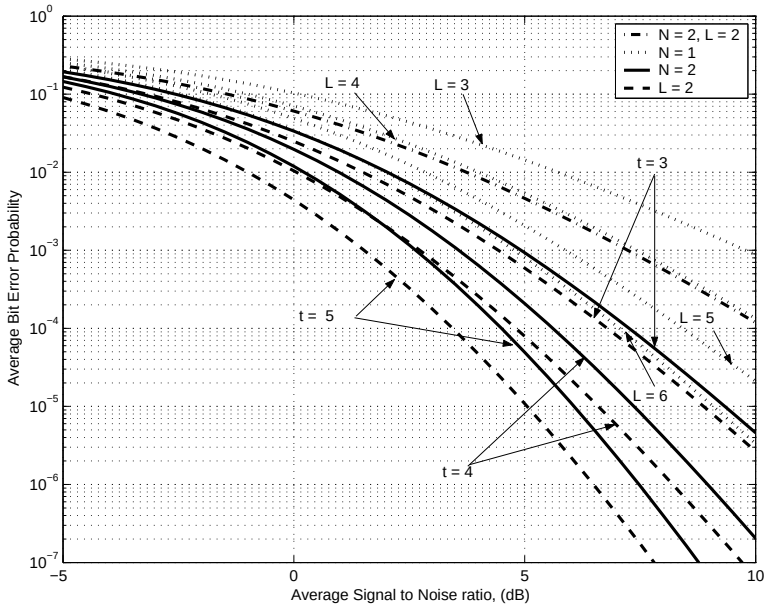

Figure 3.2. Average BEP of DBPSK with MIMO EGC over Rayleigh fading channels.

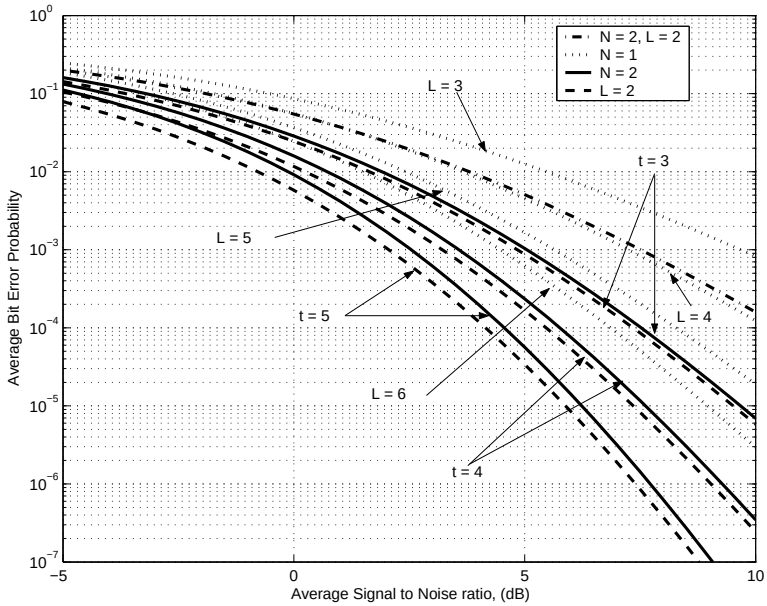

Figure 3.3. Average BEP of DQPSK with MIMO EGC over Rayleigh fading channels.

QPSK with MRC receive diversity ($L = 3, 4, 5$) and single transmit antenna ($N = 1$) is about 3 dB over Rayleigh fading channels. The gain penalty of DBPSK and DQPSK with MIMO EGC over the BPSK and QPSK with MIMO MRC is < 3 dB. Therefore, DBPSK and DQPSK with MIMO EGC can be considered as attractive candidates in wireless communication systems.

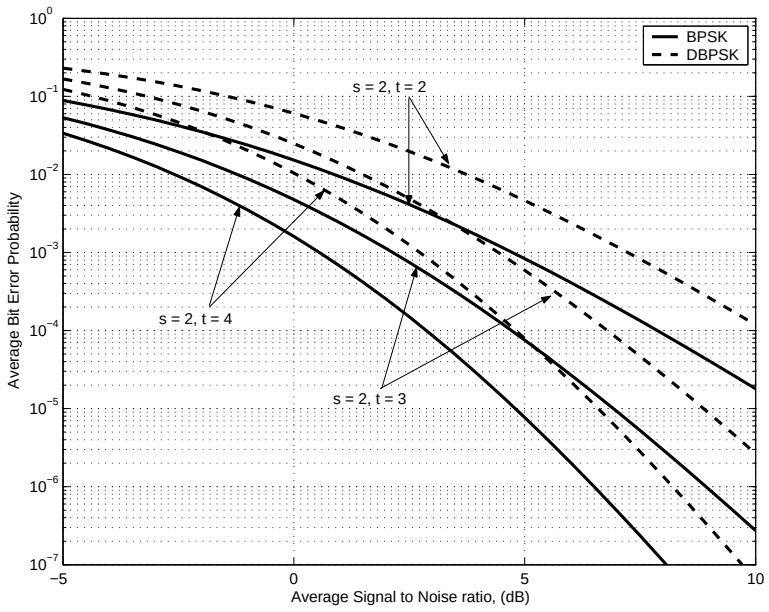

Figure 3.4. Average BEP of BPSK with MIMO MRC and DBPSK with MIMO EGC over Rayleigh fading channels.

Table 3.1. Gain penalty on decibels for DBPSK and DQPSK with MIMO EGC over BPSK and QPSK with MIMO MRC over Rayleigh fading channels at average BEP 10^{-4}

(s, t)	DBPSK	DQPSK
$(2, 2)$	2.330	2.717
$(2, 3)$	2.074	2.631
$(2, 4)$	1.938	2.593

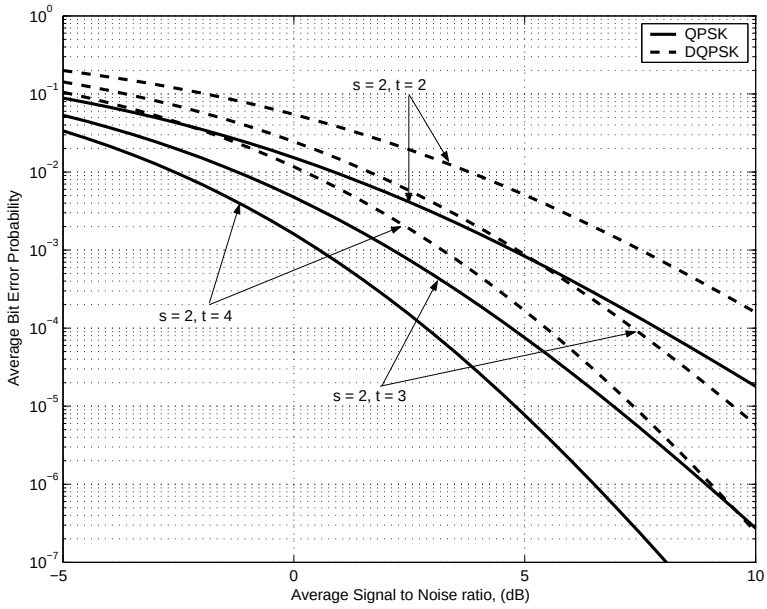

Figure 3.5. Average BEP of QPSK with MIMO MRC and DQPSK with MIMO EGC over Rayleigh fading channels.

3.7 Conclusion

The average BEP for DBPSK and DQPSK with MIMO EGC over independent Rayleigh fading channels has been derived. The proposed structure for the differential phase-shift keying (DPSK) with MIMO EGC provides a reduced-complexity and low-cost receiver for MIMO systems compared to the coherent phase-shift keying system (PSK) with MIMO MRC. Two approaches are introduced to analyze the error rates of DQPSK. Finite closed form expressions for the average BEP of DBPSK and DQPSK are presented. The results provided in this study can be helpful in the design of the practical MIMO EGC DBPSK and DQPSK systems.

CHAPTER 4

PSK SYSTEMS WITH IMPERFECT CARRIER PHASE RECOVERY

Using Fourier series expansion and associated Legendre functions, the average bit error probability (BEP) of the binary and quaternary phase shift keying (BPSK and QPSK respectively) on a single channel (no diversity) in the presence of different kinds of slow fading channels (Rayleigh, Nakagami-m, and Rician), phase recovery error, and additive white Gaussian noise (AWGN) has been evaluated. The detection loss and phase precision for both of BPSK and QPSK have been calculated. The series expressions of the average BEP proposed in our study are found to be converged with reasonable number of terms.

4.1 Background and Previous Work

The performance of PSK systems in the presence of imperfect carrier phase recovery has been studied extensively since 1960s. Starting with the problem of modeling the statistics of the carrier phase error, Tikhonov and Viterbi [59],[25] succeeded in the early 1960s to model the probability density function (pdf) of the carrier phase error with a first-order phase-locked loop (PLL). Then, many attempts have been introduced to analyze and evaluate the performance of PSK systems with imperfect phase recovery and AWGN; Lindsey in 1966, was one of the people who addressed the performance of BPSK in the presence of imperfect carrier phase recovery and AWGN [27]. Prabhu in 1976

analyzed the performance of BPSK and QPSK using the Fourier series expansion [26]. Simon has used the Maclaurin series expansion to evaluate the BEP of unbalanced QPSK systems [28]. Weber in 1976 was the first author who demonstrated the impact of fading channels on the performance of PLL [60]. Recently, Najib and Prabhu have proposed a new technique to compute the BEP of the partially coherent BPSK and QPSK over Rayleigh fading channels with equal gain combiner (EGC), and their technique was based on Gram-Charlier series expansion [29]. After that time, Simon and Alouini extended the approach in [28] to include the effects of several types of slow flat fading channels, however, they only consider the first two nonzero terms of the Maclaurin series expansion of the conditional BEP. Moreover, they demonstrate the Gaussian approximation to model phase error distribution [30]. The authors in [31], [32], propose infinite series expressions for the average BEP of PSK systems with imperfect phase recovery over fading channels. However, their analysis is based on approximation the cumulative distribution function (cdf), and the error expressions require either numerical integration of an infinite integral [32] or evaluation the moments of the EGC decision variable [31].

In this Chapter, we demonstrate the evaluation of the performance of BPSK and QPSK in the presence of three system imperfections: phase recovery error, slow multipath fading, and AWGN over a single channel (no diversity). The problem is formulated in Section 4.2. In Section 4.3, the average conditional BEP (on the phase error and channel fading) is expanded using the Fourier series method, then the series expression of the average BEP is averaged over the pdf of phase error. The average BEP of the BPSK and QPSK over Nakagami-m and Rician fading channels is obtained in Sections 4.4 and 4.5 respectively. The average BEP expressions are given in terms of infinite series involving the associated Legendre functions of the first or the second kinds. In Section 2.6, the average BEP of the Nakagami-m and Rician faded BPSK and QPSK with imperfect phase recovery is plotted and compared to the performance of the differential schemes of

BPSK and QPSK systems. The detection loss, due to imperfect phase recovery, and phase precision are also discussed in this Section. Finally, concluding remarks are presented in Section 4.7.

4.2 System Model

PSK modulation schemes are characterized by the fact that the information sequence carried by the transmitted carrier is contained in the phase. The low-pass representation of the mth transmitted PSK signal $s_m(t)$ takes the form:

$$s_m(t) = \begin{cases} u_M(t)\exp(\jmath\theta_m), & 0 \le t \le T \\ 0, & \text{elsewhere} \end{cases} \quad m = 1, 2, \ldots, M \tag{4.1}$$

where $u_M(t)$ is the pulse shaping signal and it is assumed to be constant during the pulse interval T (rectangular shaping pulse) and it has the following form

$$u_M(t) = \begin{cases} \sqrt{\frac{2E_s}{T}}, & 0 \le t \le T \\ 0, & \text{elsewhere} \end{cases} \tag{4.2}$$

in which $E_s = E_b \log_2 M$ is the symbol energy, θ_m is the modulation phase of the mth signal, which can take 0 or π in case of BPSK and $-3\pi/4, -\pi/4, \pi/4,$ or $3\pi/4$ in case of QPSK.

The low-pass equivalent of the mth received signal $r_m(t)$ can be described by

$$r_m(t) = \alpha\exp(\jmath\ \varphi)u_M(t)\exp(\jmath\ \theta_m) + n(t) \tag{4.3}$$

where α is the fading amplitude, which is due to the time-invariant multipath characteristics on the channel. φ is a random phase shift introduced by the channel and it is uniformly distributed between $[-\pi, \pi]$. The additive term $n(t)$ represents the zero mean complex-valued Gaussian noise, and it has a single-sided power spectral density of $2N_0$ W/Hz.

Coherent reception techniques require a perfect knowledge of the carrier's phase [2]. The receiver can estimate the carrier's phase using either a suppressed carrier-tracking loop or a pilot tone [24]. In the suppressed carrier-tracking loop, the receiver constructs a coherent replica of the carrier by passing the information-bearing signal through a carrier synchronization loop (e.g., a squaring loop, costas loop, or decision feedback loop). On the other hand, the pilot tone method needs the transmitter to transmit a separate unmodulated carrier (referred as a pilot tone) besides the modulated carrier, and the receiver in turn constitutes a coherent version of the carrier by feeding the pilot tone to PLL. The PLL in the pilot tone method is designed to have a narrow bandwidth to reduce the effect of unwanted adjacent frequencies, but a portion of the transmitted power is allocated to the pilot tone [2]. Carrier synchronization loop method is more widely used since the total transmitted power is allocated to the information bearing signal [3]. The single channel coherent PSK receiver is depicted in Figure 4.1. Regardless of the devoted phase estimation technique, the coherent receiver produces an estimate $\hat{\varphi}$. Due to thermal noise [26], which is present in the recovery circuit, and due to the random modulation [26] that may present in the carrier, the estimation process results in a residual carrier phase error defined as $\varepsilon = \varphi - \hat{\varphi}$, this situation is denoted by partially coherent reception [25]. The statistics of ε in the presence of AWGN (excluding the effect of channel fading) for a first order PLL have been discussed extensively [59]-[25]. The stationary pdf of the carrier phase error has been shown to be modeled by a Tikhonov distribution, which can expressed as [26]

$$f_{\varepsilon}(\varepsilon) = \frac{\exp(\gamma \cos(\varepsilon))}{2\pi I_0(\gamma)}, \quad |\varepsilon| \leq \pi \tag{4.4}$$

where $I_n(.)$ denotes the nth-order modified Bessel function of the first kind, γ is the carrier loop signal-to-noise-ratio (SNR) and is given by

$$\gamma = \frac{2P_s}{N_0 B_L} \tag{4.5}$$

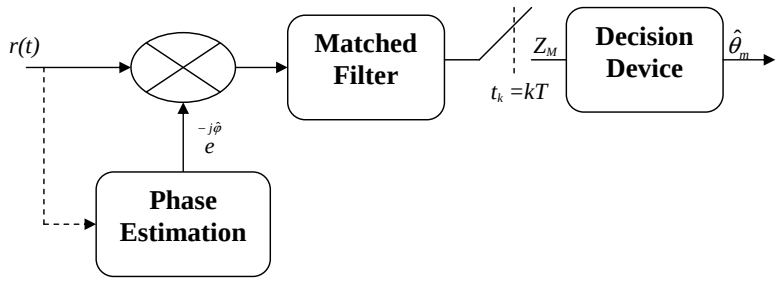

Figure 4.1. Single channel coherent PSK receiver.

where P_s denotes the power of the unmodulated carrier (assuming the pilot tone method is employed), and B_L is the loop bandwidth.

In Figure 4.1, Z_M is the output of the match filter and it can be shown that it is given by

$$\begin{aligned} Z_M(\theta_m) =& \exp(-\jmath\ \hat{\varphi}) \int_0^T r_m(t) u_M(t) dt \\ =& 2E_s \alpha \exp[\jmath\ (\varepsilon + \theta_m)] + v_M,\ m = 1, 2, \ldots, M \end{aligned} \tag{4.6}$$

where the phase error ε is assumed to be slowly varying during the bit interval T, so that it can be considered constant within the signaling interval T. With respect to the noise term v_M, it can be shown that

$$\begin{aligned} v_M =& \exp(-\jmath\ \hat{\varphi}) \int_0^T n(t) u_M(t) dt \\ =& v_{M,I} + \jmath\ v_{M,Q} \end{aligned} \tag{4.7}$$

provided that $v_{M,I}$ and $v_{M,Q}$ are zero mean Gaussian-distributed random processes with equal variances

$$\sigma^2_{v_{M,I}} = \sigma^2_{v_{M,Q}} = 2E_s N_0 \tag{4.8}$$

4.3 Conditional Probability

In this Section, the conditional BEP (on fading amplitude) of BPSK and QPSK with imperfect phase recovery is derived using Fourier series expansion.

4.3.1 BPSK Analysis

Assuming equally probable symbols, the conditional (on phase error and channel fading) BEP for BPSK can be computed from equation (4.6)-(4.8) and it can be shown to be [27], [26], [29], and [30]

$$P_2(E|\alpha,\varepsilon) = \frac{1}{2}\ \mathrm{erfc}\left(\sqrt{\rho}\ \alpha\cos(\varepsilon)\right) \tag{4.9}$$

where erfc(.) is the complementary error function, $\rho = \frac{E_b}{N_0}$ is the SNR per bit, and $\cos(\varepsilon)$ is the loss factor due to imperfect phase recovery. In [61], Prabhu has introduced an interesting expansion for the error function erf(.). He has shown that the erf($\sqrt{\rho}\ \cos(\varepsilon)$) (since it is periodic in ε with period 2π) can be expanded using Fourier series expansion into the following converging infinite series

$$\mathrm{erf}(\sqrt{\rho}\cos(\varepsilon)) = 2\sqrt{\frac{\rho}{\pi}}\sum_{\ell=0}^{\infty}\ \frac{(-1)^{\ell}}{2\ell+1}\cos[(2\ell+1)\varepsilon]\exp(-\frac{\rho}{2})\left\{I_{\ell}\left(\frac{\rho}{2}\right)+I_{\ell+1}\left(\frac{\rho}{2}\right)\right\} \tag{4.10}$$

It should pointed out that there are many forms in which the erf(.) function can be expressed as an infinite series [62], the series expression in (4.10) is chosen since it is fast to converge for all values ($\sigma_{\varepsilon} \neq 0$) [26], where σ_{ε} is the standard deviation of ε. Equation (4.9) can be transformed into the following form :

$$\begin{aligned} P_2(E|\alpha,\varepsilon) =& \frac{1}{2} + \alpha\sqrt{\frac{\rho}{\pi}}\ \sum_{\ell=0}^{\infty}\ \frac{(-1)^{\ell+1}}{2\ell+1}\cos[(2\ell+1)\varepsilon] \\ & \times\left\{I_{\ell}\left(\frac{\alpha^2\ \rho}{2}\right)+I_{\ell+1}\left(\frac{\alpha^2\rho}{2}\right)\right\}\exp\left(-\frac{\alpha^2\rho}{2}\right) \end{aligned} \tag{4.11}$$

by averaging the previous expression over the pdf of ε, one can get

$$\begin{aligned} P_2(E|\alpha) =& \int_{-\pi}^{\pi} P_2(E|\alpha,\varepsilon) f_{\varepsilon}(\varepsilon)d\varepsilon \\ =& \frac{1}{2} + \alpha\ \sqrt{\frac{\rho}{\pi}}\ \sum_{\ell=0}^{\infty}\frac{(-1)^{\ell+1}}{2\ell+1}\ \frac{I_{2\ell+1}(\gamma)}{I_0(\gamma)} \\ & \times\left\{I_{\ell}\left(\frac{\alpha^2\ \rho}{2}\right)+I_{\ell+1}\left(\frac{\alpha^2\rho}{2}\right)\right\}\exp\left(-\frac{\alpha^2\rho}{2}\right) \end{aligned} \tag{4.12}$$

with [6]

$$I_n(z) = \frac{1}{\pi}\int_0^{\pi} \exp(-z\cos(\theta))\cos(n\theta)d\theta \tag{4.13}$$

4.3.2 QPSK Analysis

In QPSK, M=4 and θ_m can take the values of $-3\pi/4, -\pi/4, \pi/4,$ or $3\pi/4$. The mapping of the information symbols (k bits where $k = \log_2(M)$) can be achieved in many ways [2]. The favored technique is the way in which adjacent phases differ by one binary digit, this coding technique is known as Gray encoding. The reason behind the effectiveness and preference of Gray codes is that an error is more probable to be occurred for its nearest neighbors, so it is better to make adjacent symbols differ in only one digit so that the adjacent symbol is accompanied by one and only one bit error [24]. Assuming equally probable symbols, the conditional (on phase error and channel fading) bit error probability for QPSK can be derived from equations (4.6)-(4.8) and it can be shown to be [26], [29], and [30]

$$P_4(E|\alpha,\varepsilon) = \frac{1}{4}\text{erfc}(\sqrt{2\rho}\alpha\cos[\frac{\pi}{4}+\varepsilon]) + \frac{1}{4}\text{erfc}(\sqrt{2\rho}\ \alpha\cos[\frac{\pi}{4}-\varepsilon]) \tag{4.14}$$

the Fourier series expansion of (4.14) is given by

$$\begin{aligned} P_4(E|\alpha,\varepsilon) =& \frac{1}{2} + \alpha\sqrt{\frac{2\rho}{\pi}}\sum_{\ell=0}^{\infty}\frac{(-1)^{\ell+1}}{2\ell+1}\exp\left(-\alpha^2\rho\right)\left\{I_\ell(\alpha^2\ \rho) + I_{\ell+1}(\alpha^2\ \rho)\right\} \\ & \times\cos[(2\ell+1)\varepsilon]\cos[(2\ell+1)\frac{\pi}{4}] \end{aligned} \tag{4.15}$$

and the conditional BEP on the fading amplitude is

$$\begin{aligned} P_4(E|\alpha) =& \frac{1}{2} + \alpha\sqrt{\frac{2\rho}{\pi}}\sum_{\ell=0}^{\infty}\frac{(-1)^{\ell+1}}{2\ell+1}\frac{I_{2\ell+1}(\gamma)}{I_0(\gamma)}\exp\left(-\alpha^2\rho\right) \\ & \times\left\{I_\ell(\alpha^2\rho) + I_{\ell+1}(\alpha^2\ \rho)\right\}\cos[(2\ell+1)\frac{\pi}{4}] \end{aligned} \tag{4.16}$$

4.4 Analysis of Nakagami-m Fading

In this Section, we will demonstrate the case when the fade amplitude α is assumed to be frequency-nonselective, slowly varying, and Nakagami-m distributed. The pdf of α can be written as [4]

$$f_\alpha(\alpha) = \frac{2m^m \alpha^{2m-1}}{\Gamma(m)} \exp\left(-m\alpha^2\right), \quad \alpha \geq 0 \tag{4.17}$$

where without loss of generality, the mean square value of α is normalized to one. The performance of BPSK and QPSK in the presence of AWGN, Nakagami-m fading, and phase recovery noise can be evaluated by averaging the conditional BEP expressions over the pdf of α. It can be shown that the average BEP in case of BPSK is

$$\begin{aligned} P_2(E) =& \frac{1}{2} + \sum_{\ell=0}^{\infty} \frac{(-1)^{\ell+1}\ 2\ m^{\frac{m}{2}} I_{2\ell+1}(\gamma) \exp(-\jmath m\pi)}{(2\ell+1)\pi\ \Gamma(m) I_0(\gamma)(\rho+m)^{\frac{m}{2}}} \\ & \times \left\{ Q^m_{\ell-\frac{1}{2}}\left(1+\frac{2m}{\rho}\right) + Q^m_{\ell+\frac{1}{2}}\left(1+\frac{2m}{\rho}\right) \right\} \end{aligned} \tag{4.18}$$

and it can be expressed as

$$P_2(E) = \frac{1}{2} + \sum_{\ell=0}^{\infty} \frac{(-1)^{\ell+1} I_{2\ell+1}(\gamma)\sqrt{\rho}\ m^{\frac{1}{2}(m-\frac{1}{2})} Z_1(\ell, m, \rho)}{(2\ell+1) I_0(\gamma)\ \sqrt{\pi}\ \Gamma(m)(\rho+m)^{\frac{1}{2}(m+\frac{1}{2})}} \tag{4.19}$$

where

$$\begin{aligned} Z_1(\ell, m, \rho) =& \Gamma(m+\ell+0.5) P^{-\ell}_{m-\frac{1}{2}}\left(\frac{\rho+2m}{2\sqrt{m(m+\rho)}} \right) \\ & + \Gamma(m+\ell+1.5) P^{-(\ell+1)}_{m-\frac{1}{2}}\left(\frac{\rho+2m}{2\sqrt{m(m+\rho)}} \right) \end{aligned} \tag{4.20}$$

given that [44]

$$P^{-\mu}_{\nu}(z) = \frac{(z_1^2-1)^{-\frac{1}{2}(\nu+1)}}{\Gamma(\nu+\mu+1)} \int_0^\infty \exp\left\{ \frac{-tz}{\sqrt{z^2-1}} \right\} I_\mu(t) t^\nu dt \tag{4.21}$$

where $\mathrm{Re}(\nu+\mu) > -1, \mathrm{Re}(z) > 1$, $P^\mu_\nu(.)$ is the μth order and νth degree of the associated Legendre functions of the first kind. In literature, the associated Legendre functions

that have integral order and half-odd degree are commonly known as toroidal harmonics [45]-[46]. In Appendix A, we address briefly the main characteristics of the associated Legendre functions.

In the case of QPSK, the average BEP for QPSK can also be verified to be as

$$\begin{aligned} P_4(E) =& \frac{1}{2} + \sum_{\ell=0}^{\infty} \frac{(-1)^{\ell+1} 2\ m^{\frac{m}{2}} I_{2\ell+1}(\gamma) \exp(-\jmath m\pi)}{(2\ell+1)\pi\ \Gamma(m) I_0(\gamma)(2\rho+m)^{\frac{m}{2}}} \\ & \times \left\{ Q^m_{\ell-\frac{1}{2}}\left(1+\frac{m}{\rho}\right) + Q^m_{\ell+\frac{1}{2}}\left(1+\frac{m}{\rho}\right) \right\} \cos[(2\ell+1)\frac{\pi}{4}] \end{aligned} \tag{4.22}$$

or

$$P_4(E) = \frac{1}{2} + \sum_{\ell=0}^{\infty} \frac{(-1)^{\ell+1} I_{2\ell+1}(\gamma)\sqrt{2\rho}\ m^{\frac{1}{2}(m-\frac{1}{2})}}{(2\ell+1) I_0(\gamma)\sqrt{\pi}\ \Gamma(m)(2\rho+m)^{\frac{1}{2}(m+\frac{1}{2})}} Z_2(\ell, m, \rho) \cos[(2\ell+1)\frac{\pi}{4}] \tag{4.23}$$

where

$$\begin{aligned} Z_2(\ell, m, \rho) =& \Gamma(m+\ell+0.5) P^{-\ell}_{m-\frac{1}{2}}\left(\frac{\rho+m}{\sqrt{m(2\rho+m)}}\right) \\ & + \Gamma(m+\ell+1.5) P^{-(\ell+1)}_{m-\frac{1}{2}}\left(\frac{\rho+m}{\sqrt{m(2\rho+m)}}\right) \end{aligned} \tag{4.24}$$

4.5 Analysis of Rician (Nakagami-n) Fading

In Rician fading environment, there will be a fundamental line-of-sight (LOS) signal from the transmitter to the receiver with additional weaker paths resulting from reflections. If we assume that the amplitude fades α is frequency-nonselective and slowly varying, then the normalized pdf of α is given by [4]

$$\begin{aligned} f_\alpha(\alpha) =& 2(1+n^2)\alpha\ \exp\left(-(1+n^2)\alpha^2 - n^2\right) I_0\left(2n\alpha\sqrt{1+n^2}\ \right), \qquad \alpha \geq 0 \\ =& 2(1+n^2)\alpha \exp\left(-(1+n^2)\alpha^2 - n^2\right) \sum_{k=0}^{\infty} \frac{(1+n^2)^k (n\alpha)^{2k}}{(k!)^2}, \qquad \alpha \geq 0 \end{aligned} \tag{4.25}$$

where n is the Nakagami-n fading parameter. The average BEP for BPSK can be shown to be

$$\begin{aligned} P_2(E) =& \frac{1}{2} + \sum_{\ell=0}^{\infty} \frac{(-1)^{\ell+1}\ 2\ I_{2\ell+1}(\gamma)}{\pi(2\ell+1)I_0(\gamma)} \sum_{k=0}^{\infty} \frac{(-1)^{k+1} n^{2k}}{(k!)^2 \exp(n^2)} \\ & \times \sqrt[k+1]{\frac{1+n^2}{\rho+n^2+1}} \left\{ Q_{\ell-\frac{1}{2}}^{k+1}\left(1+\frac{2(n^2+1)}{\rho}\right) + \ Q_{\ell+\frac{1}{2}}^{k+1}\left(1+\frac{2(n^2+1)}{\rho}\right)\right\} \end{aligned} \tag{4.26}$$

and it can be expressed as

$$\begin{aligned} P_2(E) =& \frac{1}{2} + \sum_{\ell=0}^{\infty} \frac{(-1)^{\ell+1} I_{2\ell+1}(\gamma) \exp(-n^2)\sqrt{\rho}}{(2\ell+1)\sqrt{\pi}\ I_0(\gamma)} \\ & \times \sum_{k=0}^{\infty} \frac{n^{2k}(1+n^2)^{\frac{1}{2}(k+\frac{1}{2})}}{(k!)^2(\rho+1+n^2)^{\frac{1}{2}(k+\frac{3}{2})}} Z_3(\ell,k,n,\rho) \end{aligned} \tag{4.27}$$

where

$$\begin{aligned} Z_3(\ell,k,n,\rho) =& \Gamma(k+l+1.5)P_{k+\frac{1}{2}}^{-\ell}(z_3) + \Gamma(k+\ell+2.5)P_{k+\frac{1}{2}}^{-(\ell+1)}(z_3) \\ z_3 =& \frac{\rho+2(1+n^2)}{2\sqrt{(1+n^2)(\rho+1+n^2)}} \end{aligned} \tag{4.28}$$

The average BEP for QPSK is

$$\begin{aligned} P_4(E) =& \frac{1}{2} + \sum_{\ell=0}^{\infty} \frac{(-1)^{\ell+1}\ 2\ I_{2\ell+1}(\gamma)}{\pi(2\ell+1)I_0(\gamma)} \sum_{k=0}^{\infty} \frac{(-1)^{k+1} n^{2k}}{(k!)^2 \exp(n^2)} \sqrt[k+1]{\frac{1+n^2}{2\rho+n^2+1}} \\ & \times \left\{ Q_{\ell-\frac{1}{2}}^{k+1}\left(1+\frac{n^2+1}{\rho}\right) + \ Q_{\ell+\frac{1}{2}}^{k+1}\left(1+\frac{n^2+1}{\rho}\right)\right\} \cos[(2\ell+1)\frac{\pi}{4}] \end{aligned} \tag{4.29}$$

and also it can be expressed as

$$\begin{aligned} P_4(E) =& \frac{1}{2} + \sum_{\ell=0}^{\infty} \frac{(-1)^{\ell+1}\sqrt{2\rho}\ I_{2\ell+1}(\gamma)}{(2\ell+1)\sqrt{\pi} I_0(\gamma)\exp(n^2)} \cos[(2\ell+1)\frac{\pi}{4}] \\ & \times \sum_{k=0}^{\infty} \frac{n^{2k}(1+n^2)^{\frac{1}{2}(k+\frac{1}{2})}}{(k!)^2(2\rho+1+n^2)^{\frac{1}{2}(k+\frac{3}{2})}} Z_4(\ell,k,n,\rho) \end{aligned} \tag{4.30}$$

where

$$\begin{aligned} Z_4(\ell,k,n,\rho) =& \Gamma(k+\ell+1.5)P_{k+\frac{1}{2}}^{-\ell}(z_4) + \Gamma(k+\ell+2.5)P_{k+\frac{1}{2}}^{-(\ell+1)}(z_4) \\ z_4 =& \frac{\rho+1+n^2}{\sqrt{(1+n^2)(2\rho+1+n^2)}} \end{aligned} \tag{4.31}$$

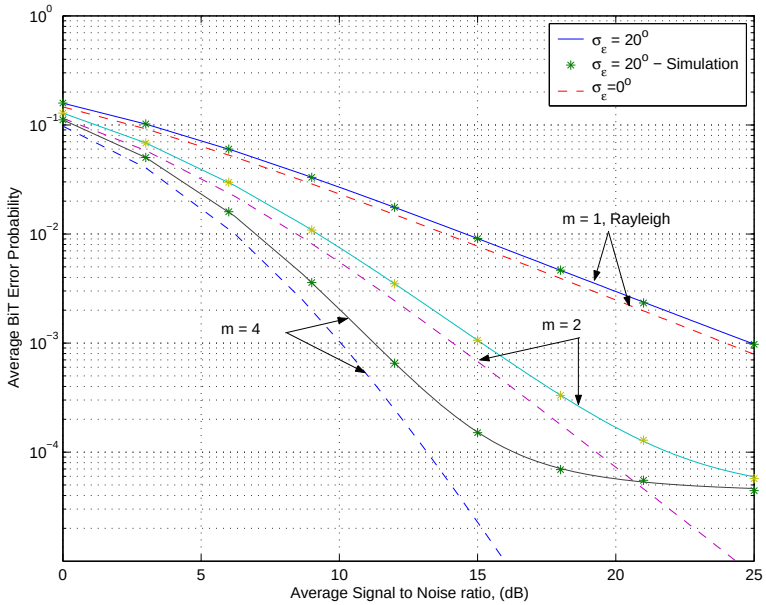

Figure 4.2. Average BEP of BPSK in the presence of AWGN, Nakagami-m fading, and phase recovery error ($\sigma_\varepsilon = 20^o$).

4.6 Discussion of Results

The average BEP of BPSK and QPSK over Nakagami-m fading channel with imperfect phase recovery for various combinations of m and σ_ε is plotted in Figures 4.2,4.3 respectively. In the same way, Figures 4.4, 4.5 show the average BEP for BPSK and QPSK over Rician fading channel. The accuracy of our analysis is demonstrated by quasi-analytic simulation [63]. Quasi-analytic simulations were performed by averaging the conditional BEP expressions in (4.9) and (4.14) over simulated random variables α, ϵ for 10^7 bits. Figures 4.2, 4.3, 4.4, 4.5 show an excellent agreement between the numerical and simulation results. It can be recognized from these results that the system performance degradation, due to the imperfect phase recovery, of the QPSK system is more severe than the degradation of BPSK system.

It is obvious from Figures 4.2, 4.3, 4.4, 4.5 that the lack of perfect phase recovery in coherent systems leads to an extra system performance degradation relative to the

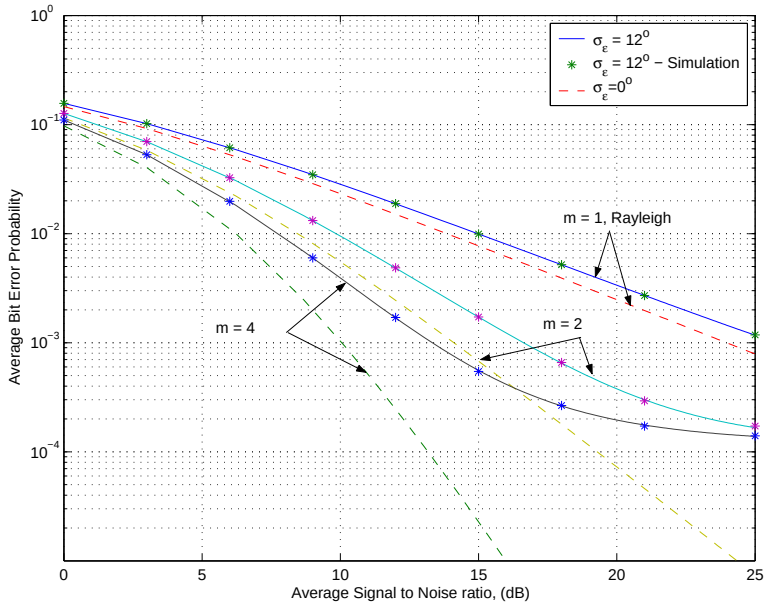

Figure 4.3. Average BEP of QPSK in the presence of AWGN, Nakagami-m fading, and phase recovery error ($\sigma_\varepsilon = 12^o$).

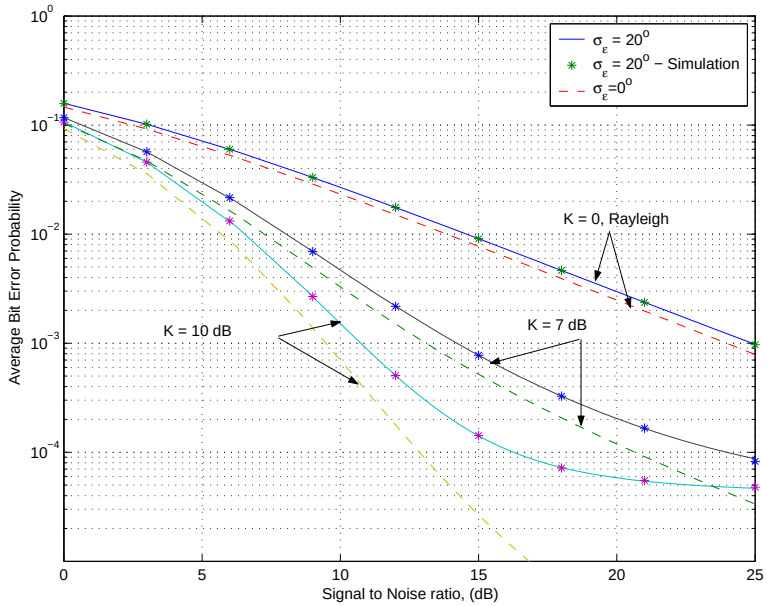

Figure 4.4. Average BEP of BPSK in the presence of AWGN, Rician fading, and phase recovery error ($\sigma_\varepsilon = 20^o$).

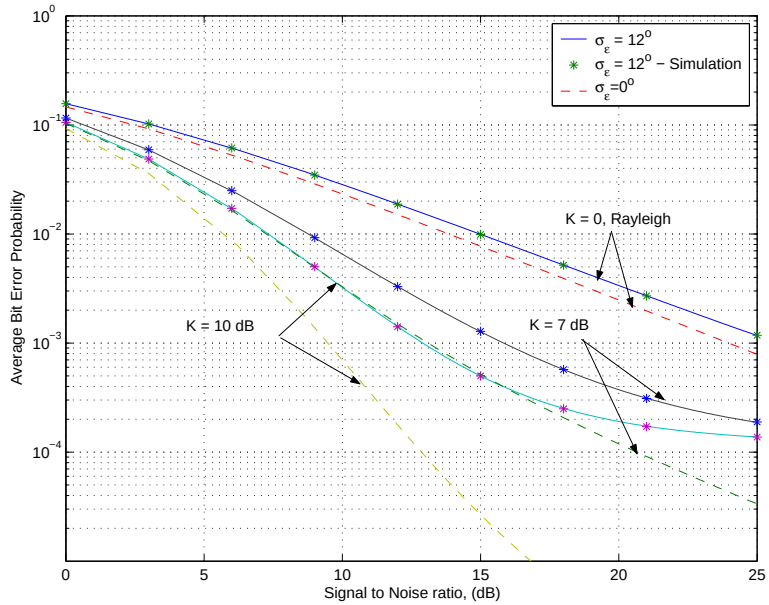

Figure 4.5. Average BEP of QPSK in the presence of AWGN, Rician fading, and phase recovery error ($\sigma_\varepsilon = 12^o$).

original penalty due to the existing noise impairments (channel fading and AWGN). In the literature, it is common to translate the increase in a certain average BEP into an equivalent increase of SNR that maintain the same BEP as that of a system without phase recovery noise. This increase in SNR is usually referred to as the noisy reference loss [28], [30] or detection loss [29], and the later will be used in our context. Computation of the detection loss for PSK systems is so important in the design of the practical coherent PSK receivers [28], [29], and [30]. The detection loss of BPSK and QPSK systems over Rayleigh fading channel at average BEP of (10^{-3}) is shown in Table 4.1, where the the blank spaces denote a virtual loss of ∞. Table 4.1 indicates that imperfect phase recovery can cause more penalty in QPSK than BPSK systems, the reason behind the severity in QPSK system is the induced cross coupling, which is resulted from imperfect phase recovery, between the two orthogonal components of the QPSK system [64]. Gray mapping of the information bits into the signal vectors produces QPSK that is equivalent

Table 4.1. Detection loss in decibels for BPSK and QPSK over Rayleigh fading at BEP 10^{-3}

σ_ϵ	BPSK	QPSK
8^o	0.087	0.390
10^o	0.139	0.722
12^o	0.205	1.822
14^o	0.289	9.527
16^o	0.397	
18^o	0.561	
20^o	0.928	

to the combination of two BPSK systems modulated onto quadrature components of the carrier [64]. Under the imperfection of AWGN and channel fading, the two binary components of the QPSK can be detected orthogonally and the total BEP is the same as BPSK [2]. On the other hand, the existence of the phase recovery error will destroy the orthogonality between the two components. The resulting cross coupling causes a severe system performance degradation for the QPSK system [29], and [64]. The values of detection loss in Table 4.1 are in agreement with the values given in [29].

The detection loss for BPSK and QPSK in the case of Nakagami-m is shown in Table 4.2 for two values of the fading parameter m at BEP of 10^{-4}, and the detection loss for Rician fading are provided for two values of the fading parameter K (10 dB and 7 dB) in Table 4.3.

Comparing the values in Figures 4.2, 4.3, 4.4, 4.5, Table 4.1, 4.2, 4.3 one can recognize that the detection loss at a certain average BEP is dependent upon the modulation scheme, the included noise impairments, and indeed the statistical properties of phase synchronization error (standard deviation σ_ε).

Computation of the average BEP of BPSK and QPSK using the infinite series expressions proposed in our study is found to be convergent with reasonable number of

Table 4.2. Detection loss in decibels for BPSK and QPSK in the presence of AWGN, Nakagami-m fading, and phase recovery error at average BEP 10^{-4}

σ_ϵ	$m = 2$		$m = 4$	
	BPSK	QPSK	BPSK	QPSK
8^o	0.089	0.648	0.091	1.063
10^o	0.144	1.599	0.151	2.587
12^o	0.216		0.234	
14^o	0.314		0.360	
16^o	0.467		0.581	
18^o	0.855		1.112	
20^o	2.614		3.134	

Table 4.3. Detection loss in decibels for BPSK and QPSK in the presence of AWGN, Rician fading, and phase recovery error at average BEP 10^{-4}

σ_ϵ	$K = 10$ dB		$K = 7$ dB	
	BPSK	QPSK	BPSK	QPSK
8^o	0.079	1.035	0.056	0.473
10^o	0.147	2.596	0.138	1.278
12^o	0.233		0.213	
14^o	0.356		0.300	
16^o	0.581		0.434	
18^o	1.160		0.871	
20^o	3.400		3.317	

terms. It should be pointed out that these infinite series expressions have alternating sign and they satisfy the conditions of Leibniz theorem for series convergence [65]. According to Leibniz theorem for alternating series [65], any alternating series $\pm\sum_{j=0}^{\infty}(-1)^{j+1}c_j$ (where $c_j \geq 0, \forall j$) converges if it satisfies two conditions: it is a decreasing sequence i.e. ($c_{j+1} \leq c_j$), and $\lim_{j\to\infty} c_j = 0$. Leibniz has also shown that the residual sum (truncating error) is less than the absolute value of the first neglecting term i.e. $|R_n| \leq c_{j+1}$, where the residual sum $R_n = \pm\sum_{j=n+1}^{\infty}(-1)^{j+1}c_j$ and $|.|$ denotes the absolute value. It can be shown that our series expressions for the average BEP of the faded BPSK and QPSK

with imperfect phase recovery meet Leibniz's conditions. Table 2.4 shows the required number of terms for the BEP expressions of BPSK and QPSK under Nakagami-m fading to reach a truncation error $\leq 10^{-14}$ over (0 dB - 25 dB) SNR's range. The average BEP of Rician faded BPSK and QPSK is expressed in terms of double series expression, the number of iterations required to reach a truncation error of $\leq 10^{-14}$ for the outer series (with index ℓ) in the average BEP expression is shown in Table 2.5, where the inner infinite series (with index k) requires (23-53) terms to converge with an accuracy of 10^{-14} for the given values of the fading parameter K, σ_ϵ, and SNR's range. The convergence of the inner series (with index k) can be proved by the comparison with series expression of the modified Bessel function of the first kind.

The approach proposed in [30] analyzes the performance of faded PSK systems under imperfect phase recovery using the Maclaurin series. It can be shown that under approximation adopted in [30], the average BEP of Rayleigh faded BPSK with phase recovery error is given by

$$P_2(E) \simeq \frac{1}{2}\left[\frac{\sqrt{1+\rho}-\sqrt{\rho}}{\sqrt{1+\rho}} + \frac{\sigma_\varepsilon^2}{2}\frac{\sqrt{\rho}}{(1+\rho)^{\frac{3}{2}}}\right] \tag{4.32}$$

Illustrations in Figure 4.6 are the exact and approximated average BEP of Rayleigh faded BPSK under phase recovery error, where the exact value is computed using (4.19) and the approximated value is evaluated using (4.32). It is obvious from Figure 4.6 that the results of the exact and approximate average BEP expressions are in agreement for small and moderate SNR, but the difference between the two is getting large at high SNR (above 30 dB), the reason behind this difference can be attributed to the fact that the approximated error probability consists only the first two nonzero terms of the Maclaurin series expansion of the conditional BEP.

Coherent PSK systems provide performance improvement over noncoherent (differential) systems [12]. The noncoherent receptions of PSK systems avoid the need for

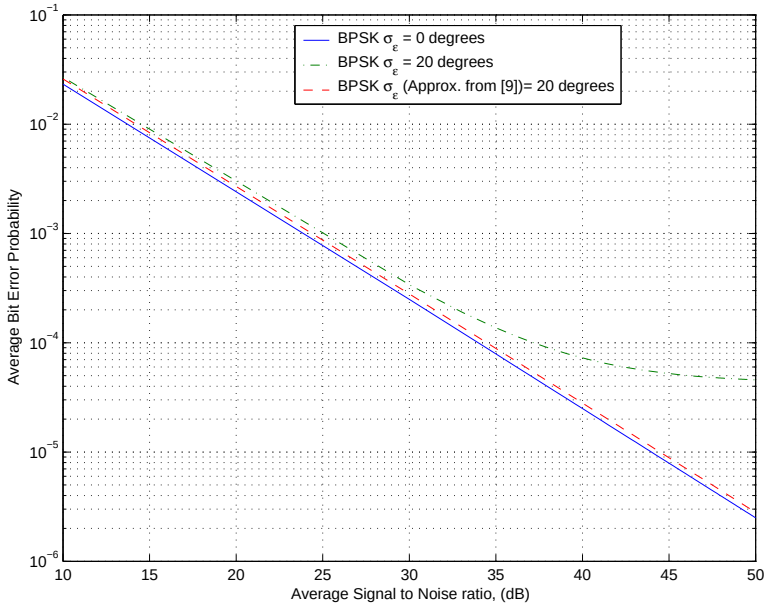

Figure 4.6. The average bit error probability of BPSK in the presence of AWGN, Rayleigh fading, and phase recovery error for exact and approximate evaluations.

carrier recovery, and therefore achieve fast synchronization [12]. Also, the receiver implementation in case of differential systems is simpler than coherent receivers [12]. For the previous reasons, it is necessary to study the performance of coherent PSK systems in the presence of imperfect phase recovery and differential form of PSK systems. In the following analysis, the fading amplitude and the phase variations over two consecutive symbols are assumed to be constant. In Figure 4.7, the average BEP of the BPSK with phase error ($\sigma_\varepsilon = 20^o$) and differential binary phase shift keying (DBPSK) system under Nakagami-m fading is plotted, and Figure 2.8 shows the average BEP of the Nakagami-m faded QPSK with phase error ($\sigma_\varepsilon = 12^o$) and differential quaternary phase shift keying (DQPSK) systems.

Equivalently, Figures 4.9,4.10 show the performance of the coherent (BPSK and QPSK) and noncoherent (DBPSK and DQPSK) systems over Rician fading. Figures 4.7, 4.8, 4.9, 4.10 indicate that the performance of coherent PSK systems with imperfect phase

Table 4.4. The number of iterations required to reach a truncation error $\leq 10^{-14}$ for the series expression of the average BEP of Nakagami-m faded BPSK and QPSK over (0dB-25dB) SNR

m	BPSK		QPSK	
	$\sigma_\epsilon = 12^o$	$\sigma_\epsilon = 20^o$	$\sigma_\epsilon = 12^o$	$\sigma_\epsilon = 20^o$
1	$12-20$	$10-14$	$14-20$	$11-14$
2	$11-20$	$9-14$	$13-20$	$10-14$
4	$11-20$	$9-14$	$12-20$	$10-14$
6	$10-20$	$9-14$	$12-20$	$10-14$

Table 4.5. The number of iterations required to reach a truncation error $\leq 10^{-14}$ for the series expression of the average BEP of Rician faded BPSK and QPSK over (0dB-25dB) SNR

K	BPSK		QPSK	
	$\sigma_\epsilon = 12^o$	$\sigma_\epsilon = 20^o$	$\sigma_\epsilon = 12^o$	$\sigma_\epsilon = 20^o$
0	$12-20$	$10-14$	$14-20$	$11-14$
3 dB	$11-20$	$9-14$	$13-20$	$10-14$
7 dB	$11-20$	$9-14$	$12-20$	$10-14$
10 dB	$9-20$	$9-14$	$11-20$	$10-14$

recovery shows an improvement over the differential PSK systems till a certain limit, after that point differential systems become more effective. Another measure of interest is the phase precision [29], phase precision at certain average BEP and SNR in the differential form determines the standard deviation of the phase error that maintains the same BEP and SNR in the coherent scheme. Table 4.6, 4.7 show the phase precision requirements for BPSK and QPSK over Nakagami-m and Rician fading channels at average BEP of 10^{-3}. It can be recognized from these two tables that QPSK system needs more stringent phase precision than BPSK system.

Through our analysis, the carrier phase error ε is modeled by Tikhonov distribution. The Tikhonov model is applicable for both of the carrier's phase estimation

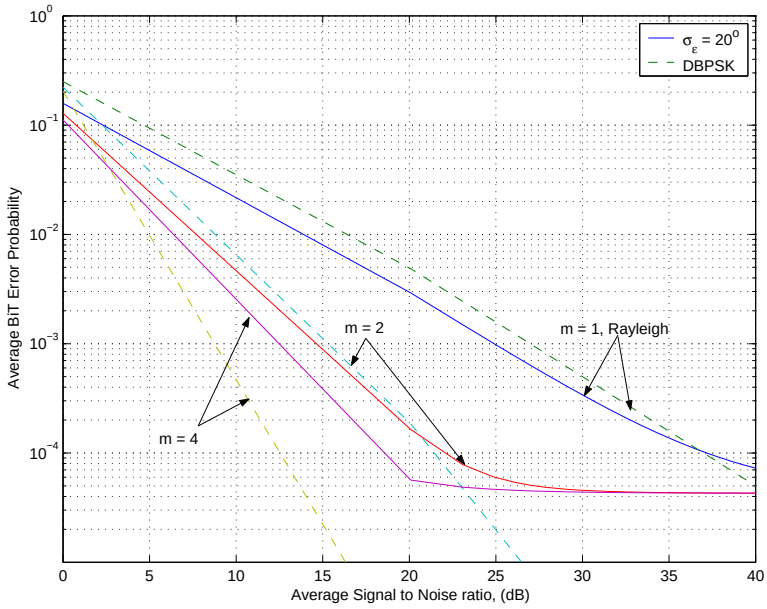

Figure 4.7. Average BEP of BPSK with phase recovery error ($\sigma_\varepsilon = 20^o$) and DBPSK in the presence of and Nakagami-m fading, and AWGN.

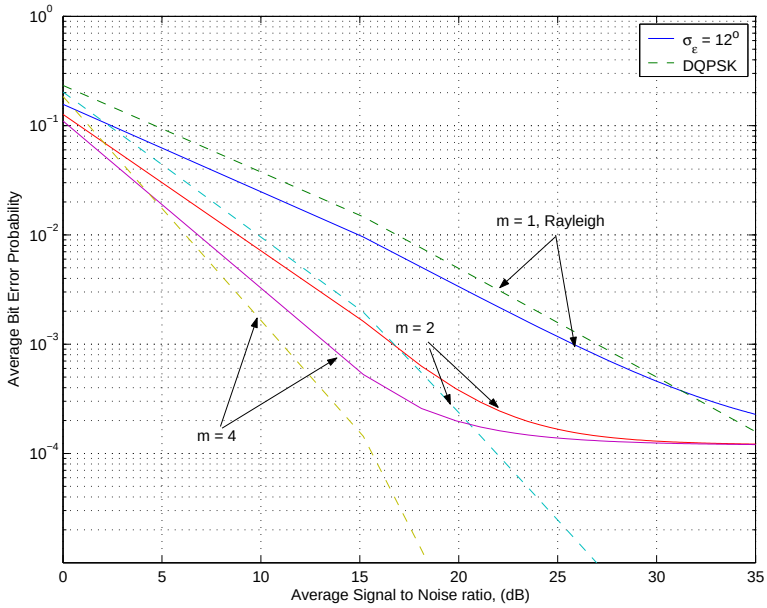

Figure 4.8. Average BEP of QPSK with phase recovery error ($\sigma_\varepsilon = 12^o$) and DQPSK in the presence of Nakagami-m fading, and AWGN.

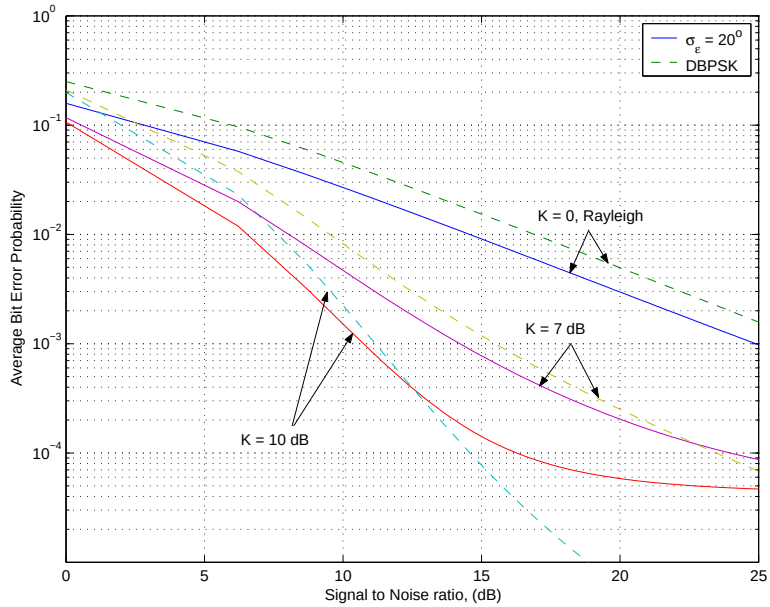

Figure 4.9. Average BEP of BPSK with phase recovery error ($\sigma_\varepsilon = 20^o$) and DBPSK in the presence of Rician fading, and AWGN.

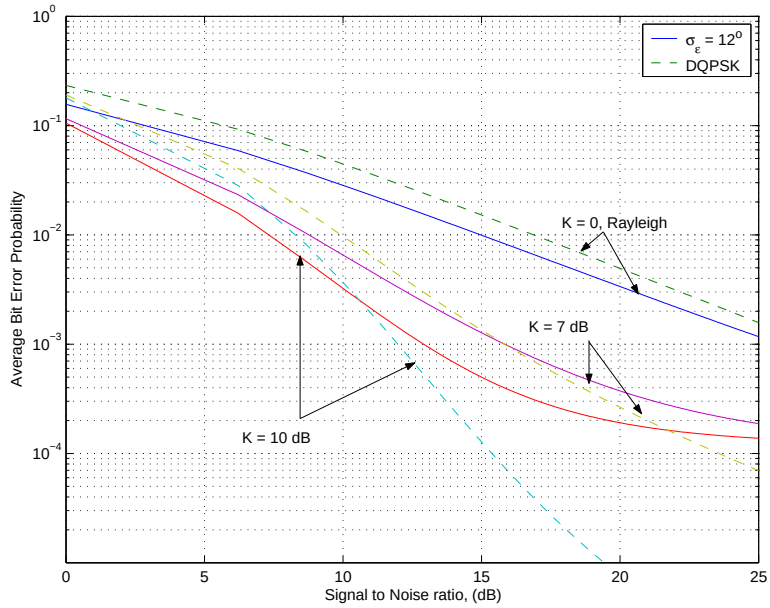

Figure 4.10. Average BEP of QPSK with phase recovery error ($\sigma_\varepsilon = 12^o$) and DQPSK in the presence of Rician fading, and AWGN.

Table 4.6. Phase precision requirements for coherent Nakagami-m faded BPSK and QPSK to achieve average BEP of10^{-3} as that of their differential versions

m	BPSK	QPSK
1	22.93°	12.77°
2	22.34°	12.09°
4	21.22°	11.28°
6	20.63°	10.95°
8	20.29°	10.78°
10	20.08°	10.68°

Table 4.7. Phase precision requirements for coherent Rician faded BPSK and QPSK to achieve average BEP of10^{-3} as that of their differential versions

K	BPSK	QPSK
2	22.90°	12.72°
4	22.81°	12.62°
6	22.55°	12.29°
8	21.89°	11.67°
10	21.00°	11.15°

techniques, the suppressed carrier-tracking loop and the pilot tone, when the coherent receiver employs a first order PLL in the presence of AWGN. The Tikhonov model can also be appropriate for characterization of the statistics of the phase error when a second order PLL is utilized under the same circumstances and provided that the loop SNR is sufficiently large [24]. It should be pointed out that the effect of channel fading on the performance of the PLL was excluded in our analysis. Demonstration the channel fading on the performance of PLL implies that the loop SNR, γ, is a random variable and it is proportional to the fading power (α^2) [66]. In this case, the degradation factor $\frac{I_{2\ell+1}(\gamma)}{I_0(\gamma)}$ in the BEP expressions needs to be averaged over the pdf of γ.

Thus far, the emphasis of this Chapter was to analyze the performance of BPSK and QPSK in the presence of channel fading, AWGN, and imperfect phase recovery. In most

cases, the series expressions of the average BEP can be calculated with a considerable accuracy by using small number of terms of the expansion. The accuracy of the BEP expressions is verified by comparison with quasi-analytic simulation. Simulation results confirm the accuracy of our BEP expressions and underline the potential of our approach. The numerical results of the detection loss in our study agree with those given in [29]. Computation of the average BEP was shown to be stable over a wide range of SNR with different combinations of the fading parameter (m or K) and the variance of the phase noise (σ_{ε}^2). Thus, it was possible to calculate the decrease in the mean SNR due to the imperfect phase recovery. These results are useful in the design of PSK systems. For example, the detection loss can be interpreted as an additional margin in the power link budget to compensate for the power loss due phase recovery error [29].

4.7 Conclusion

Using the Fourier series expansion and the associated Legendre functions, the average BEP of BPSK and QPSK systems was computed in the presence of AWGN, slow flat multipath channel fading, and imperfect phase recovery. The series expressions of the average BEP proposed in our study are found to be convergent with reasonable number of terms. The detection loss and phase precision have been calculated for several fading distributions. It has been shown that imperfect phase recovery can lead to a severe system performance degradations for QPSK system. Also, it is verified that QPSK system needs more stringent phase precision than BPSK system. The numerical results provided in this study are in agreement with the approach proposed in [29], and they can be helpful in the design of the practical coherent PSK receivers.

CHAPTER 5

MQAM WITH MRC DIVERSITY RECEPTION

A method for computing the exact average symbol error probability (SEP) of the rectangular M-ary quadrature amplitude modulation (MQAM) with maximal ratio combining (MRC) diversity over L independent and equal-correlated Nakagami-m fading channels with *arbitrary* fading index m is presented. Two models of MQAM receivers are analyzed. Closed-form expressions are provided for the average SEP in terms of the Appell and Gauss hypergeometric functions. Simplified error expressions are proposed when the product Lm is either integer or half-integer. The distinction between the performance of the two MQAM schemes is discussed. Finally, the penalty in signal-to-noise ratio (SNR) due to equal-correlated Nakagami-m channel fading is investigated.

5.1 Introduction

MQAM is widely used in high-rate data transmission over wireless links [67]. The Nakagami-m distribution can be used to characterize a variety of mobile radio fading environments. Nakagami-m fading model can model Rayleigh channel fading ($m = 1$), one-sided Gaussian distribution ($m = \frac{1}{2}$), unfaded channel ($m = \infty$), and it can also approximate the Rician fading distribution.

The average SEP of the faded MQAM systems has been studied extensively in the literature. Starting with the pioneering work of Proakis, he has analyzed the average SEP of MQAM over additive white Gaussian noise (AWGN) [2]. In [68], the authors

studied the average SEP of MQAM with MRC reception over independent Rayleigh fading channels. Goldsmith and Alouini in [33] have presented a moment generating function (MGF)-based approach to analyze the average SEP for MQAM over several independent fading channels, moreover they used alternative form of the Gaussian and Marcum Q-functions to reach SEP expressions, which involve a single finite-range integral. The authors in [69],[34] proposed closed-form expressions for the average SEP of of MQAM over independent and correlated Nakagami-m fading channels, however the closed form expressions are restricted for positive integer fading index m. By contrast, in this Chapter, closed-form expressions are provided for the average SEP with arbitrary fading index m over independent and equally-correlated Nakagami-m fading channels. Moreover, simplified error expressions are proposed when the product Lm is either integer or half-integer. The average SEP expressions are given in terms of the Appell and Gauss hypergeometric functions.

This Chapter is organized as follows, the problem for the common model of MQAM is formulated in Section 5.2. In Section 5.3, the average SEP of MQAM over independent identically distributed (iid) Nakagami-m fading channels is obtained by averaging the conditional probability over the probability density function (pdf) of the total SNR per bit at the combiner output. In Section 5.4, the analysis of the SEP of MQAM is extended to the case of equal-correlated Nakagami-m channel fading. Section 5.5, clarifies the structure and performance analysis of the simplified model of MQAM. Results are discussed in Section 5.6. Finally, concluding remarks are presented in Section 5.7.

5.2 System Model

MQAM modulation schemes are characterized by the fact that the information sequence is encoded in the amplitudes of two phase-quadrature carriers. The average SEP

of MQAM is mainly a function of the minimum distance of the signal constellation and the average transmitted signal power. For this reason, it is appropriate to choose the signal constellation that corresponds to the minimum average transmitted power for a given constellation size (M) and minimum distance. Signal constellation of MQAM can be arranged in many ways [2]. Rectangular MQAM is frequently employed since: first MQAM can be generated using two PAM signals modulated into two phase-quadrature carriers, second they can be easily demodulated, and third the average transmitted power required to achieve a given minimum distance with rectangular MQAM is slightly greater than the required average power for the optimum MQAM signal constellation. Assuming rectangular MQAM with equally probable symbols and $\log_2(M)$ is even, the ith transmitted signal $s_i(t)$ takes the form:

$$\begin{aligned} s_i(t) =& A_{ic} u_M(t) \cos(\omega_c t) - A_{is} u_M(t) \sin(\omega_c t) \\ =& \sqrt{A_{ic}^2 + A_{is}^2}\, u_M(t) \cos\left\{ \omega_c t + \tan^{-1}\left(\frac{A_{is}}{A_{ic}} \right) \right\} \end{aligned} \tag{5.1}$$

where $A_{ic}, A_{is} = d(2i - 1 - \sqrt{M})$, $i \in \{1, 2, \ldots, \sqrt{M}\}$, d is a scaling parameter, ω_c is the radian carrier frequency, and $u_M(t)$ is the pulse shaping signal and it is assumed to be constant during the pulse interval T (rectangular shaping pulse) and it has the following form

$$u_M(t) = \begin{cases} \sqrt{\frac{2}{T}}, & 0 \le t \le T \\ 0, & \text{elsewhere} \end{cases} \tag{5.2}$$

The received signal on the ℓth channel can be expressed as

$$r_{i\ell}(t) = \alpha_\ell u_M(t) \{ A_{ic} \cos(\omega_c t + \varphi_\ell) - A_{is} \sin(\omega_c t + \varphi_\ell) \} + n_\ell(t) \tag{5.3}$$

where $n_\ell(t)$ is the zero mean AWGN, which has a double-sided power spectral density of $N_0/2$ W/Hz. φ_ℓ is the random phase introduced by the ℓth channel, which is uniformly distributed between $[-\pi, \pi]$, and α_ℓ is the fading envelope. The channel parameters α_ℓ

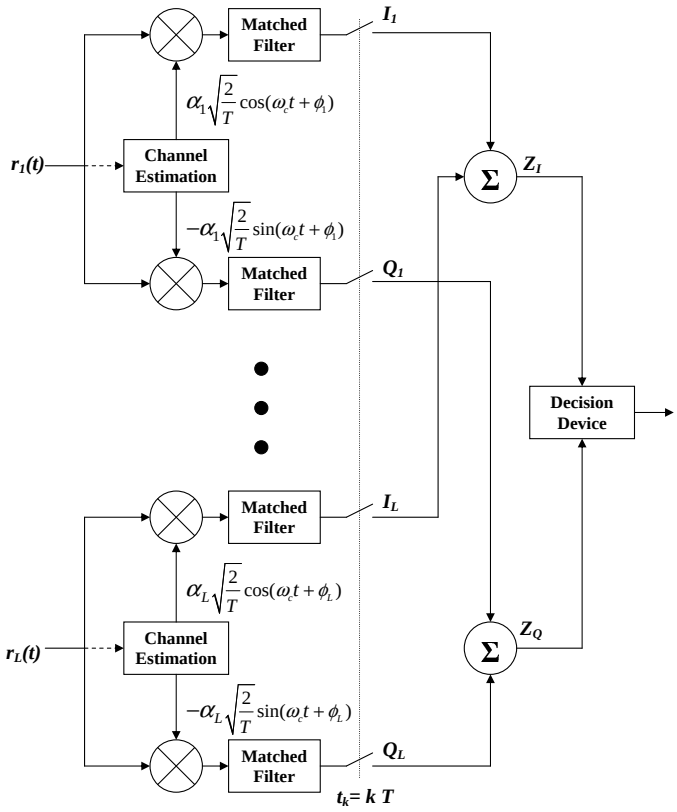

Figure 5.1. Common quadrature MQAM receiver with MRC diversity.

and φ_ℓ are assumed to be slowly varying, so that they can be considered constant over the signaling interval T.

The demodulation and detection of the received MQAM signals can be accomplished using the common quadrature coherent MQAM receiver. Figure 5.1 shows the block diagram of L-branch quadrature MQAM receiver with MRC diversity. Assuming perfect channel estimation, the conditional SEP of the rectangular MQAM can be written as [2]

$$P_M(e|\gamma_t) = 2q\ \mathrm{erfc}(\sqrt{p\gamma_t}) - q^2\mathrm{erfc}^2(\sqrt{p\gamma_t}) \tag{5.4}$$

where $\gamma_t = \frac{E_b}{N_0} \sum_{\ell=1}^{L} \alpha_\ell^2 = \sum_{\ell=1}^{L} \gamma_\ell$ is the total conditional SNR per bit and E_b is the average transmitted energy per bit, which is given by

$$E_b = \frac{1}{\sqrt{M}\log_2(M)} \sum_{m=1}^{\sqrt{M}} (A_{mc}^2 + A_{ms}^2) = \frac{2d^2(M-1)}{3\log_2(M)} \tag{5.5}$$

The conditional SEP in (5.4) can be written in terms of the confluent hypergeometric function ${}_1F_1(x;y;z)$ [6]

$$\begin{aligned} P_M(e|\gamma_t) =& 2q - q^2 + \frac{4q(q-1)\sqrt{p\gamma_t}e^{-p\gamma_t}}{\sqrt{\pi}} \; {}_1F_1(1;1.5;p\gamma_t) \\ & - \frac{4q^2 p\gamma_t e^{-2p\gamma_t}}{\pi} \left({}_1F_1(1;1.5;p\gamma_t)\right)^2 \end{aligned} \tag{5.6}$$

where we have used the fact [6]

$$\text{erf}(x) = 1 - \text{erfc}(x) = \frac{2xe^{-x^2}}{\sqrt{\pi}} \; {}_1F_1(1;1.5;x^2) \tag{5.7}$$

5.3 Statistically Independent Nakagami-m Channel Fading

If the channel fades α_ℓ is assumed to be frequency-nonselective, slowly varying, and Nakagami-m distributed, then the pdf of α_ℓ can be written as [4]

$$f_{\alpha_\ell}(\alpha_\ell) = \frac{2m_\ell^{m_\ell} \alpha_\ell^{2m_\ell - 1}}{\Omega_\ell^{m_\ell}\Gamma(m_\ell)} \; e^{-\frac{m_\ell \alpha_\ell^2}{\Omega_\ell}}, \quad \alpha_\ell \geq 0 \tag{5.8}$$

where $\Gamma(.)$ is the Gamma function and m_ℓ is the Nakagami-m fading parameter for the ℓth branch, which ranges from 0.5 to ∞ , and Ω_ℓ is the mean squared of α_ℓ. Assuming the fades α_ℓ's on all the channels are identically distributed ($m_\ell = m$ and $\Omega_\ell = \Omega, \forall \ell \in \{1, 2, ..., L\}$), the pdf of the total conditional SNR γ_t can be expressed as

$$f_{\gamma_t}(\gamma_t) = \left(\frac{m}{\bar{\gamma}}\right)^{Lm} \frac{\gamma_t^{Lm-1}}{\Gamma(Lm)} \; e^{-\frac{m\gamma_t}{\bar{\gamma}}}, \quad \gamma_t \geq 0 \tag{5.9}$$

where $\bar{\gamma} = \frac{\Omega E_b}{N_0}$ is the average SNR per bit per branch. The total average SEP of MQAM is

$$P_M(e) = \int_0^\infty P_M(e|\gamma_t) f_{\gamma_t}(\gamma_t) d\gamma_t = 2q - q^2 + H_1 - H_2 \tag{5.10}$$

where H_1 is

$$H_1 = \frac{4q(q-1)\sqrt{p\bar{\gamma}}m^{Lm}\Gamma(Lm+0.5)}{\sqrt{\pi}\Gamma(Lm)(m+p\bar{\gamma})^{Lm+0.5}}\ {}_2F_1\left(Lm+0.5,1;1.5;\frac{p\bar{\gamma}}{m+p\bar{\gamma}}\right) \tag{5.11}$$

given that for $\mathrm{Re}(b)>0$, and $|k|<|h|$ [58]

$$\int_0^\infty {}_1F_1(a;c;kt)t^{b-1}e^{-st}dt = \frac{\Gamma(b)}{s^b}\ {}_2F_1\left(a,b;c;\frac{k}{s}\right) \tag{5.12}$$

where ${}_2F_1(w,x;y;z)$ is the Gaussian hypergeometric function [6]. H_2 is given by

$$H_2 = \frac{4q^2\bar{\gamma}pLm^{Lm+1}}{\pi(m+2p\bar{\gamma})^{Lm+1}}F_2\left(Lm+1;1,1;1.5,1.5;\frac{p\bar{\gamma}}{m+2p\bar{\gamma}},\frac{p\bar{\gamma}}{m+2p\bar{\gamma}}\right) \tag{5.13}$$

provided that for $\mathrm{Re}(d)>0$, and $|k_1|+|k_2|<|h|$ [70]

$$\int_0^\infty {}_1F_1(a_1;b_1;k_1t)\ {}_1F_1(a_2;b_2;k_2t)t^{d-1}e^{-ht}dt = h^{-d}\Gamma(d)F_2\left(d;a_1,a_2;b_1,b_2;\frac{k_1}{h},\frac{k_2}{h}\right) \tag{5.14}$$

given that $F_2(d;a_1,a_2;b_1,b_2;x,y)$ is the Appell's hypergeometric function [44], which is defined by

$$F_2(d;a_1,a_2;b_1,b_2;x,y) = \sum_{m,n=0}^{\infty}\frac{(d)_{m+n}(a_1)_m(a_2)_n}{(b_1)_m(b_2)_n m!n!}x^m y^n \tag{5.15}$$

where $(\delta)_m$ is the shifted factorial. The average SEP can be further reduced for the following two cases

5.3.1 Lm is Integer

When Lm is integer, H_1 can be reduced into the following expression

$$H_1 = \frac{4q(q-1)\sqrt{p\bar{\gamma}}\ \Gamma(Lm+0.5)}{\sqrt{\pi(m+p\bar{\gamma})}\Gamma(Lm)}\sum_{k=0}^{Lm-1}\frac{(0.5)_k(1-Lm)_k}{k!(1.5)_k}\left(\frac{\bar{\gamma}p}{m+\bar{\gamma}p}\right)^k \tag{5.16}$$

provided that [71]

$$\begin{aligned} {}_2F_1(a,b;c;z) &= (1-z)^{c-a-b}\ {}_2F_1(c-a,c-b;c;z) \\ {}_2F_1(-n,b;c;z) &= \sum_{k=0}^{n}\frac{(-n)_k(b)_k}{(c)_k k!} \quad , \quad n \text{ is integer} \end{aligned} \tag{5.17}$$

and H_2 can be simplified as

$$H_2 = \frac{4q^2 p\bar{\gamma}}{\pi(m+2p\bar{\gamma})} \sum_{k=0}^{Lm-1} \left(\frac{m}{m+2\bar{\gamma}p}\right)^k \, {}_2F_1\left(1, k+1; 1.5; \frac{p\bar{\gamma}}{m+2p\bar{\gamma}}\right) \tag{5.18}$$

given that for any positive integer n (proved in Appendix B)

$$F_2\left(n; 1, 1; 1.5, 1.5; \frac{k}{h}, \frac{k}{h}\right) = \frac{h^{n-1}}{(n-1)(h-2k)^{n-1}} \sum_{j=0}^{n-2} \left(\frac{h-2k}{h}\right)^j \, {}_2F_1\left(1, j+1; 1.5; \frac{k}{h}\right) \tag{5.19}$$

5.3.2 Lm is Half-Integer

If Lm is half integer, H_2 can be reduced to (using the identity in [70, eq. 3.2]),

$$\begin{aligned} H_2 = &\frac{4q^2 pLm^{Lm+1}}{\pi(m+2p\bar{\gamma})^{Lm-1}} \sum_{k=0}^{Lm-0.5} \left\{ \frac{(0.5-Lm)_k}{(1.5)_k} \sum_{r=0}^{Lm-0.5+k} \frac{(0.5-Lm-k)_r(-p\bar{\gamma})^{r+k}}{(1.5)_r(m+p\bar{\gamma})^{r+k+2}} \right. \\ &\left. \times \; {}_2F_1\left(1+r, 1+k; 1.5+r; \frac{(p\bar{\gamma})^2}{(m+p\bar{\gamma})^2}\right) \right\} \end{aligned} \tag{5.20}$$

5.4 Equal-Correlated Nakagami-m Channel Fading

In equal-correlated Nakagami-m fading, the power correlation between any two fading envelopes is assumed to be constant and it equals λ

$$\lambda = \frac{\mathrm{cov}(\gamma_i, \gamma_j)}{\sqrt{\mathrm{var}(\gamma_i)\mathrm{var}(\gamma_j)}}, \quad i \neq j, \quad i, j = 1, 2, \cdots, L \tag{5.21}$$

Assuming the fades α_ℓ's on all the channels are identically distributed, then the pdf of the total conditional SNR γ_t can be expressed as [36]

$$f_{\gamma_t}(\gamma_t) = \frac{m^{Lm}\gamma_t^{Lm-1} e^{-\frac{m\gamma_t}{\bar{\gamma}(1-\rho)}}}{\bar{\gamma}^{Lm}(1-\rho)^{m(L-1)}(1-\rho+L\rho)^m \Gamma(Lm)} \, {}_1F_1\left(m; Lm; \frac{Lm\rho\gamma_t}{\bar{\gamma}(1-\rho)(1-\rho+L\rho)}\right) \tag{5.22}$$

where $\lambda = \rho^2$ and ρ is the correlation coefficient between the accompanying Gaussian process that are used to generate the Nakagami-m random variables at the input of the L-branch receiver [36].

The total average SEP of MQAM is

$$P_M(e) = \int_0^\infty P_M(e|\gamma_t) f_{\gamma_t}(\gamma_t) d\gamma_t = 2q - q^2 + T_1 - T_2 \tag{5.23}$$

where T_1 and T_2 are given by

$$\begin{aligned} T_2 =& \frac{4q(q-1)\sqrt{\bar{\gamma}p/\pi} m^{Lm} (1-\rho)^{m+0.5} \Gamma(Lm+0.5)}{\Gamma(Lm)(m+p\bar{\gamma}(1-\rho))^{Lm+0.5}(1-\rho+L\rho)^m} \\ & \times F_2\left(Lm+0.5; 1, m; 1.5, Lm; \frac{p\bar{\gamma}(1-\rho)}{m+p\bar{\gamma}(1-\rho)}, \frac{Lm\rho}{(1-\rho+L\rho)(m+p\bar{\gamma}(1-\rho))}\right) \end{aligned} \tag{5.24}$$

$$\begin{aligned} T_3 =& \frac{4q^2 p\bar{\gamma} m^{Lm}(1-\rho)^{m+1}}{\pi(1-\rho+L\rho)^m (m+2p\bar{\gamma}(1-\rho))^{Lm+1}} \sum_{k=0}^{\infty} \left\{ \frac{(m)_k}{k!} \right. \\ & \times (Lm+k)\left(\frac{Lm\rho}{(1-\rho+L\rho)(m+2p\bar{\gamma}(1-\rho))}\right)^k \\ & \left. \times F_2\left(Lm+k+1; 1, 1; 1.5, 1.5; \frac{p\bar{\gamma}(1-\rho)}{m+2p\bar{\gamma}(1-\rho)}, \frac{p\bar{\gamma}(1-\rho)}{m+2p\bar{\gamma}(1-\rho)}\right)\right\} \end{aligned} \tag{5.25}$$

When Lm is integer, T_2 can be written in the following form

$$\begin{aligned} T_2 =& \frac{4q^2 p\bar{\gamma}(1-\rho)^{m+1}}{\pi(1-\rho+L\rho)^m (m+2p\bar{\gamma}(1-\rho))} \sum_{k=0}^{\infty} \left\{ \frac{(m)_k (L\rho)^k}{(1-\rho+L\rho)^k k!} \right. \\ & \left. \times \sum_{j=0}^{Lm+k-1} \left(\frac{m}{m+2p\bar{\gamma}(1-\rho)}\right)^j {}_2F_1\left(1, j+1; 1.5; \frac{p\bar{\gamma}(1-\rho)}{m+2p\bar{\gamma}(1-\rho)}\right)\right\} \end{aligned} \tag{5.28}$$

5.5 Simplified Exact Analysis

In the quadrature MQAM receiver depicted in Figure 5.1, the input to the decision device has to be compared with the M possible transmitted signals. When M is large, the structure of the decision device becomes more complex, costly, and it may introduce some delay in the detection process. An alternative realization for the quadrature MQAM receiver can be drawn as shown in Figure 5.2. In this case, the inphase and the quadrature

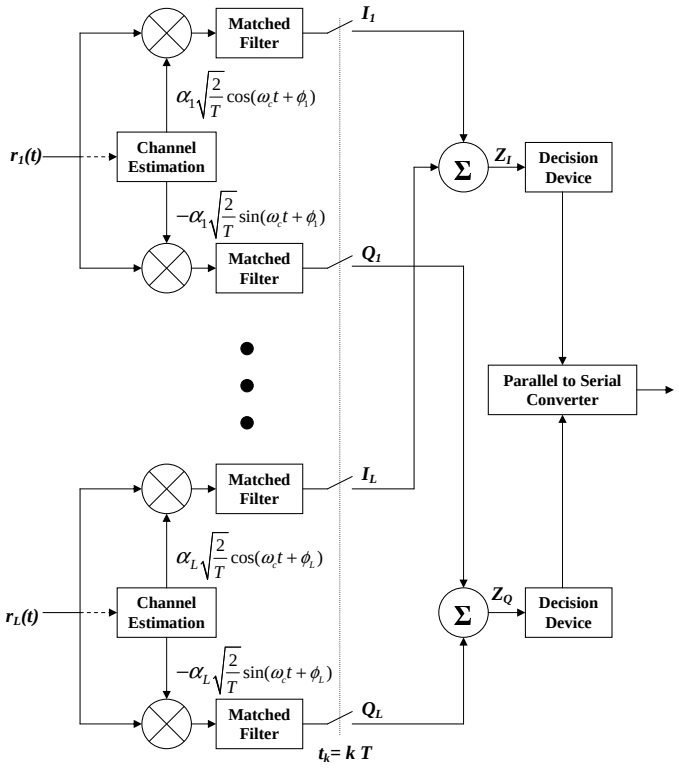

Figure 5.2. Simplified quadrature MQAM receiver with MRC diversity.

components of the received waveform are demodulated and detected independently. The receiver implementation requires two decision devices with size of $\sqrt{M}$, which lead to a simpler receiver-structure than the one considered in Section 5.2. For this reason it can be considered as an attractive candidates in high-rate data transmission over wireless links.

The total average SEP of the simplified MQAM system can be expressed as

$$P_M(e) = 1 - (1 - P_I(e))(1 - P_Q(e)) \tag{5.29}$$

where $P_I(e|\gamma_t)$ and $P_Q(e|\gamma_t)$ are the conditional SEP of the inphase and the quadrature components. Since $\log_2(M)$ is even, $P_I(e)$ and $P_Q(e)$ are equal and they are equivalent to the average SEP of PAM, $P_{\sqrt{M}}(e)$, with $\sqrt{M}$ signals, then

$$P_M(e) = 2P_{\sqrt{M}}(e) - P^2_{\sqrt{M}}(e) \tag{5.30}$$

The conditional SEP $P_{\sqrt{M}}(e|\gamma_t)$ is [2]

$$P_{\sqrt{M}}(e|\gamma_t) = q - \frac{2q\sqrt{p\gamma_t}e^{-p\gamma_t}}{\sqrt{\pi}}\ {}_1F_1(1; 1.5; p\gamma_t) \tag{5.31}$$

5.5.1 Statistically Independent Nakagami-m Channel Fading

In case of independent Nakagami-m channel fading, $P_{\sqrt{M}}(e)$ can be evaluated with the aid of (5.12)

$$P_{\sqrt{M}}(e) = q - \frac{2q\sqrt{p\bar{\gamma}}m^{Lm}\Gamma(Lm+0.5)}{\sqrt{\pi}\Gamma(Lm)(m+p\bar{\gamma})^{Lm+0.5}}\ {}_2F_1\left(Lm+0.5, 1; 1.5; \frac{p\bar{\gamma}}{m+p\bar{\gamma}}\right) \tag{5.32}$$

5.5.2 Equal-Correlated Nakagami-m Channel Fading

Under equal-correlated Nakagami-m channel fading, $P_{\sqrt{M}}(e)$ can be evaluated using (5.14). The average SEP $P_{\sqrt{M}}(e)$ is given as

$$\begin{aligned} P_{\sqrt{M}}(e) = q &- \frac{2q\sqrt{\bar{\gamma}p/\pi}m^{Lm}(1-\rho)^{m+0.5}\Gamma(Lm+0.5)}{\Gamma(Lm)(m+p\bar{\gamma}(1-\rho))^{Lm+0.5}(1-\rho+L\rho)^m} \\ &\times F_2\left(Lm+0.5; 1, m; 1.5, Lm; \frac{p\bar{\gamma}(1-\rho)}{m+p\bar{\gamma}(1-\rho)}, \frac{Lm\rho}{(1-\rho+L\rho)(m+p\bar{\gamma}(1-\rho))}\right) \end{aligned} \tag{5.33}$$

5.6 Discussion of Results

The average SEP versus average SNR per bit per branch (i.e $\bar{\gamma}$) for MQAM with MRC diversity over independent Nakagami-m fading channels is plotted for various combinations of the number of branches L, the fading parameter m, and the constellation size M in Figures 5.3, 5.4. In the same way, Figure 5.5 shows the average SEP of 16-QAM with MRC diversity over equal-correlated Nakagami-m. Comparison between the average SEP curves of the two MQAM models in Figures 5.3, 5.4 reveals that the discrepancy between them diminishes for higher diversity order, greater fading index m, or as the

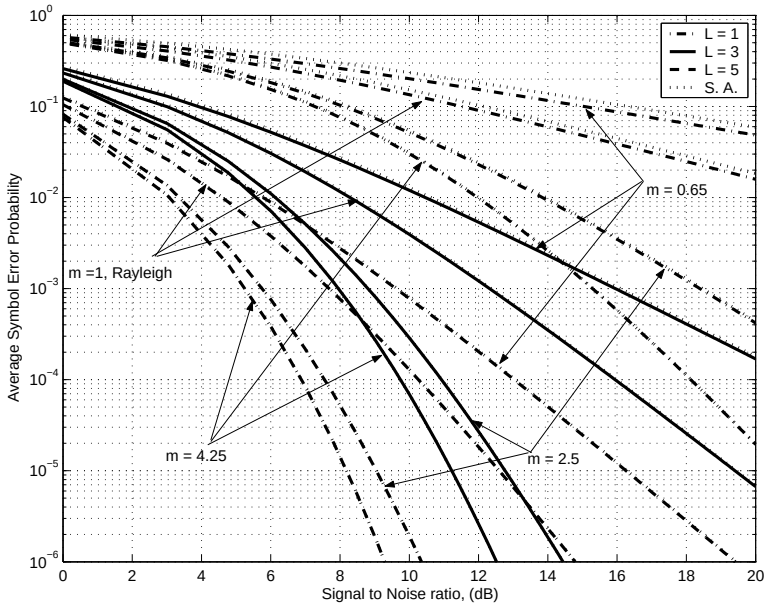

Figure 5.3. Average SEP of 16-QAM with MRC diversity over independent Nakagami-m fading channels and S. A. denotes the simplified approach.

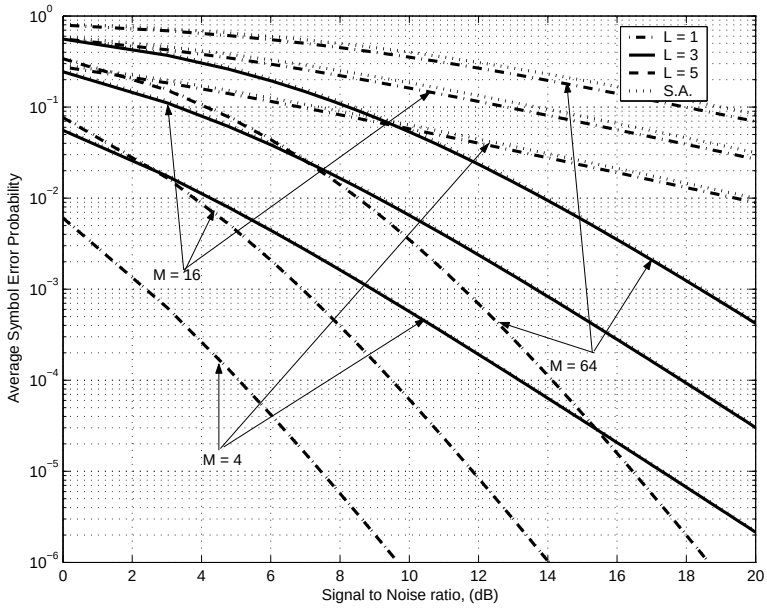

Figure 5.4. Average SEP of MQAM with MRC diversity over independent Nakagami-m ($m = 0.83$) fading channels and S. A. denotes the simplified approach.

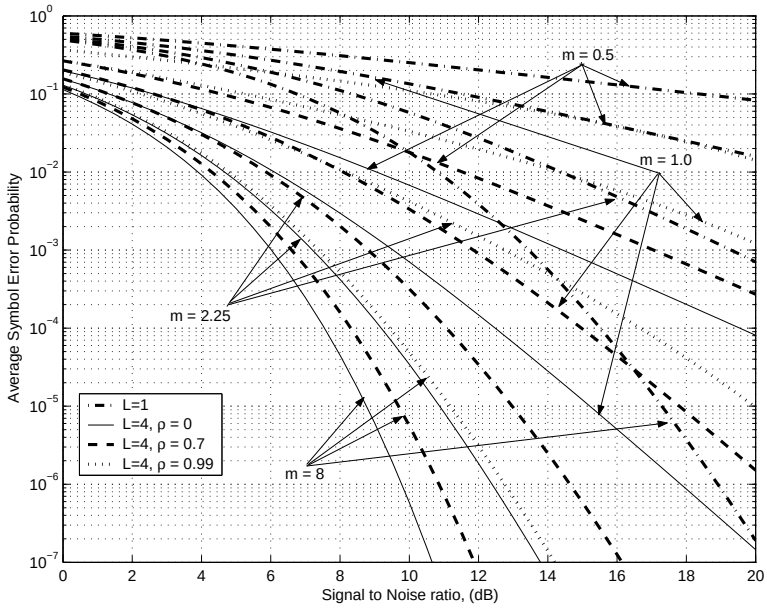

Figure 5.5. Average SEP of 16-QAM with MRC diversity over equal-correlated Nakagami-m fading channels.

received SNR per branch increases. It should be pointed that the average SEP of the simplified model is always higher or equal than the SEP of the common model (proved in Appendix B). Table 5.1 shows the penalty in SNR for the simplified model of the MQAM to achieve the same level of performance (at SEP = 10^{-4}) with the common quadrature MQAM receiver with MRC diversity over independent Nakagami-m fading channels. The results in Table 5.1 indicate that the difference between the average SEP of the two models is less that 0.13 dB when the product $Lm \geq 2$ at SEP = 10^{-4}. It is worthwhile to note that as long as the product Lm is equal, then the penalty in SNR between the two MQAM configurations will be identical. Figure 5.6 compares the average SEP of the common and simplified models for 16-MQAM with MRC diversity over Rayleigh fading channels. The percentage of difference is defined as $100 \times (P_{S.M.}(e) - P_{C.M.}(e))/P_{C.M.}(e)$ where $P_{S.M.}(e), P_{C.M.}(e)$ denote the average SEP of the common and simplified models

Table 5.1. Gain penalty in decibels of the simplified model over the common 16-QAM with MRC diversity over Nakagami-m fading channels at average SEP of 10^{-4}

m	$L = 1$	$L = 2$	$L = 4$
0.5	2.1546	0.6362	0.1299
1	0.6362	0.1299	0.0177
2	0.1299	0.0177	0.0021
4	0.0177	0.0021	0.0004
6	0.0051	0.0007	0.0001
8	0.0021	0.0004	0.0001

Table 5.2. Correlation loss on decibels for 16-QAM with MRC diversity over equal-correlated Nakagami-m fading channels at average BEP 10^{-4}

m	$L = 2$		$L = 4$	
	$\rho = 0.4$	$\rho = 0.9$	$\rho = 0.4$	$\rho = 0.9$
0.5	0.379	3.606	0.801	6.035
1	0.374	3.540	0.741	5.618
2	0.334	2.986	0.588	4.403
4	0.245	1.871	0.394	2.709
6	0.187	1.287	0.293	1.874
8	0.150	0.969	0.232	1.418

respectively. Notice that the percentage difference is less than 10% higher than the SEP of the common model when $Lm \geq 2$.

It can be recognized from Figure 5.5 that equal power correlation between the L branches causes an extra system performance degradation relative to the original penalty due to the present noise impairments (channel fading and AWGN). In the literature, it is common to translate the increase in a certain average SEP into an equivalent increase of SNR that maintain the same SEP as that without correlation. In our context, we will refer to this increase in SNR as the correlation loss. Computation of correlation loss is important in the design of the practical MQAM receivers. For example, the correlation loss can be interpreted as an additional margin in the power link budget to compensate

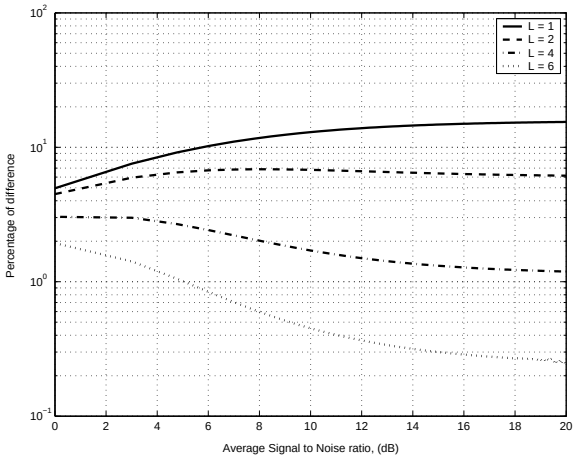

Figure 5.6. Comparison between the average SEP of the common and simplified models for 16-MQAM with MRC diversity over Nakagami-m ($m = 1.0$) fading channels.

for the power loss due to correlation. The correlation loss of 16-QAM system over equal-correlated Nakagami-m fading channels at average BEP of (10^{-4}) are given in Table 5.2. In Table 5.2, it is observed that the correlation loss is getting smaller for higher fading index m (less severe fading condition) and it is getting larger for higher diversity order L (higher correlation among more diversity branches). An interesting aspect of the correlation among the diversity reception can be observed when $\rho \rightarrow 1.0$. The L-diversity branches of the combiner act as a single channel (no diversity) when $\rho \rightarrow 1.0$. In Figure 5.5, the average SEP curves of 16-QAM degrades towards the nondiversity case and the only improvement is the gain that comes from adding the power from the diversity branches. It can be recognized from Figure 5.5 that improvement is a 6 dB gain (comes from quadrupling the power) for the fourth branch combiner.

5.7 Conclusion

The average SEP for MQAM with MRC diversity over equal-correlated Nakagami-m fading channels with *arbitrary* fading index m has been derived. No approximations are

assumed in our analysis. Two models of MQAM receivers, the common and simplified models, are analyzed. Closed-form expressions are proposed for the average SEP in terms of the Appell and Gauss hypergeometric functions. Moreover, simplified error expressions are proposed when the product Lm is either integer or half integer. The distinction between the performance of the two MQAM systems is discussed. Particularly, the simplified model penalty over the common is computed for the Nakagami-m fading channels. It is observed that the percentage difference between the average SEP of the two models is less than 10% higher than the SEP of the common model when $Lm \geq 2$. Thus, the average SEP of the simplified model can be considered as a tight upper bound on the average SEP of the common MQAM system. The correlation loss due to the equal-correlated Nakagami-m fading is computed. Finally, the results can be easily extended to analyze the performance of MPAM systems.

CHAPTER 6

CONCLUSION

This dissertation presents a unified framework to analyze the error rates of of wireless communication systems over independent and correlated fading channels. This framework is based on the integral definition of the associated Legendre functions. Using the associated Legendre functions we were able to derive closed-form expressions for the average BEP of DQPSK over L-branch independent Nakagami-m with integer Lm. In addition to that, we propose and analyze a reduced-complexity and low-cost MIMO system for wireless communications. The proposed structure is based on DPSK system with MIMO employing EGC receive diversity. The performance of PSK systems in the presence of imperfect recovery over fading channels was also analyzed using the associated Legendre functions approach. We also derive the average SEP for MQAM with MRC diversity over independent and equal-correlated Nakagami-m fading channels with arbitrary fading index m.

6.1 Contributions

In Chapter two, we introduce the associated Legendre fuctions approach and present a relatively simple error rate expressions for the performance of DPSK systems diversity reception over independent and arbitrarily correlated Rayleigh, Nakagami-m, and Rician fading channels. The associated Legendre functions approach can lead to finite closed-form expressions for the average BEP of DQPSK over L independent Rayleigh and

Nakagami-m channels, when the product Lm is integer. The error rates of DQPSK over arbitrarily correlated Nakagami-m and Rician fading channels are given in terms of a finite sum of a finite-range integral. Besides, a finite-series closed-form expression is given for the average BEP of differential binary phase shift keying (DBPSK) with EGC over independent Rician fading channels. The penalty in SNR due to arbitrarily correlated channel fading is investigated. It is observed that the system performance degradation due to the correlation among the diversity branches in Rician fading channels is more severe than that in Nakagami-m fading channels as a result of the presence of the specular component.

In Chapter three, we present and analyze the proposed structure for the DPSK with MIMO EGC. The proposed structure provides a reduced-complexity and low-cost receiver for MIMO systems compared to the coherent PSK with MIMO MRC. The average BEP for DBPSK and DQPSK with MIMO EGC over independent Rayleigh fading channels has been derived. Two approaches are introduced to analyze the error rates of DQPSK. Finite closed-form expressions for the average BEP of DBPSK and DQPSK are presented.

In Chapters two and three, the associated Legendre functions approach was devoted to analyze the performance of DPSK systems. In Chapter four, this approach is extended to analyze the performance of PSK systems with imperfect phase recovery over fading channels. Using the Fourier series expansion and the associated Legendre functions, the average BEP of BPSK and QPSK systems was computed in the presence of AWGN, slow flat multipath channel fading, and imperfect phase recovery. The series expressions of the average BEP proposed in our study are found to be convergent with reasonable number of terms.

In Chapter five, the average SEP for MQAM with MRC diversity over equal-correlated Nakagami-m fading channels with *arbitrary* fading index m has been derived.

No approximations are assumed in our analysis. Closed-form expressions are proposed for the average SEP in terms of the Appell and Gauss hypergeometric functions.

6.2 Future Work

Many possible extensions have attracted the author's attention during the course of research and are worthy for further study. These topics include the following:

- Performance analysis of DPSK systems in the presence cochannel interference.
- Study the impact of selective and/or fast fading on the error rates of DPSK systems.
- The results in this study can be extended to include the Weibull fading model.
- Extension the structure of DPSK system with MIMO EGC onto the noncoherent frequency shift keying (FSK) with MIMO employing EGC receive diversity.
- Additional work is also needed to include the cochannel interference in the analysis of DPSK system with MIMO EGC.

APPENDIX A

THE ASSOCIATED LEGENDRE FUNCTIONS

In this appendix we will show how can we compute the value of the associated Legendre functions of the second kind $Q_\nu^\mu(.)$. The associated Legendre functions are the solution of the following differential equation [6], [72]

$$\left(1-z^2\right)\frac{d^2u}{dz^2}-2z\frac{du}{dz}+\left[\nu(\nu+1)-\frac{\mu^2}{1-z^2}\right]u=0 \tag{A.1}$$

where ν and μ are real numbers, and z may be complex. The above differential equation has two solutions denoted as $P_\nu^\mu(z)$ and $Q_\nu^\mu(z)$ which are called the μth order and νth degree of the associated Legendre functions of the first and second kind respectively [6] and [72]. The associated legendre functions satisfy, among others, two important recurrence equations [6] and [72]

$$(\nu-\mu+1)P_{\nu+1}^\mu(z)-(2\nu+1)zP_\nu^\mu(z)+(\nu+\mu)P_{\nu-1}^\mu(z)=0 \tag{A.2}$$

$$P_\nu^{\mu+2}(z)-\frac{2(\mu+1)z}{\sqrt{z^2-1}}P_\nu^{\mu+1}(z)+(\nu-\mu)(\nu+\mu+1)P_\nu^\mu(z)=0 \tag{A.3}$$

and $Q_\nu^\mu(z)$ satisfy the same relations. In (A.2) $P_\nu^\mu(z)$ is the dominant solution, and $Q_\nu^\mu(z)$ is the minimal solution [71]. On the other hand, in (A.3) $P_\nu^\mu(z)$ is the minimal solution and $Q_\nu^\mu(z)$ is the dominant solution [71]. To ensure the stability of recurrence equations, dominant solution needs to be applied only in the forward recursion, and minimal solution have to be applied only in the backward recursion [71] and [45]-[48]. So, $P_\nu^\mu(z)$ in (A.2) can be applied only for forward recursion, and $Q_\nu^\mu(z)$ can be applied in the backward recursion, and the order will be reversed in (A.3). So the recurrence relations (A.2) and (A.3) can be used to compute the value of $Q_\nu^\mu(z)$, but the only requirement are the starting points (at least two). The starting points can be found using different criteria, closed form representation, continued fractions, power series, and numerical integration. For example $Q_\nu^{-\frac{1}{2}}(z)$ and $Q_\nu^{\frac{1}{2}}(z)$ are given by [6]

$$\begin{aligned}
Q_\nu^{-\frac{1}{2}}(z)&=-\frac{\sqrt{-2\pi}}{2\nu+1}\left(z^2-1\right)^{-\frac{1}{4}}\left(z+\sqrt{z^2-1}\right)^{-\nu-\frac{1}{2}}\\
Q_\nu^{\frac{1}{2}}(z)&=\sqrt{-\frac{\pi}{2}}\left(z^2-1\right)^{-\frac{1}{4}}\left(z+\sqrt{z^2-1}\right)^{-\nu-\frac{1}{2}}
\end{aligned} \tag{A.4}$$

equation (A.3) combined with (A.4) can be used to find $Q_\nu^{m+\frac{1}{2}}(z)$ where m is an integer. For arbitrary values of ν, μ, and $|z| > 1$, the starting points can be computed using [6]

$$Q_\nu^\mu(z) = \frac{e^{\jmath\mu\pi}\sqrt{\pi}\ \Gamma(\nu+\mu+1)\,(z^2-1)^{\mu/2}}{2^{\nu+1}\Gamma(\nu+1.5)z^{\nu+\mu+1}}\ {}_2F_1\left(1+(\nu+\mu)/2, (1+\nu+\mu)/2; \nu+3/2; 1/z^2\right) \tag{A.5}$$

where ${}_2F_1(w, x; y; z)$ is the Gaussian hypergeometric function [6].

APPENDIX B

PROOFS FOR THE AVERAGE SEP OF MQAM

B.1 Proof of equation (5.19)

In this Section, we will prove the evaluation of the Appells hypergeometric function given in (5.19). Assuming n is integer, then it can be shown (with the aid of (5.7) and (5.14)) that

$$\begin{aligned} F_2\left(n;1,1;1.5,1.5;\frac{k}{h},\frac{k}{h}\right) &= \frac{h^n}{\Gamma(n)}\int_0^\infty \left({}_1F_1(1;1.5;kx)\right)^2 x^{n-1}e^{-xh}dx \\ &= \frac{\pi h^n}{4k\Gamma(n)}\int_0^\infty \text{erf}^2(\sqrt{kx})x^{n-2}e^{-x(h-2k)}dx \end{aligned} \tag{B.1}$$

Integration by parts can be used to evaluate the last integral by substituting $u = \text{erf}^2(\sqrt{kx})$ and $v = \int x^{n-2}e^{-x(h-2k)}dx$, then

$$\begin{aligned} &\int_0^\infty \text{erf}^2(\sqrt{kx})x^{n-2}e^{-x(h-2k)}dx = \frac{2\sqrt{k}(n-2)!}{\sqrt{\pi}(h-2k)^{n-1}} \\ &\times\sum_{\ell=0}^{n-2}\frac{(h-2k)^\ell}{\ell!}\int_0^\infty \text{erf}(\sqrt{kx})x^{\ell-0.5}e^{-x(h-k)}dx \end{aligned} \tag{B.2}$$

where we have used [58]

$$\int z^\ell e^{-az}dz = \frac{-\ell!e^{-az}}{a^{\ell+1}}\sum_{j=0}^{\ell}\frac{a^j}{j!}z^j, \qquad \ell \text{ is integer} \tag{B.3}$$

Since [58]

$$\begin{aligned} \int_0^\infty \text{erf}(\sqrt{kx})x^{\ell-0.5}e^{-x(h-k)}dx &= 2\sqrt{\frac{k}{\pi}}\int_0^\infty {}_1F_1(1;1.5;kx)x^\ell e^{-xh}dx \\ &= \frac{2\sqrt{k}\Gamma(\ell+1)}{\sqrt{\pi}h^{\ell+1}}\,{}_2F_1\left(1,\ell+1;1.5;\frac{k}{h}\right) \end{aligned} \tag{B.4}$$

Combining (B.1)-(B.4), then

$$F_2\left(n;1,1;1.5,1.5;\frac{k}{h},\frac{k}{h}\right) = \frac{h^{n-1}}{(n-1)(h-2k)^{n-1}}\sum_{\ell=0}^{n-2}\frac{(h-2k)^\ell}{h^\ell}\,{}_2F_1\left(1,\ell+1;1.5;\frac{k}{h}\right) \tag{B.5}$$

B.2 The average SEP of the common and simplified models

The average SEP of the common quadrature MQAM is

$$P_M(e) = 2q\ \mathrm{E}\{\mathrm{erfc}(\sqrt{p\gamma_t})\} - q^2\mathrm{E}\{\mathrm{erfc}^2(\sqrt{p\gamma_t})\} \tag{B.6}$$

and the average SEP of the simplified model of MQAM is

$$P_M(e) = 2q\ \mathrm{E}\{\mathrm{erfc}(\sqrt{p\gamma_t})\} - q^2\left(\mathrm{E}\{\mathrm{erfc}(\sqrt{p\gamma_t})\}\right)^2 \tag{B.7}$$

where E{.} denotes the statistical expectation. Since

$$\begin{aligned} &\mathrm{E}\{(\mathrm{erfc}(\sqrt{p\gamma_t}) - \mathrm{E}\{\mathrm{erfc}(\sqrt{p\gamma_t})\})^2\} \geq 0 \\ \Rightarrow\ &\mathrm{E}\{\mathrm{erfc}^2(\sqrt{p\gamma_t})\} - (\mathrm{E}\{\mathrm{erfc}(\sqrt{p\gamma_t})\})^2 \geq 0 \\ \Rightarrow\ &\mathrm{E}\{\mathrm{erfc}^2(\sqrt{p\gamma_t})\} \geq (\mathrm{E}\{\mathrm{erfc}(\sqrt{p\gamma_t})\})^2 \end{aligned} \tag{B.8}$$

from the previous inequality, we can conclude that the average SEP of the simplified model is always greater or equal to the SEP of the common quadrature MQAM.

REFERENCES

[1] R. E. Ziemer and R. L. Peterson, *Introduction to Digital Communication.* Upper Saddle River, NJ: Prentice Hall, 2001.

[2] J. Proakis, *Digital Communications.* New York, NY: McGraw-Hill, 1989.

[3] M. Simon and M. Alouini, *Digital Communication over Fading Channels: A Unified Approach to Performance Analysis.* New York, NY: John Wiley, 2000.

[4] M. Nakagami, "The m distribution A general formula for intensity distribution of rapid fading," *in Statistical Methods in Radio Wave Propagation*, pp. 3–36, 1960.

[5] S. O. Rice, "Statistical properties of a sine wave plus random noise," *Bell Syst. Tech. J.*, vol. 27, pp. 109–157, Jan. 1948.

[6] M. Abramowitz and I. Stegun, *Handbook of Mathematical Functions.* NY: Dover, 1972.

[7] D. Brennan, "Linear diversity combining techniques," *Proc. IRE*, vol. 47, pp. 1075–1102, June 1959.

[8] W. B. M. Schwartz and S. Stein, *Communication Systems and Techniques.* New York, NY: McGraw-Hill, 1966.

[9] A. Goldsmith, *Wireless Communications.* Cambridge: Cambridge University Press, 2004.

[10] G. Stuber, *Principles of Mobile Communications.* Norwell, MA: Kluwer, 1996.

[11] L. Ahlin and J. Zander, *Principles of Wireless Communications.* Sweden: Studentlitteratur, 1998.

[12] K. Feher, "MODEMs for emerging digital cellular-mobile radio system," *IEEE Trans. Veh. Technol.*, vol. 40, pp. 355–365, May 1991.

[13] C. L. T. T. Tjhung and N. P. Secord, "A unified performance of DQPSK in slow Rician fading," *Electron. Lett.*, vol. 28, no. 18, pp. 1763–1765, Aug. 1992.

[14] J. Weng and S. Leung, "Analysis of DPSK with equal gain combining in Nakagami fading channels," *Electron. Lett.*, vol. 33, no. 8, pp. 654–656, Apr. 1997.

[15] M. Simon and M.-S. Alouini, "A unified approach to the probability of error for noncoherent and differentially coherent modulations over generalized fading channels," *IEEE Trans. Commun.*, vol. 46, pp. 1625–1638, Dec. 1998.

[16] Y. Ma and T. J. Lim, "Bit error probability for MDPSK and NCFSK over arbitrary Rician fading channels," *IEEE J. Select. Areas Commun.*, vol. 18, pp. 2179–2186, Nov. 2000.

[17] Y. Ma and Q. T. Zhang, "Accurate evaluation for MDPSK with noncoherent diversity," *IEEE Trans. Commun.*, vol. 50, pp. 1189–1200, 2002.

[18] I. Ghareeb and M. Abu-Sbeih, "Performance of QDPSK signals with postdetection equal gain diversity combining in arbitrarily correlated Nakagami-m fading channels," *IEEE Commun. Lett.*, vol. 5, pp. 441–443, Nov. 2001.

[19] T. K. Y. Lo, "Maximum ratio transmission," *IEEE Trans. Commun.*, vol. 47, p. 14581461, Oct. 1999.

[20] R. K. M. P. A. Dighe and S. S. Jamuar, "Analysis of transmit-receive diversity in Rayleigh fading," *IEEE Trans. Commun.*, vol. 51, p. 694703, Apr. 2003.

[21] B. D. Rao and M. Yan, "Performance analysis of maximal ratio transmission with two receive antennas," *IEEE Trans. Commun.*, vol. 51, p. 894895, 2003.

[22] M. Kang and M.-S. Alouini, "A comparative study on the performance of MIMO MRC systems with and without cochannel interference," *IEEE Trans. Commun.*, vol. 52, pp. 1417– 1425, Aug. 2004.

[23] A. J. Grant, "Performance analysis of transmit beamforming," *IEEE Trans. Commun.*, vol. 52, pp. 738– 744, Apr. 2005.

[24] W. Lindsey and M. Simon, *Telecommunication Systems Engineering.* Upper Saddle River, NJ: Prentice Hall, 1973.

[25] A. Viterbi, *Principles of Coherent Communication.* New York, NY: McGraw-Hill, 1966.

[26] V. K. Prabhu, "PSK performance with imperfect carrier phase recovery," *IEEE Trans. Aerosp. Electron. Syst.*, vol. ASE-12, pp. 275–286, Mar. 1976.

[27] W. C. Lindsey, "Phase-shift-keyed signal detection with noisy reference signals," *IEEE Trans. Aerosp. Electron. Syst.*, vol. ASE-2, pp. 393–401, July 1966.

[28] M. K. Simon, "Error probability performance of unbalanced QPSK receivers," *IEEE Trans. Commun.*, vol. COM-26, pp. 1390–1397, May 2001.

[29] M. A. Najib and V. K. Prabhu, "Analysis of equal-gain diversity with partially coherent fading signals," *IEEE Trans. Veh. Technol.*, vol. 49, pp. 783–791, May 2000.

[30] M. Simon and M. Alouini, "Simplified noisy reference loss evaluation for digital communication in the presence of slow fading and carrier phase recovery," *IEEE Trans. Veh. Technol.*, vol. 50, pp. 783–791, Mar. 2001.

[31] M. A. Smadi and V. K. Prabhu, "Performance analysis of generalized-faded coherent PSK channels with equal-gain combining and carrier phase error," *IEEE Trans. Wireless Commun.*, vol. 5, pp. 509–513, Mar. 2005.

[32] ——, "Performance analysis of generalized-faded coherent PSK channels with equal-gain combining and carrier phase error," *IEE Proceedings-Comm.*, vol. 153, pp. 349–354, June 2006.

[33] M. Alouini and A. Goldsmith, "A unified approach for calculating error rates of linearly modulated signals over generalized fading channels," *IEEE Trans. Commun.*, vol. 47, pp. 1324–1334, Sept. 1999.

[34] A. Annamalai and C. Tellambura, "Error rates for Nakagami-m fading multichannel reception of binary and M-ary signals," *IEEE Trans. Commun.*, vol. 49, pp. 58–68, Jan. 2001.

[35] E. K. Al-Hussaini and A. Al-Bassiouni, "Performance of MRC diversity systems for the detection of signals with Nakagami fading," *IEEE Trans. Commun.*, vol. COM-33, pp. 1315–1319, Dec. 1985.

[36] V. A. Aalo, "Performance of maximal-ratio diversity systems in a correlated Nakagami-m fading environment," *IEEE Trans. Commun.*, vol. 43, pp. 2360–2369, Aug. 1995.

[37] J. H. L. F. Patenaude and J. Y. Chouinard, "Noncoherent diversity reception over Nakagami-m fading channels," *IEEE Trans. Commun.*, vol. 46, pp. 985–991, Aug. 1998.

[38] Q. Zhang, "Exact analysis of postdetection combining for DPSK and NFSK systems over arbitrarily correlated Nakagami channels," *IEEE Trans. Commun.*, vol. 46, pp. 1459–1467, Nov. 1998.

[39] J. Proakis, "Probabilities of error for adaptive reception of M-phase signals," *IEEE Trans. Commun. Technol.*, vol. COM-16, pp. 71–81, Feb. 1968.

[40] ——, "On the probability of error for multichannel reception of binary signals," *IEEE Trans. Commun. Technol.*, vol. COM-16, pp. 68–71, Feb. 1968.

[41] S. Parl, "A new method of calculating the generalized q function," *IEEE Trans. Inform. Theory*, vol. IT-26, pp. 121–124, Jan. 1980.

[42] J. Gurland, "Distribution of the maximum of the arithmetic mean of correlated random variables," *Annals of Math. Statistics*, vol. 26, pp. 294–300, June 1995.

[43] G. F. P. Lombardo and M. M. Rao, "MRC performance for binary signals in Nakagami-m fading with general branch correlation," *IEEE Trans. Commun.*, vol. 47, pp. 44–52, Jan. 1999.

[44] A. Erdelyi, *Higher Transcendental Functions.* New York, NY: McGraw-Hill, 1982, vol. II.

[45] J. Segura and A. Gil, "Evaluation of toroidal harmonics," *Comput. Phys. Comm.*, vol. 124.

[46] A. G. J. Segura and N. M. Temme, "Computing toroidal functions for wide ranges of the parameters," *J. Comput. Phys.*, vol. 161.

[47] ——, "Evaluation of Legendre functions of arguments greater than one," *J. Comput. Phys.*, vol. 105.

[48] ——, "A code to evaluate prolate and oblate spherical harmonics," *J. Comput. Phys.*, vol. 108.

[49] C. Tellambura and V. Bhargava, "Unified error analysis of DQPSK in fading channels," *Electron. Lett.*, vol. 30, no. 25, pp. 2210–2211, Dec. 1994.

[50] R. K. Mallik and M. Z. Win, "Error probability of binary NFSK and DPSK with postdetection combining over correlated Rician channels," *IEEE Trans. Commun.*, vol. 48, pp. 1975–1978, Dec. 2000.

[51] R. R. Pawula, "A new formula for MDPSK system error probability," *IEEE Commun. Lett.*, vol. 2, pp. 271–272, Oct. 1998.

[52] Y. Ma, "Impact of correlated diversity branches in Rician fading channels," *IEEE ICC*, vol. 1, pp. 473–477, May 2005.

[53] Q. T. Zhang, "Error performance of noncoherent MFSK with L-diversity on correlated fading channels," *IEEE Trans. Wireless Commun.*, vol. 1, pp. 531–539, 2002.

[54] C.-Y. S. Chang and P. J. McLane, "Bit-error-probability for noncoherent orthogonal signals in fading with optimum combining for correlated branch diversity," *IEEE Trans. Inform. Theory*, vol. 43, pp. 263–247, Jan. 1997.

[55] J. K. Cavers, "Single-user and multiuser adaptive maximal ratio transmission for Rayleigh channels," *IEEE Trans. Veh. Technol.*, vol. 49, pp. 2043–2050, Nov. 2000.

[56] R. L.-U. Choi and R. D. Murch, "New transmit schemes and simplified receivers for MIMO wireless communication systems," *IEEE Trans. Wireless Commun.*, vol. 2, pp. 1217–1230, Apr. 2003.

[57] A. T. James, "Distributions of matrix variates and latent roots derived from normal samples," *Ann. Math. Statist.*, vol. 35.

[58] I. Gradeshteyn and I. Ryzhik, *Table of Integrals, Series, and Products*. San Diego, CA: Academic Press, 1994.

[59] V. I. Tikhonov, "Phase-lock automatic frequency control operation in the presence of noise," *Automata. Remote Contr.*, vol. 21, pp. 209–214, Mar. 1960.

[60] W. Weber, "Performance of phase-locked loops in the presence of fading communication channels," *IEEE Trans. Commun.*, vol. COM-24, pp. 487–499, May 1976.

[61] V. K. Prabhu, "Error-rate consideration for digital phase-modulation systems," *IEEE Trans. Commun.*, vol. COM-17, pp. 33–42, Feb. 1969.

[62] Y. L. Luke, *Integrals of Bessel Functions*. New York, NY: McGraw-Hill, 1962.

[63] V. Prabhu, "Techniques for estimating the bit error rate in the simulation of digital communication systems," *IEEE J. Select. Areas Commun.*, vol. SAC-2, pp. 153–170, Jan. 1984.

[64] S. A. Rhodes, "Effect of noisy phase reference on coherent detection of offset-QPSK signals," *IEEE Trans. Commun.*, vol. COM-22, pp. 1064–1055, Aug. 1974.

[65] R. Bartle and D. R. Sherbert, *Introduction to Real Analysis*. New York, NY: John Wiley, 1982.

[66] T. Eng and L. B. Milstein, "Partially coherent DS-SS performance in frequency selective multipath fading," *IEEE Trans. Commun.*, vol. 45, pp. 110–118, Jan. 1997.

[67] S. Sampei, *Applications of Digital Wireless Technologies to Global Wireless Communications*. Englewood Cliffs, NJ: Prentice-Hall, 1997.

[68] T. T. T. J. Lu and C. C. Chai, "Error probability performance of L-branch diversity reception of MQAM in Rayleigh fading," *IEEE Trans. Commun.*, vol. 46, pp. 179–181, Feb. 1998.

[69] C. T. A. Annamalai and V. K. Bhargava, "Exact evaluation of maximal-ratio and equal-gain diversity receivers for M-ary QAM on nakagami fading channels," *IEEE Trans. Commun.*, vol. 47, pp. 1335–1344, Sept. 1999.

[70] N. Saad and R. Hall, "Integrals containing confluent hypergeometric functions with applications to perturbed singular potentials," *J. Phys. A:Math. Gen.*, vol. 36, pp. 7771–7788, 2003.

[71] N. Temme, *Special Functions; An Introduction to the Classical Functions of Mathematical Physics*. New York, NY: John Wiley, 1996.

[72] N. Lebedev, *Special Functions and their Applications*. Englewood Cliffs, NJ: Prentice-Hall, 1965.

BIOGRAPHICAL STATEMENT

Iyad Al Falujah was born in Amman, Jordan, in 1975. He received his B.S. degree from University of Technology, Iraq, in 1997, his M.S. degree from Jordan University of Science and Technology, Jordan, in 2000, and Ph.D. degrees from The University of Texas at Arlington in 2007, all in Electrical Engineering. Between 1999 and 2000, he was working as designer and developer engineer at International Technical Engineering, Amman, Jordan. From 2000 to 2001, he was a lecture member in the department of Electronic Technology, at Dammam College of Technology, Saudi Arabia. His current research interest is in the area of CDMA communications for mobile cellular systems. He is a member of several IEEE societies.